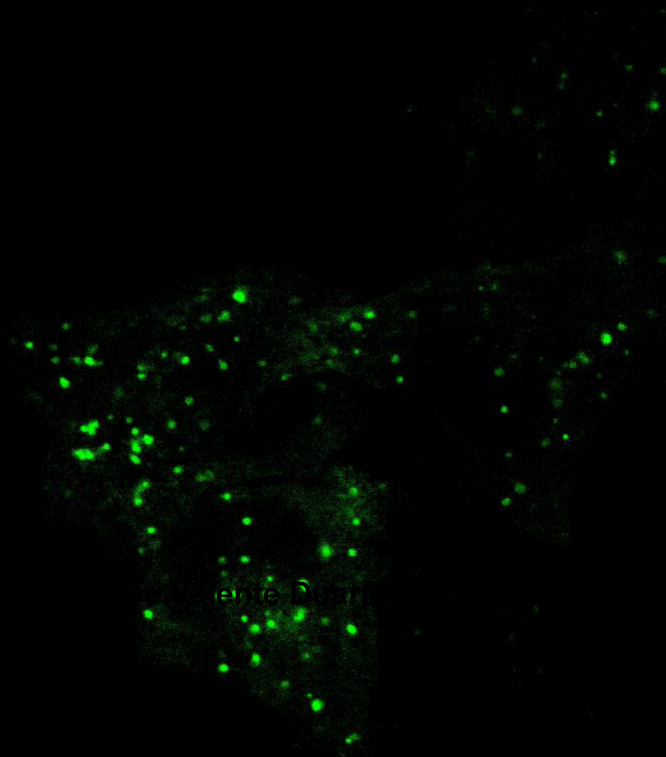


Dibenzofuran exposure: cellular and mitochondrial damage



UNIVERSIDADE DE COIMBRA

Filipe Valente Duarte | 2012



UNIVERSIDADE DE COIMBRA

Dibenzofuran exposure: cellular and mitochondrial damage

Dissertação apresentada à Faculdade de Ciências e Tecnologia da Universidade de Coimbra, para cumprimento dos requisitos necessários à obtenção do grau de Doutor em Biociências (Especialidade Biologia Celular e Molecular), realizada sob a orientação científica do Professor Doutor Carlos Palmeira (Universidade de Coimbra e Centro de Neurociências e Biologia Celular da Universidade de Coimbra) e co-orientação da Professora Doutora Anabela Rolo (Centro de Neurociências e Biologia Celular da Universidade de Coimbra).

Dissertation presented to the Faculty of Sciences and Technology of the University of Coimbra in partial fulfillment of the requirements for the degree of Doctor of Philosophy in Biosciences (Specialty Molecular and Cell Biology), under supervision of Professor Carlos Palmeira (University of Coimbra, and Center for Neurosciences and Cell Biology of University of Coimbra) and co-supervision of Professor Anabela Rolo (Center for Neurosciences and Cell Biology of University of Coimbra).

"The only real mistake is the one from which we learn nothing."

Henry Ford

"Success is not final, failure is not fatal: it is the courage to continue that counts."

Winston Churchill

"It always seems impossible until it's done."

Nelson Mandela

Index / Table of contents

Index / Table of contents	I
Agradecimientos / Acknowledgements	V
Abstract	VII
Resumo	IX
List of Abbreviations	XI
1. General introduction	1
1.1. Environmental pollution	3
1.1.1. Toxicants exposure and disease	5
1.1.2. Dioxins and Dibenzofurans	10
1.1.3. Molecular targets of exposure and toxicity	12
1.2. Mitochondria: general view	16
1.2.1. Respiratory chain, OXPHOS and energy production	20
1.2.2. Generation of reactive oxygen species	24
1.2.3. Mitochondrial permeability transition (MPT)	28
1.2.3.1. Molecular composition of the mitochondrial permeability transition pore (mPTP)	30
1.2.3.2. Regulation of mPTP	36
1.2.3.3. Physiological role of mPTP	38
1.2.4. Calcium homeostasis	40
1.3. Mitochondria and cell death	43
1.3.1. Mitochondria in apoptosis	43
1.4. Mitochondrial shape and dynamics	45
1.5. Autophagy	49
1.5.1. Physiological functions of autophagy/Autophagy and disease	53
1.5.2. Selective autophagy	60
1.5.2.1. Mitophagy - Selective degradation of mitochondria	61
1.6. Mitochondrial biogenesis and mitophagy: quality control and mitochondrial abundance regulation	62
1.7. Aims / Objectives	64

2. Materials and Methods	67
2.1. Materials	69
2.2. List of antibodies used	69
2.3. Animals	69
2.4. Isolation of mitochondria	70
2.5. Mitochondrial transmembrane potential ($\Delta\Psi_m$) measurements	70
2.6. Mitochondrial respiration / Oxygen consumption	71
2.7. ATPase activity	71
2.8. Cytochrome c oxidase (COX) activity	72
2.9. Mitochondrial permeability transition (MPT)	72
2.10. Measurement of mitochondrial calcium fluxes / calcium retention capacity	73
2.11. Immunoprecipitation of ANT and western blot detection of CypD	73
2.12. Carboxyatractyloside (CAT) titration	74
2.13. Western blotting analysis with lung mitochondria	74
2.14. Cell line	74
2.15. Cell culture	74
2.16. Cell death/viability	75
2.17. LDH leakage	75
2.18. Cell proliferation	75
2.19. MTT reduction assay	76
2.20. Adenine nucleotides content	76
2.21. Measurement of mitochondrial membrane potential ($\Delta\Psi_m$) in A549 cells	77
2.22. Oxygen consumption in A549 cells	77
2.23. Measurement of ROS production	78
2.24. Nuclear morphology (apoptosis)	78
2.25. LysoTracker accumulation	78
2.26. LC3 subcellular distribution	79
2.27. Western blotting analysis with A549 cell extracts	79
2.28. DNA isolation and real-time qPCR	79
2.29. Statistical analysis	80

3. Exposure to Dibenzofuran affects lung mitochondrial function <i>in vitro</i>	81
3.1. Introduction	83
3.2. Results	84
3.3. Discussion	90
4. Dibenzofuran-induced mitochondrial dysfunction: interaction with ANT carrier	93
4.1. Introduction	95
4.2. Results	97
4.3. Discussion	111
5. Exposure to Dibenzofuran triggers autophagy in lung cells	117
5.1. Introduction	119
5.2. Results	120
5.3. Discussion	132
6. General discussion	137
 Bibliography	 149

Agradecimentos / Acknowledgements

Gostaria de agradecer de forma geral a todos aqueles que, de alguma maneira, contribuíram para a concretização deste trabalho.

O primeiro agradecimento particular vai para o Professor Doutor Carlos Palmeira e Professora Doutora Anabela Rolo. Agradeço-lhes sinceramente por toda a disponibilidade, constante e desde sempre; por todos os ensinamentos; por toda a amizade verdadeira; por toda a sinceridade; e sobretudo pela paciência e por todo o incentivo e esforço colocados em fazer de mim (ou pelo menos tentar) um melhor cientista. Espero um dia conseguir retribuir pelo menos parte daquilo que me proporcionaram. Obrigado.

I would also like to deeply thank Professor Luca Scorrano and his lab team at the Venetian Institute of Molecular Medicine (Padova, Italy), especially Dr. Lígia Gomes. You all took me in so friendly and professionally that not for a single day I felt homesick. Thanks for all the collaboration and scientific improvement.

Agradeço à Faculdade de Ciências e Tecnologia da Universidade de Coimbra e ao Centro de Neurociências e Biologia Celular da Universidade de Coimbra, respectivamente a instituição que me aceitou no Curso de Doutoramento em Biociências (FCTUC) e a instituição de acolhimento (CNC).

Agradeço à Fundação para a Ciência e a Tecnologia (FCT), cuja Bolsa de Doutoramento (SFRH/BD/38372/2007) me permitiu a realização deste trabalho.

A todos os meus amigos, colegas da Universidade, colegas de curso, professores e funcionários que foram cruzando o meu caminho e deixando o seu contributo na minha vida e no meu percurso.

Agradeço igualmente a todos os meus amigos do Hóquei, a minha “segunda família”, também responsável por grande parte daquilo que sou.

Um agradecimento particular a todos os colegas de laboratório do Departamento de Zoologia e em especial aos colegas do MitoLab: obrigado Ana, Ana e João, por tudo aquilo que partilhámos até aqui no laboratório, fora dele, em dias bons e menos bons. O sucesso devo-o também a vocês. Obrigado.

Agradeço à minha família todo o apoio incondicional.

Em particular à minha mãe, sempre presente e de olhos abertos, verdadeira responsável pelo que sou hoje.

Ao meu pai, longe mas verdadeiramente perto.

Ao meu irmão, sempre presente e de olhos fechados. Não é preciso abri-los. As minhas conquistas são igualmente conquistas suas.

Um beijinho especial à Beatriz, que veio marcar indelevelmente a minha vida e ensinar-me uma coisa nova a cada dia.

À Marta. Sorrindo sempre, dá-me a força necessária e faz-me gostar de viver.
You were wonderful tonight.

Abstract

In the modern world, one of the main issues that mankind tries to control and improve, concerning its well-being, is health. In the last decades, several progresses have been achieved in order to improve health and also to increase overall lifespan. However, modern lifestyle also brought changes that continuously threaten health. In an “industrial” world, environmental pollution increased largely, and its effects are reflected deeply in disease development rates and incidence percentages.

Human exposure to pollutants can occur via various pathways, including inhalation of contaminated air and dust, ingestion of contaminated water and food, dermal exposure to chemical or contaminated products, or fetal exposure during pregnancy. Dibenzofuran (DBF) is a “dioxin-like” chemical that is known to be toxic. This pollutant has been identified in tobacco smoke and listed as a pollutant of concern due to its persistence in the environment and potential for bioaccumulation; its exposure has been reported to cause reproductive injury, endocrine disruption and respiratory damage. Nevertheless and although the lung is a primary site of exposure for many inhaled chemical contaminants, studies about pollutants-induced toxic effects in lung function are scarce.

In this work we tested the toxic effects of DBF *in vitro* in isolated mitochondria, organelles that play a central role in cell life and death. Mitochondria were isolated from lung, primary target organ of exposure to pollutants through inhalation, and from the liver, the main organ responsible for accumulating and metabolize xenobiotics. In the lung mitochondria, DBF caused a decrease in the mitochondrial phosphorylative efficiency and interfered with the mitochondria permeability transition (MPT) induction. Liver mitochondrial function was also impaired by DBF, which caused increased phosphorylative lag phase, reduced mitochondrial state 3 respiration, as well as disturbance of the calcium loading capacity and MPT. Moreover, we identified an interaction of DBF with the adenine nucleotide translocase (ANT), a mitochondrial component that is involved in both the phosphorylative system and in MPT induction.

Exposure of lung epithelial cells A549 to the pollutant caused a reduction in cell proliferation, associated with a decreased mitochondrial activity (lower MTT reduction and reduced oxygen consumption rate) and impairment of ATP production. DBF exposure triggered autophagy in A549 cells probably as a cytoprotective mechanism.

In summary, our results indicate that mitochondria are probably a target in DBF-induced toxicity. A decrease in the mitochondrial phosphorylative efficiency elicited by Dibenzofuran, with subsequent decrease in ATP content, are damaging results from exposure to Dibenzofuran; also inhibition of lung cell proliferation and mitochondrial activity, as well as autophagy triggering seem to be critical events in DBF-induced function impairment. Yet, further studies focused on understanding the upstream molecular mechanisms, by which metabolic pathways are deregulated, may ultimately help to develop therapeutic strategies and to prevent diseases related to pollutants exposure.

Resumo

No mundo moderno de hoje, um dos principais aspectos que o Homem tenta controlar e melhorar, no que respeita ao seu bem-estar, é a sua saúde. Nas últimas décadas, vários progressos foram feitos de forma a conseguir melhorar a saúde e também aumentar a esperança média de vida. No entanto, o estilo de vida moderno trouxe também algumas mudanças que constantemente ameaçam a saúde. Numa sociedade dita “industrial”, a poluição ambiental aumentou grandemente; em consequência disso os seus efeitos refletem-se largamente nas taxas de desenvolvimento de doenças e percentagens de incidência.

A exposição humana a poluentes ambientais pode ocorrer por diversas vias, nomeadamente inalação de ar contaminado e de poeiras, ingestão de comida e água contaminadas, exposição por contacto dérmico com químicos ou produtos contaminados, ou ainda exposição fetal durante a gravidez. O Dibenzofurano (DBF) é um composto químico semelhante a dioxinas, conhecido por ser tóxico. Este poluente foi identificado no fumo de tabaco e listado como um poluente preocupante devido às suas características de persistência no ambiente e potencial para bioacumulação. Foi já reportado que a exposição a DBF prejudica a reprodução, causa disrupção endócrina e dano respiratório. Contudo, e apesar de o pulmão ser um órgão primário de exposição a vários contaminantes químicos inalados, são ainda escassos os estudos sobre os efeitos tóxicos induzidos por poluentes na função pulmonar.

Neste trabalho foram testados os efeitos tóxicos do DBF *in vitro*, utilizando mitocôndrias isoladas, desempenhando estes organelos um papel central na vida e morte celular. As mitocôndrias foram isoladas a partir de pulmão, órgão alvo da exposição a poluentes por inalação, e a partir de fígado, o principal órgão responsável por acumular e metabolizar compostos xenobióticos. Nas mitocôndrias de pulmão, a exposição a DBF causou uma redução na eficiência da fosforilação mitocondrial e interferiu com a indução de permeabilidade transitória mitocondrial (MPT). A função mitocondrial no fígado também foi inibida pela exposição a DBF, que causou um aumento da *lag phase* fosforilativa, redução do estado 3 da respiração mitocondrial, bem como um distúrbio na capacidade de retenção de cálcio pelas mitocôndrias e

na indução de MPT. Além destes efeitos, foi identificada uma interação do DBF com o translocador de nucleótidos de adenina (ANT), um componente mitocondrial que está envolvido tanto no sistema fosforilativo como na indução de MPT.

A exposição de células epiteliais pulmonares (células A549) ao poluente causou uma redução da proliferação celular, associada a um decréscimo na atividade mitocondrial (diminuição na redução de MTT e na taxa de consumo de oxigênio) e a uma diminuição da produção de ATP. A exposição a DBF despoletou nas células A549 mecanismos de autofagia, provavelmente como um mecanismo de proteção celular em resposta ao dano causado.

Em síntese, os resultados indicam que a mitocôndria é provavelmente um alvo envolvido na toxicidade causada pela exposição a DBF. Um decréscimo da eficiência fosforilativa mitocondrial causado pelo DBF, com consequente decréscimo na quantidade de ATP, são efeitos danosos da exposição a este poluente. Também a inibição da proliferação de células pulmonares e da atividade mitocondrial, assim como a indução de autofagia, parecem ser fenômenos causados pela exposição a DBF e consequente dano. Porém, estudos adicionais focados na compreensão dos mecanismos moleculares que levam à desregulação de vias metabólicas são necessários, podendo contribuir para o desenvolvimento de novas estratégias terapêuticas e para a prevenção de doenças relacionadas com a exposição a poluentes.

List of Abbreviations

- α -1 - ATZ - α -1-antitrypsin Z
- $\Delta\Psi_m$ - Transmembrane potential
- $\Delta\mu H^+$ - Electrochemical gradient
- A549 - Human lung epithelial cell line
- ADOA - Autosomal-dominant optic atrophy
- ADP - Adenosine diphosphate
- AhR - Aryl hydrocarbon receptor
- AIF - Apoptosis-inducing factor
- AKT - v-akt murine thymoma viral oncogene homolog, also known as PKB
- AMP - Adenosine monophosphate
- AMPK - AMP-activated protein kinase
- ANT - Adenine nucleotide translocase
- APAF1 - Apoptotic protease activating factor 1
- ARNT - AhR nuclear translocator
- ATG - Autophagy-related genes (and proteins)
- ATP - Adenosine triphosphate
- Bcl2 - B-cell lymphoma 2, apoptosis regulator protein
- Bcl-XL - B-cell lymphoma-extra large, apoptosis regulator protein
- BKA - Bongkrelic acid
- BSA - Bovine serum albumin
- cAMP - Cyclic adenosine monophosphate
- CAT - Carboxyatractyloside
- CK - Creatine kinase
- CL - Cardiolipin
- CMA - Chaperone-mediated autophagy
- CMT2A - Charcot-Marie-Tooth Disease type 2A
- CNS - Central nervous system
- COPD - Chronic obstructive pulmonary disease
- COX-2 - Cyclooxygenase-2
- CsA - Cyclosporine A
- CYP1A1 - Cytochrome P450 1A1

CypA - Cyclophilin A
CypD - Cyclophilin D
Cyt c – Cytochrome c
DAPI - 4',6-diamidino-2-phenylindole
DAPK - Death-associated protein kinase
DBF - Dibenzofuran
DNA - Deoxyribonucleic acid
DNP - 2,4-dinitrophenol
DRAM - Damage-regulated autophagy modulator
DRP1/DLP1 - Dynamin-related protein 1
DSBs - DNA double strand breaks
EGF - Epidermal growth factor
EGFR - Epithelial growth factor receptor
EGTA - Ethylene glycol tetraacetic acid
EM - Electron microscopy
ER - Endoplasmic reticulum
ETC - Electron transport chain
FADH₂ - flavin adenine dinucleotide (reduced form)
FBS – Fetal bovine serum
Fe/S clusters - Iron/Sulfur clusters proteins
Fis1 - Mitochondrial fission 1 protein
GPx - Glutathione peroxidase
GST - Glutathione-S-transferase
H₂DCF-DA - 2',7'-Dichlorodihydrofluorescein diacetate
H₂O₂ - Hydrogen peroxide
HK – Hexokinase
HOCL - Hypochlorous acid
HPLC - High-performance liquid chromatography
IMS - Intermembrane space
I/R - Ischemia/Reperfusion
JNK - c-Jun N-terminal kinase
LAMP-2 - Lysosomal-associated membrane protein 2
LCINS - Lung cancer in never smokers
LDH – Lactate dehydrogenase

MAC - Mitochondrial apoptosis-induced channels
MAPK - Mitogen-activated protein kinase
MCF-10A - Human mammary epithelial cell line
MCU - Mitochondrial calcium uniporter
MFNs – Mitofusins proteins
MIM - Mitochondrial inner membrane
MnSOD - Manganese superoxide dismutase
MOM - Mitochondrial outer membrane
MPT - Mitochondrial permeability transition
mPTP - Mitochondrial permeability transition pore
mRNA - Messenger RNA
mRyR - Mitochondrial ryanodine receptor
mtDNA - Mitochondrial DNA
MTT - 3-[4,5-dimethylthiazol-2-yl]-2,5-diphenyl tetrazolium bromide
mtUPR - mitochondrial unfolded protein response
NAD⁺ - Nicotinamide adenine dinucleotide, oxidized form
NADH - Nicotinamide adenine dinucleotide, reduced form
NADPH - Nicotinamide adenine dinucleotide phosphate, reduced form
NAFLD – Non-alcoholic fatty liver disease
ALT – alanine aminotransferase
NO - Nitric oxide
NOS - Nitric oxide synthase
O₂^{•-} - Superoxide radical
OH[•] - Hydroxyl radical
ONOO⁻ - Peroxynitrite
OPA1 - Optic atrophy protein 1
OXPHOS - Oxidative phosphorylation
PAHs - Polycyclic aromatic hydrocarbons
PBR - Peripheral benzodiazepine receptor
P_iC - Mitochondrial phosphate carrier
PCBs - Polychlorinated biphenyls
PCDDs - Polychlorinated dibenzodioxins
PCDFs - Polychlorinated dibenzofurans
PGE₂ - Prostaglandin E₂

PGF_{2α} - Prostaglandin F_{2α}
PKs - Protein kinases
PNs - Pyridine nucleotides
PS – Phosphatidylserine
PTEN - Phosphatase and tensin homolog
PVDF - Polyvinylidene difluoride
RCR – Respiratory control ratio
RNA – Ribonucleic acid
RNS - Reactive nitrogen species
ROS - Reactive oxygen species
rRNA - Ribosomal RNA
siRNA - Small interfering RNA
Sox9 - Transcriptor factor of the Sox gene family
TCA cycle - Citric acid cycle, also known as Krebs cycle
TCDD - tetrachlorodibenzo-*p*-dioxin
TCDF - tetrachlorodibenzofuran
TGF-α - Transforming growth factor-α
THP-1 - human promonocytic leukemia cell line
TMPD - Tetramethylphenylene-diamine
TNF-α - Tumor necrotizing factor-α
TOM - Translocase of the outer membrane
TOR - Target of rapamycin
TPP⁺ - tetraphenylphosphonium
tRNA - Transfer RNA
TSCs - Tuberous sclerosis protein
TSPO - mitochondrial outer membrane translocator protein of 18 kDa
UCPs - Mitochondrial uncoupling proteins
VDAC - Voltage-dependent anion channel
VOCs - Volatile organic compounds
WHO - World Health Organization
XRE - Xenobiotic response element

Chapter 1

General introduction

In the modern world, one of the main issues that mankind tries to control and improve, concerning its well-being, is health. In the last decades, several progresses have been achieved in order to improve health and also to increase overall lifespan. However, modern lifestyle also brought changes that continuously threaten health. In an “industrial” world, environmental pollution increased largely, and its effects are reflected deeply in disease development rates and incidence percentages.

Chemicals definitely became part of our daily lives. Moreover, they may cause diseases. One important question that decision-makers have to address, in order to prioritize efforts to protect us from the harmful effects of chemicals, is related to which fraction of the current disease burden are caused by chemical exposure, and also which are the chemicals of greatest concern.

Unsurprisingly, chemicals exposure not only affects health but also economy, as modern societies spend more and more money trying to either cure people from diseases or prevent them from getting ill.

1.1. Environmental pollution

Chemicals, whether of natural origin or produced by human activities, are part of our environment. Their chemical, physical and toxicological properties vary greatly; while many are not hazardous or persistent, some are life-threatening on contact and some persist in the environment, accumulate in the food chain, travel large distances from where they are released, and are harmful to human health in small amounts (Prüss-Ustün et al., 2011). Human exposure can occur at different stages of the existence of a chemical in the environment, including through occupational exposure during manufacture, use and disposal, consumer exposure, exposure to contaminated products or environmental exposure to toxic waste. Exposure can occur via various pathways, including inhalation of contaminated air and dust, ingestion of contaminated water and food, dermal exposure to chemical or contaminated products, or fetal exposure during pregnancy (Table 1.1.1).

Table 1.1.1 - Examples of sources and pathways of human exposure to chemicals (from Prüss-Ustün et al., 2011).

Exposure media	Example sources of exposure and exposure pathways	Examples of chemicals
Outdoor air	Inhalation of toxic gases and particles from vehicle and industrial emissions, or naturally occurring sources such as volcanic emission or forest fires.	Sulfur dioxide, nitrogen oxides, ozone, suspended particulate matter, lead, benzene, dioxins and dioxins-like compounds
Indoor air	Inhalation of pollutants released during indoor combustion of solid fuels, tobacco smoking, or from construction materials and furnishings, contaminants in indoor air and dust.	Suspended particulate matter, nitrous oxide, sulfur oxides, carbon monoxide, formaldehyde, polyaromatic hydrocarbons (PAH), mercury, lead dust from lead-based paints, benzene, asbestos, mycotoxins, phthalates, polybrominated diphenyl ether fire retardants (PBDEs)
Drinking water	Ingestion of drinking water contaminated with toxic chemicals from industrial effluents, human dwellings, agricultural runoff, oil and mining wastes, or from natural sources.	Pesticides, herbicides, fertilizers, metals (copper, lead, mercury, selenium, chromium), arsenic, fluoride, nitrate, cyanide, industrial solvents, petroleum products, disinfection by-products.
Food	Consumption of food contaminated with chemicals at toxic levels through agricultural practices, industrial processes, environmental contamination, and natural toxins.	Pesticides, methylmercury, lead, cadmium, dioxins, aflatoxin.
Non-food consumer products	Exposure by ingestion, inhalation or dermal exposure to toxic chemicals contained in toys, jewelry and decoration items, textiles, or food containers, consumer chemical products	Lead, mercury, cadmium, phthalates, formaldehyde, dyes, fungicides or pesticides.
Soil	Ingestion (particularly for children) or inhalation of soil contaminated through industrial processes, agricultural processes or inadequate household and industrial waste management.	Heavy metals, pesticides, and persistent organic pollutants.
Occupational exposure	Chronic or acute exposures through inhalation, dermal absorption, or secondary ingestion of toxic chemicals or by-products of industrial processes such as agriculture, mining or manufacturing.	Pesticides, benzene, heavy metals, solvents, suspended particulate matter.
Human to human	Fetal exposure to toxic chemicals during pregnancy (through placental barrier) or through consumption of contaminated breast milk.	Heavy metals, pesticides, benzene, etc.

Pollution implicates the insertion of contaminants into a natural environment that causes instability, disorder, harm or discomfort to the ecosystem (i.e. physical systems or living organisms). Pollution can take the form of chemical substances, noise, heat or light. Pollutants, the components of pollution, can be either foreign substances or naturally occurring contaminants.

Air pollution has long been known to be detrimental to health, particularly that of the respiratory system, yet epidemiologic estimates of the respiratory effects of air pollution have suggested relatively small effects compared with those of other environmental exposures. However, effects estimated at a population level ignore individuals' susceptibility to air pollution, which may be associated with genetic factors, together with non-genetic factors such as age, time spent outdoors, and level of physical exercise (Minelli et al., 2011).

1.1.1. Toxicants exposure and disease

Environmental pollution can lead to the development of several diseases or promote the exacerbation of conditions already prevailing.

When one thinks about air pollution, it is mandatory to think of respiratory morbidity and respiratory diseases. Ambient air pollution is associated with a considerable burden of global disease (Figure 1.1.1). The World Health Organization estimated that exposure to fine particulate air pollution caused 800,000 deaths and 6.4 million lost years of healthy life in the world's cities in 2000. The developing countries of Southeast Asia accounted for two-thirds of this burden (Cohen et al., 2005; Su et al., 2011).

The effects of air pollutants continue to be at a high level of interest within the scientific, regulatory, and public communities. This is because of the need to address critical gaps in understanding how air pollution contributes to human health problems and how we can effectively attenuate them. A great deal of information exists concerning the effects of gaseous air pollutants but our current understanding of such effects, including the effects of mixed components on human mortality and morbidity, are limited. Also

limited is our understanding about the level of metabolic changes associated with changes in oxidative stress and how such changes modulate health.

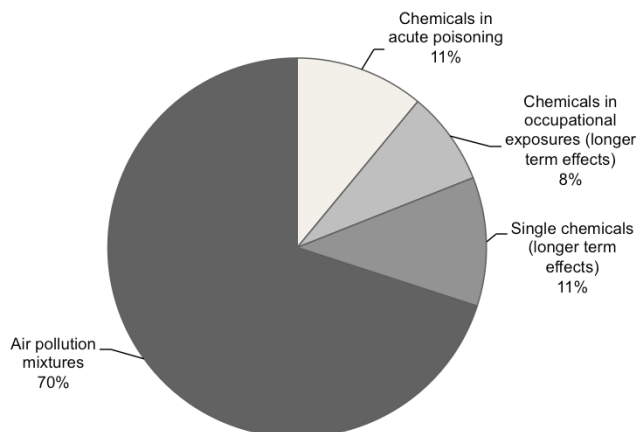


Figure 1.1.1 – Distribution of known burden of disease in DALYs - Disability-adjusted life years. Adapted from Prüss-Ustün et al., 2011.

Several health problems have been associated with air pollution and oxidative stress, such as chronic obstructive pulmonary disease (COPD) (Chiba et al., 2012), cardiovascular diseases (Gentner and Weber, 2010; Nemmar et al., 2011; Jules et al., 2012; Martinelli et al., 2012), asthma (Lehmann et al., 2001; Lehmann et al., 2002), inflammation (Lehmann et al., 2008) and lung cancer (Katanoda et al., 2011; Couraud et al., 2012). Particularly tobacco use is the oldest (Doll and Hill, 1950) and most well-established (Khuder, 2001) risk factor for lung cancer, and lung cancer is the most common cause of cancer death (1.38 million, 18.2% of the total) (Ferlay et al., 2010; Jemal et al., 2011). The World Health Organization (WHO) estimates that 25% of lung cancer worldwide occurs in never smokers (Jemal et al., 2011). This percentage is probably closer to 10–15% in Western countries (Sun et al., 2007; Scagliotti et al., 2009). If considered as an independent entity, lung cancer in never smokers (LCINS) was already the 7th largest cause of cancer-related mortality in the world some years ago (Parkin

et al., 2005) and a top-ten cause of death in the United States (Thun et al., 2006; Blair and Freeman, 2006).

Apart from air pollution and respiratory diseases, many studies have also demonstrated that exposure to environmental chemicals has other severe adverse health effects, including neurotoxicity, immunotoxicity, developmental toxicity, hepatotoxicity, kidney toxicity and lymphomas (Bakke et al., 2007; Tabrez and Ahmad, 2009; Purdue et al., 2011). The liver is the major site of trichloroethylene (TCE) metabolism and TCE hepatotoxicity has been well documented in humans and experimental animal models (Yang et al., 2012). Occupational exposure to TCE has also been found to cause non-cancer liver diseases, such as hepatic necrosis, fatty liver, and cirrhosis (Thiele et al., 1982; Pantucharoensri et al., 2004). TCE-associated hepatotoxicity involves increased oxidative stress and TCE treatment has also been found to cause genotoxic effects in HepG2 cells, which probably result from TCE-induced oxidative DNA damage (Hu et al., 2008). Moreover, human beings exposed to chromium, nickel or arsenic under environmental or occupational settings show increased risk of asthma, nasal septum and skin ulcerations, allergic and contact dermatitis, as well as respiratory cancers (Salnikow and Zhitkovich, 2008; Soudani et al., 2011). Experimental animals models exposed to chromium also exhibit acute tissue damage, including testicular lesions, kidney tubular necrosis, and liver damage (Pedraza-Chaverri et al., 2005). The damage has been associated with the intracellular generation of toxic chromium intermediates, which are considered as strong oxidants; ROS generated in excess cause injury to cellular proteins, lipids and DNA, leading to oxidative stress (Soudani et al., 2011). Still, polychlorinated biphenyls (PCBs), lead, and mercury are common pollutants that have been associated with significant dose-dependent increase for ALT elevation not explained by viral hepatitis, hemochromatosis, or alcohol abuse, presenting a relationship between low-level environmental pollution and the development of liver disease and non-alcoholic fatty liver disease - NAFLD (Cave et al., 2010).

Table 1.1.2 presents a brief summary about diseases with suspected or already confirmed linkage to chemicals.

Table 1.1.2 - Main disease groups with suspected or confirmed linkage to chemicals (from Prüss-Ustün et al., 2011).

Diseases/disease groups	Examples of exposures	Examples of associated outcomes
Respiratory infections and chronic respiratory diseases	Occupational exposures to dusts, gases, irritant chemicals, fumes Second-hand smoke; occupational exposures to cleaning-agents, pesticides, hairdressing chemicals etc. Second-hand smoke	Chronic Obstructive Pulmonary Disease (COPD) Asthma onset and exacerbation Acute lower respiratory infections Asbestosis, Bronchitis, pneumoconiosis, silicosis
Perinatal conditions	Maternal exposure to pesticides or other chemicals	Low-birth-weight and preterm infants
Congenital anomalies	Maternal exposure to pesticides, polychlorinated biphenyls (PCBs), polychlorinated dibenzofurans (PCDFs), lead, mercury, other endocrine disruptors	Various birth defects
Diseases of the blood	Lead, arsine, naphthalene, benzene	Anemia, methaemoglobinemia
Cancers	Occupational exposures to carcinogens, aflatoxins in food, second-hand smoke, outdoor air pollution by carbon particles associated with polycyclic aromatic hydrocarbons, asbestos, arsenic; volatile organic compounds such as benzene, pesticides, dioxins. etc.	Numerous cancer sites, including of the lung, skin, liver, brain, kidney, prostate, bone marrow, bladder
Neuropsychiatric and developmental disorders	Lead, methylmercury, polychlorinated biphenyls (PCBs), arsenic, toluene etc.	Cognitive development, mental retardation, Parkinson disease, Attention-deficit disorder, Minamata disease
Sense organ diseases	Carbon disulfide, mercury, lead	Hearing loss
Cardiovascular diseases	Ultrafine particles in polluted air, lead, arsenic, cadmium, mercury, pollutant gases, solvents, pesticides, second-hand smoke	Ischemic heart disease, cerebrovascular disease
Diabetes mellitus	Arsenic, N-3-pyridylmethyl-N'-p-nitrophenyl urea (rodenticide), 2,3,7,8-Tetrachlorodibenzo-p-dioxin.	Diabetes Type II

Systemic autoimmune diseases	Crystalline silica dust	Systemic sclerosis, systemic lupus erythematosus, rheumatoid arthritis, systemic small vessel vasculitis
Endocrine diseases	Ethanol, hexachlorobenzene	Porphyria
Genito-urinary diseases	Beryllium, cadmium, lead	Calculus of kidney, chronic renal disease
Digestive diseases	Ethanol, chloroform, carbon tetrachloride, manganese	Hepatitis, cholestasis, pancreatitis
Skin diseases	Antiseptics, aromatic amines, cement, dyes, formaldehyde, artificial fertilizers, cutting oils, fragrances, glues, lanolins, latex, metals, pesticides, potassium dichromate, preservatives	Atopic dermatitis, allergic and irritant contact dermatitis, chloracne, hyperkeratosis
Musculoskeletal diseases	Cadmium, lead	Osteoporosis, gout
Oral conditions	Fluoride	Dental fluorosis
Poisonings	Accidental ingestion of household products, occupational exposures and accidents, intentional self-harm by ingestion of pesticides	Unintentional poisonings, self-inflicted injuries

Based on recent estimations, the global burden of disease attributable to environmental exposure and management of selected chemicals sums to at least 4.9 million deaths (or 86 million DALYs - “Disability-adjusted life years”, a weighted measure of years of life lost due to premature death, and years lived with disability) per year (Prüss-Ustün et al., 2011). This represents 8.3% of the total deaths and 5.7% of the total burden of disease in DALYs worldwide. The share of the total disease burden is considerable, and supports the need for further public health considerations in this area. By far the largest disease burden is related to exposure to air pollution mixtures with 70% of the total. These estimations include available information for chemicals in a broad sense, i.e. not only industrial and agricultural chemicals but also air pollutants and some naturally occurring chemicals. Available information for industrial and agricultural chemicals and acute poisonings only (i.e. without air pollution nor contaminated drinking-water) amounts to a global burden of disease of at least 1.2 million deaths (25 million DALYs), corresponding to 2.0% of the total deaths and 1.7% of the total burden of disease worldwide (Prüss-Ustün et al., 2011).

Better insight on these diseases and linkage to toxicants exposure may direct means for more effective public health prevention and treatment of diseases associated with air pollution.

1.1.2. Dioxins and Dibenzofurans

Dibenzofuran is a heterocyclic organic compound with the chemical structure shown in Figure 1.1.2. It is an aromatic ether that has two benzene rings fused to one furan ring in the middle, having the chemical formula $C_{12}H_8O$.

Dibenzofurans often inaccurately refer to polychlorinated dibenzofurans (PCDFs), a family of organic compounds with one or several of the hydrogens in the Dibenzofuran structure replaced by chlorines (Figure 1.1.3). For example, 2,3,7,8-tetrachlorodibenzofuran (TCDF) has chlorine atoms substituted for each of the hydrogens on the number 2, 3, 7, and 8 carbons.

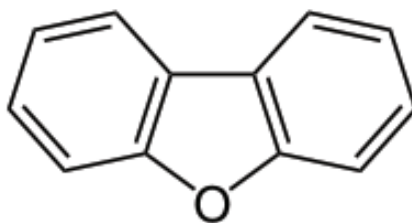


Figure 1.1.2 – Chemical structure of Dibenzofuran.

Polychlorinated dibenzofurans are structurally similar to polychlorinated dibenzodioxins (PCDDs) and these groups together are often inaccurately called “dioxins”, which represents a generic term used to denote a single compound or mixture of compounds derived from polychlorinated dibenzodioxins, with very similar structures and often found in association with them.

The toxic potency of both PCDDs and PCDFs is a function of the number and positions of chlorine substituents. PCDDs and PCDFs with a decreased number of lateral chlorine atoms (positions 2, 3, 7 and 8) or increased non-lateral chlorine atoms are generally less toxic than TCDD (Safe, 1990).

The mixture of dioxins and furans emitted from combustion sources are in both the gaseous and particulate phase, and the persistence of these substances may be a function of the phase into which they are emitted. The potency of dioxins and dibenzofurans is dependent on the chemical structure of the individual compound. Therefore, dibenzodioxin chlorinated in the 2, 3, 7, and 8 positions has been demonstrated to be carcinogen, but other chlorinated dibenzodioxins, polychlorinated dibenzofurans and non-chlorinated dibenzodioxins and dibenzofurans were evaluated as not classifiable as to their carcinogenicity to humans (McGregor et al., 1998) and the carcinogenic properties of these compounds remain unclear to the moment.

Dibenzofuran (DBF) is a white crystal-like solid that is created from the production of coal tar, used as an insecticide and to make other chemicals. It has been found in coke dust, grate ash, fly ash, and flame soot. One can be

exposed to DBF by breathing contaminated air or by eating or drinking contaminated food or water. Since it has been found in tobacco smoke, you can be exposed if you smoke cigarettes or breathe cigarette smoke. In addition, you can be exposed to Dibenzofuran if you work in an industry that makes or uses coal tar. Moreover, it can also be absorbed into your body when it comes into contact with your skin.

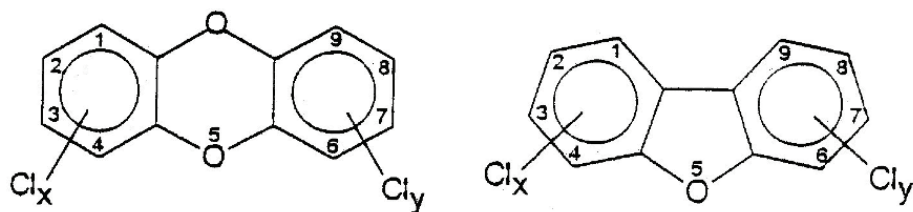


Figure 1.1.3 – General structures of PCDDs (left) and PCDFs (right).

The PCDDs and PCDFs are two series of almost planar tricyclic aromatic compounds with very similar chemical properties. The number of chlorine atoms can vary between 1 and 8. The number of positional congeners is quite large; in all there are 75 PCDDs and 135 PCDFs.

Little information is available on the effects of DBF exposure to our health. However, the information that does exist shows that short-term exposure to DBF can cause skin, eye, nose, and throat irritation. Dibenzofurans, coplanar PCBs and other dioxin-like chemicals were shown to be anti-estrogenic in oviduct porcine epithelial cell line (Hombach-Klonisch et al., 2006), reported to act as endocrine disruptors (Aoki, 2001) and to prompt menstrual effects in DBF-poisoned women (Yang et al., 2011), and testified to cause reduced fertility and alterations in pregnancy in women exposed to PCB/PCDF-contaminated cooking oil (Yang et al., 2008).

1.1.3. Molecular targets of exposure and toxicity

Many toxic agents such as dioxins, dibenzofurans, benzo[a]pyrene (B[a]P), cigarette smoke toxicants, PCBs, and other related organochlorine

compounds have been proven to cause harmful effects. Several studies have demonstrated the association between air pollution and respiratory and cardiovascular diseases (Brunekreef and Forsberg, 2005), namely changes in blood homeostasis, alterations in heart rate and atherosclerosis (Sun et al., 2010), asthma and COPD (Perez et al., 2010). These sort of chemicals can also regulate several immunological responses. Indeed, some authors have reported upregulation of the production of proinflammatory cytokines in airway epithelial cells due to cigarette smoke (Baginski et al., 2006). Cigarette smoke has also been proved a potent Th17 adjuvant and IL-17RA signaling is required for chemokine expression necessary for MMP12 induction and tissue emphysema in mice exposed to cigarette smoke (Chen et al., 2011). Studies with mice have also reported the inhibition of the antigen-presenting activity of alveolar macrophages and a decrease in interleukin-1 β mRNA expression, as well as a significant increase in DNA damage and ROS generation in alveolar macrophages (Ishida et al., 2009). Furthermore, some volatile organic compounds (VOCs) widely distributed in the environment were shown to markedly increase the expression level of cyclooxygenase-2 (COX-2), the rate-limiting enzyme of the prostaglandin pathway, in human lung cells (Mögel et al., 2011). Additionally, prostaglandin E₂ (PGE₂) and prostaglandin F_{2 α} (PGF_{2 α}), major products of the COX enzyme, were found to be upregulated in response to the same aromatic compounds, which exposure caused activation of p38 MAPK (Mögel et al., 2011). However, a complete understanding of inflammatory interactions is far from clear.

Concerning air pollution, increased concentrations of particulate matter with an aerodynamic diameter of less than 10 $\mu\text{g}/\text{m}^3$ (PM10) have been linked to an acute increase in emergency room visits, hospital admissions, respiratory symptoms, mortality rate due to respiratory and cardiovascular disease and restricted activity days due to morbidity (Pelucchi et al., 2009).

Regarding chemical toxicants, one of the most toxic dioxins, 2,3,7,8-tetrachlorodibenzo-*p*-dioxin (TCDD), induces the production of tumor necrotizing factor- α (TNF- α) in THP-1, a human promonocytic leukemia cell line (Cheon et al., 2007). TNF- α is known as a primary mediator of an acute inflammatory response, and its over-production plays a key role in many pathologic processes (Vassalli, 1992), including TCDD associated mortality,

hypersensitivity to endotoxin, an enhanced peritoneal inflammatory response, cachexia, and endometriosis (Clark et al., 1991). This compound has also been reported to increase the expression of transforming growth factor- α (TGF- α) mRNA in MCF-10A, a human mammary epithelial cell line (Davis et al., 2003). Furthermore, noxious agents such as TCDD mimic the epithelial growth factor receptor (EGFR) signaling pathway, leading to tyrosine kinase phosphorylation and its physical association with EGFR (Sewall et al., 1995). On the other hand, TCDD also blocks cell differentiation through EGFR signaling in human epidermal keratinocytes (Sutter et al., 2009). EGFR exists on the cell surface and is activated by binding of its specific ligands, including epidermal growth factor (EGF) and TGF α . Upon activation, EGFR undergoes a transition from an inactive monomeric form to an active homodimer (Yarden and Schlessinger, 1987), resulting in downstream activation and signaling transduction cascades, essentially the mitogen-activated protein kinase (MAPK), Akt (v-akt murine thymoma viral oncogene homolog; also known as PKB - protein kinase B) and c-Jun N-terminal kinase (JNK) pathways, leading to DNA synthesis and cell proliferation (Oda et al., 2005). Activation of EGFR is important for the innate immune response in human skin (Roupé et al., 2010). Though, it has been shown that TCDD inhibited EGF withdrawal-induced apoptosis in the human mammary epithelial cell line MCF-10A and that the ability of TCDD to overcome EGF withdrawal-induced apoptosis likely requires the induction of TGF- α (Davis et al., 2003), thus reporting the inhibition of apoptosis upon TCDD exposure as a potentially important mechanism of tumor promotion.

Currently it is known that the biological effects of these dioxin-like compounds are mainly mediated through binding to the arylhydrocarbon receptor (AhR). The AhR is a ligand-activated transcription factor ubiquitously distributed in the body, and after ligation of aromatic compounds (such as dioxins and dibenzofurans) to the AhR, the receptor translocates from the cytosol to the nucleus, heterodimerizes with the AhR nuclear translocator (ARNT), and binds to an enhancer sequence, called a xenobiotic response element (XRE), of several drug metabolizing enzymes, such as cytochrome P450 1A1 (CYP1A1) (Mimura and Fujii-Kuriyama, 2003; Gendy et al., 2012).

The effects of toxicants exerted through AhR binding are often related to increased reactive oxygen species (ROS) production through downstream enzymes such as cytochrome P450 (Kopf and Walker, 2010; Chiba et al., 2012). It is well established that superoxide anion and H₂O₂ are common by-products of the P450 catalytic cycle, resulting from inefficient coupling of NADPH consumption to substrate oxidation (Zangar et al., 2004), and this may represent one potential mechanism by which ROS can be produced downstream of CYP1A1 induction (Kopf and Walker, 2010). CYP1A1 is a phase I xenobiotic metabolizing enzyme that bioactivates several polycyclic aromatic hydrocarbons (PAHs) and other hydrophobic environmental procarcinogens into their ultimate carcinogenic forms (Shimada and Fujii-Kuriyama, 2004), reactive intermediates that form DNA adducts, which lead to mutagenesis and carcinogenesis. Several lines of evidence demonstrate a strong correlation between the activity of CYP1A1 and the increased risk of different human cancers such as colon, rectal and lung cancers (Slattery et al., 2004; Shah et al., 2009). Likewise, the inhibition of AhR activity and its regulated gene, CYP1A1, could result in the prevention of the toxic effects caused by the AhR ligands, including carcinogenicity (Puppala et al., 2008). In the lung, it has also been shown that Clara cells, in bronchiolar epithelium, are the most sensitive to AhR stimulation (Tritscher et al., 2000). Besides, significant progress in identifying other molecular targets for PAHs-induced toxicity has also occurred. Misregulation of AhR downstream pathways, such as conversion of arachidonic acid to prostanoids via cyclooxygenase-2 (COX-2), and altered Wnt/ β -catenin signaling downregulating transcription factor Sox9, and signaling by receptors for inflammatory cytokines, have been implicated in tissue-specific endpoints of dioxin toxicity (Yoshioka et al., 2011), shedding some more light on molecular events associated with developmental defects and diseases linked to pollutants exposure.

Furthermore, it has been reported that several pollutants induce the formation of DNA adducts in different tissues. The DNA damage and DNA adducts, when unrepaired, can then cause mutations in vital genes including tumor suppressors or oncogenes, dysregulation of which may lead to cancer initiation and progression (Halappanavar et al., 2011). Halappanavar and colleagues reported the formation of DNA adducts in the liver and lungs of

mice exposed to benzo[a]pyrene (B[a]P) by oral gavage (Halappanavar et al., 2011); other authors have shown that cigarette smoke-associated chemicals induce DNA damage, namely DNA double strand breaks (DSBs), in a human pulmonary epithelial cell model (A549 cells) (Toyooka and Ibuki, 2009), which is related to genomic instability and carcinogenesis and therefore demonstrates the strong genotoxicity of passive smoking. More recently, it has been reported an increase in the frequency of mitochondrial DNA (mtDNA) somatic mutations in lung tissues of fruit growers which had been exposed to pesticides multiple times by inhalation (Wang and Zhao, 2012). The mitochondrial genome is particularly prone to DNA damage, because of the limited DNA repair capabilities, the lack of protective histone proteins and the tolerance of damaged DNA (Wang and Zhao, 2012). Moreover, mitochondria are known to be the major source of reactive oxygen in most mammalian cell types, as well as a major target organelle for oxidative damage (Chomyn and Attardi, 2003). Mitochondrial superoxide and H₂O₂ can cause direct damage to mitochondrial proteins, result in nuclear and mitochondrial genotoxicity (Shen et al., 2005), and initiate apoptosis (Polster and Fiskum, 2004). It has been reported that dioxin causes sustained oxidative stress and damage in liver mitochondria from mice exposed to TCDD and in hepatocytes incubated with the same pollutant (Senft et al., 2002; Aly and Domènech, 2009); thus, mitochondria has also been reported as a direct target for dioxin-induced toxicity.

1.2. Mitochondria: general view

Mitochondria are cellular organelles delimited by two membranes that embrace about one tenth of the cell's proteins. These organelles, on a weight basis proportion, are able to convert between 10 000 and 50 000 times more energy per second than the sun.

Almost a century after the first descriptions of mitochondria, the acquirement of the ability to isolate them and the discovery that mitochondria contain a respiratory system and the enzymes of the tricarboxylic acid cycle and fatty acid oxidation marked the start of the bioenergetics era. This period

culminated with Peter Mitchell's chemiosmotic theory, that deserved him the Nobel Prize for chemistry in 1978.

The mitochondrion consists of four main structures or compartments: two membranes, the intermembrane space and the matrix within the inner membrane. The mitochondrial outer membrane (MOM) separates the cytosol from the intermembrane space. The MOM is responsible for interfacing with the cytosol and its interactions with cytoskeletal elements, which are important for the movement of mitochondria within a cell. This mobility is essential for the distribution of mitochondria during cell division and differentiation. The mitochondrial inner membrane (MIM) separates the intermembrane space from the matrix. The folding of the MIM (cristae) serves to increase the surface area of this membrane (Figure 1.2.1). Mitochondria also move along intermediate actin filaments, using kinesin and dynein proteins.

The MIM hosts the most important redox reactions converting the energy of nutrients into ATP. These reactions are catalyzed by the mitochondrial electron transport chain (ETC), which transports electrons from several substrates to oxygen, in the complex multistep process termed mitochondrial respiration. According to the chemiosmotic theory, mitochondrial respiration generates a transmembrane potential ($\Delta\Psi_m$) across the inner membrane, which is used by ATP synthase to phosphorylate ADP.

The MIM is normally impermeable to protons and other ions, and this solute barrier function of the MIM is critical for energy transduction. Permeabilization of the MIM dissipates $\Delta\Psi_m$ and thereby uncouples the process of respiration from ATP synthase, halting mitochondrial ATP production (Kushnareva and Newmeyer, 2010). Hence, the free energy of respiration is used to pump protons from the matrix to the intermembrane space (IMS), establishing an electrochemical gradient. Since the MIM displays an extremely low passive permeability to protons, an electrochemical gradient ($\Delta\mu_{H^+}$) is built across the membrane. The electrochemical gradient is the sum of two components: the proton concentration difference and the electrical potential difference across the membrane. The estimated magnitude of the proton electrochemical gradient is about -220 mV (negative inside) and under physiological conditions most of the gradient is in the form of electrical potential difference. The proton gradient is converted in ATP, by the F1F0-

ATP synthase. F₁F₀-ATP synthase couples the transport of the protons back to the matrix with the phosphorylation of ADP to ATP.

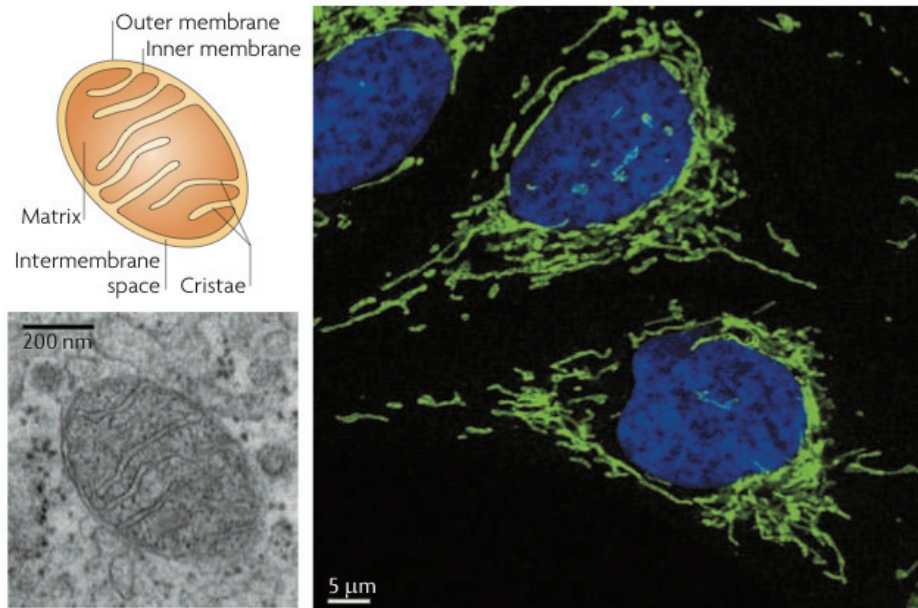


Figure 1.2.1 – Mitochondrial morphology.

Mitochondria are double membrane-bound organelles with characteristic inner membrane folds, termed cristae.

Upper left: The schematic shows the structure of mitochondria.

Bottom left: A transmission electron microscopy image of mitochondria in ultrathin sections of human fibroblast cells is also shown.

Right: In many cell types, mitochondria appear as long, tubular and sometimes branched structures that spread throughout the entire cytoplasm. Mitochondria (green) were stained in human osteosarcoma cells (U2OS) by indirect immunofluorescence using antibodies against the outer membrane protein TOM20. Nuclei (blue) were stained with DAPI (4',6-diamidino-2-phenylindole). Cells were analyzed by confocal microscopy. From Westermann, 2010.

In addition to the process of ATP formation, mitochondria are highly dynamic organelles that have been implicated in the regulation of a great and increasing number of physiological processes. Mitochondrial function is a key to cell life and death, and the deregulation of mitochondrial metabolism is

critical to the pathogenesis of disease (Figure 1.2.2). Cells need energy not only to support their vital functions but also to die gracefully, through programmed cell death, or apoptosis (Kushnareva and Newmeyer, 2010). Execution of an apoptotic program includes energy-dependent steps, including kinase signaling, formation of the apoptosome, and effector caspase activation. Furthermore, mitochondrial regulation is also present beyond cell death mechanisms. Indeed, besides oxidative ATP production, mitochondria assume other functions such as heme synthesis, β -oxidation of free fatty acids, metabolism of certain amino acids, production of free radical species, formation and export of Fe/S clusters, iron metabolism, and play a crucial role in calcium homeostasis (Duchen, 2004b; Michel et al., 2012). In addition, firstly described as a key checkpoint of intrinsic programmed cell death, accumulating data point mitochondria as a central platform involved in many cellular pathways, such as those recently highlighted participating to innate immune response (West et al., 2011) or its lipidic contribution to autophagosomal membrane genesis during starvation-induced autophagy (Hailey et al., 2010). Still, the regulatory roles of mitochondria over normal physiology include the transduction pathway that underlies the secretion of insulin in response to glucose by β -cells and in the sensing of oxygen tension necessary for oxygen sensing in the carotid body and the pulmonary vasculature. Mitochondria also house key enzyme systems quite distinct from those required for intermediary metabolism - the rate-limiting enzymes in steroid biosynthesis, and even the carbonic anhydrase required for acid secretion in the stomach (Duchen, 2004a). By accumulating calcium when cytosolic calcium levels are high, mitochondria play subtle roles in coordinating the complexities of intracellular calcium-signaling pathways, at least in some cell types, in which their contribution may be extremely important in the finer aspects of cell regulation. The physiological “uncoupling” of mitochondria plays a central role as a heat-generating mechanism in non-shivering thermogenesis in young mammals. It has also been suggested that the production of free radical species by mitochondria may play a key role as a signaling mechanism, for example, in the regulation of ion-channel activities and also in initiating cytoprotective mechanisms in stressed cells (Michel et al., 2012).

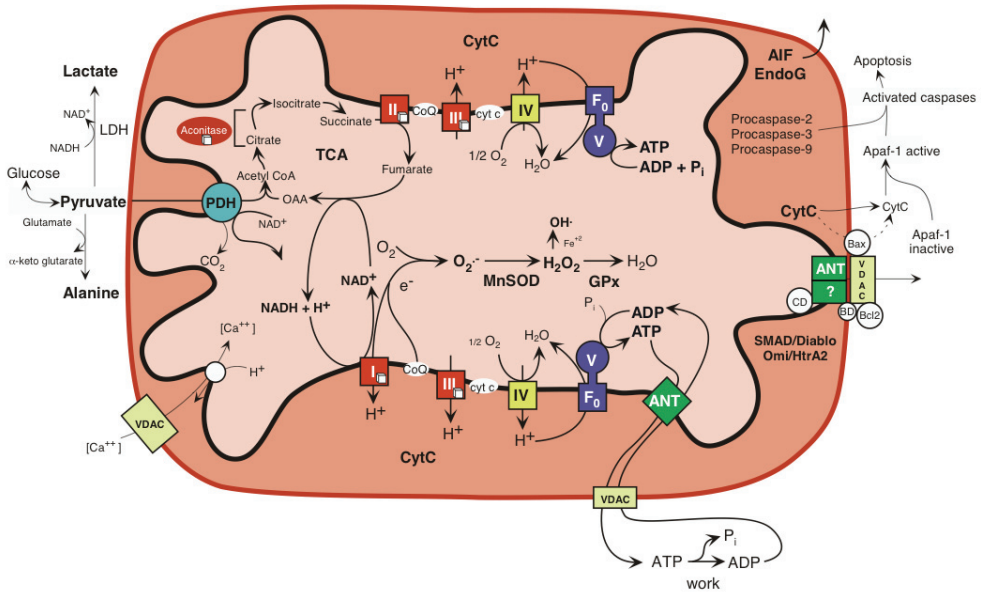


Figure 1.2.2 – Main features of mitochondrial metabolism relevant to the pathogenesis of disease.

(1) Energy production by OXPHOS, (2) ROS generation as a toxic by-product of OXPHOS, and (3) regulation of apoptosis through activation of the mitochondrial permeability transition pore (mPTP). I, II, III, IV, and V = OXPHOS complexes I–V; ADP or ATP = adenosine di- or tri-phosphate; ANT = adenine nucleotide translocase, cyt c = cytochrome c; GPx = glutathione peroxidase-1; LDH = lactate dehydrogenase; MnSOD = manganese superoxide dismutase or SOD2; NADH = reduced nicotinamide adenine dinucleotide; TCA = tricarboxylic acid cycle; VDAC = voltage dependent anion channel. From Wallace, 2005.

1.2.1. Respiratory chain, OXPHOS and energy production

Oxidative phosphorylation (OXPHOS) produces more than 95% of a cell's energy in the form of ATP under normal physiological conditions. This process involves five different protein complexes, Complex I–V, localized in the mitochondrial inner membrane.

The respiratory chain or electron transport chain (ETC; Complexes I–IV) in the MIM is associated with electron transfer components – coenzyme Q and cytochrome *c* (Figure 1.2.3). In the matrix, pyruvate oxidation, β -oxidation of fatty acids, and the TCA cycle pathways are associated.

The five protein complexes constituting the OXPHOS system are: Complex I: NADH dehydrogenase-ubiquinone oxidase, Complex II: succinate dehydrogenase-ubiquinone oxidoreductase, Complex III: ubiquinone cytochrome *c* oxidoreductase, Complex IV: cytochrome *c* oxidase, Complex V: ATP synthase (Figure 1.2.3). Mobile components of the ETC are cytochrome *c* and coenzyme Q10. Coenzyme Q can occur in oxidized form (ubiquinone – Q), reduced form (ubiquinol – QH₂) and radical form (Q \cdot), called “Q-Cycle”.

The total number of polypeptides involved directly in OXPHOS is 91 when cytochrome *c* is included. Of these proteins, some are nuclear-encoded, and some are mitochondrial-encoded in the mtDNA. MtDNA in mammals consists of ~16,5 Kb circular double-stranded DNA that encodes for only 13 subunits of the OXPHOS complexes, plus 2 rRNAs (12S rRNA and 16S rRNA), and 22 tRNAs (Attardi and Schatz, 1988). The mitochondrial genome encodes for essential proteins for the complex I, III, IV and V of the ETC, but curiously complex II subunits are all encoded by the nuclear genome. Because of its limited coding capacity mtDNA relies on nuclear genes for structural components and biological functions. Besides, nuclear-encoded genes also regulate mitochondrial transcription, translation, and mtDNA replication, thus the precise cooperation of nuclear and mtDNA expression is essential to regulate OXPHOS capacity in response to different physiological demands and disease states (Scarpulla, 2008; Peralta et al., 2011). Dysregulated mtDNA expression has been associated with human mitochondrial diseases (Shoubridge, 2001; Smeitink et al., 2006) and is also observed in normal aging process (Krishnan et al., 2007; Larsson, 2010). Moreover, there are also additional proteins required for efficient OXPHOS including those for stability, replication and transcription of mtDNA and multiple proteins acting in assembly of each of the complexes. In all, close to 300 proteins are needed for efficient OXPHOS activity. The overall process of oxidative phosphorylation is tightly controlled by transcriptional regulation at

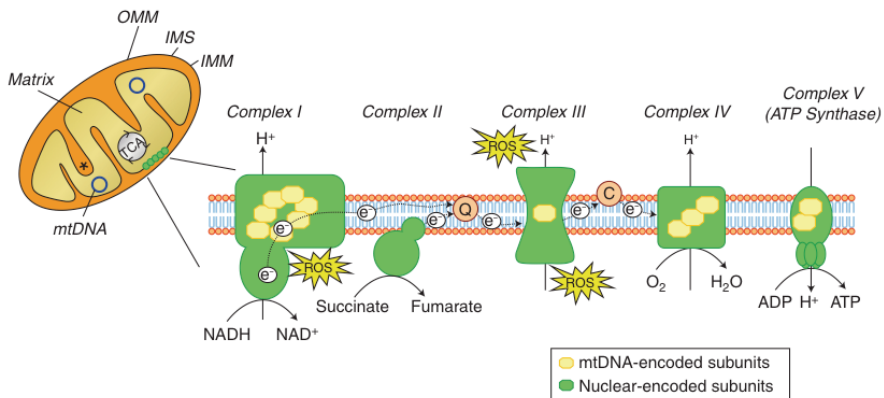


Figure 1.2.3 - Schematic representation of mitochondrial compartmentalization. Mitochondria are divided in four compartments: the outer mitochondrial membrane (OMM or MOM), the intermembrane space (IMS), the inner mitochondrial membrane (IMM or MIM), and the matrix. The respiratory chain is localized at the IMM whereas the mitochondrial DNA (mtDNA) is located in the matrix. The citric acid cycle (or Krebs cycle or TCA cycle) takes place within the mitochondrial matrix. Asterisk indicates mitochondrial cristae. The respiratory chain, also known as the electron transport chain (ETC) or oxidative phosphorylation system (OXPHOS), is composed of approximately 100 proteins, 13 of which are encoded by the mtDNA. The remaining components are encoded by the nuclear DNA and imported into the mitochondria. It consists of five protein complexes; complex I (NADH dehydrogenase) and complex II (succinate dehydrogenase) receive electrons (e^-) from intermediary metabolism, which are then transferred to coenzyme Q and subsequently delivered to complex III (cytochrome c reductase). The electron shuttling protein cytochrome c then transfers the electrons to complex IV (cytochrome c oxidase), which constitutes the final step in the ETC in which molecular oxygen is reduced to water. The electron transport is coupled to proton (H^+) pumping across the IMM by complexes I, III, and IV. The resulting proton gradient drives ATP synthesis through complex V (ATP synthase). Reactive oxygen species (ROS), in the form of superoxide, can be generated by the exit of electrons at the level of complex I and III. C, cytochrome c; Q, coenzyme Q. From Perier and Vila, 2012.

the level of DNA, translational effects via RNA levels and stability, by substrate feedback inhibition, and by post-translational modifications including phosphorylation and acetylation.

The first four complexes of the ETC receive electrons from the catabolism of carbohydrates, fats, and proteins and generate a proton gradient across the inner mitochondrial membrane. Electrons enter the chain through oxidation of either NADH at Complex I or FADH₂ at Complex II and then flow to Complex IV to reduce O₂ to H₂O. Complex I and Complex II collect these electrons, transfer them to coenzyme Q10, Complex III and Complex IV. Complex I, III and IV utilize the energy in electron transfer to pump protons across the inner mitochondrial membrane, producing a proton gradient, which is used by Complex V for ATP production from ADP and inorganic phosphate (Figure 1.2.4). The produced ATP is translocated from the mitochondria into the cytoplasm by adenine nucleotide translocase (ANT). The inner and outer mitochondrial membranes have numerous contact sites. Both of them contain a large assortment of integral and peripheral proteins as well as numerous phospholipids.

Inefficient electron transfer through complexes I-IV causes human disease in part because of loss of energy metabolism but also because insults to the various enzymes (particularly Complexes I, II and III) induce production of toxic reactive oxygen species. Defects of complex V are also a cause of mitochondrial dysfunction (Schapira, 2006; Wu et al., 2010; Abramov et al., 2011). It has also been reported that the deterioration of mitochondrial function underlies common metabolic-related diseases (Rolo and Palmeira, 2006; Palmeira et al., 2007; Turner and Heilbronn, 2008), and several studies have identified compromised oxidative metabolism, altered mitochondrial structure and dynamics, and impaired biogenesis and gene expression in insulin resistance or type 2 diabetes (T2DM) models (Cheng et al., 2010; Rolo et al., 2011; Gomes et al., 2012).

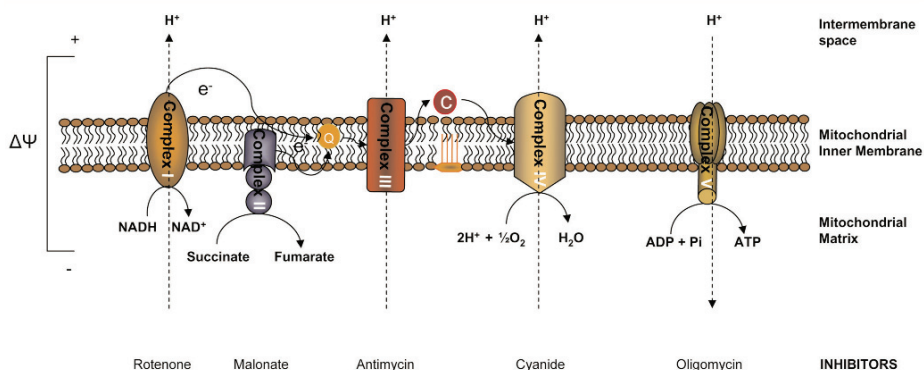


Figure 1.2.4 - Mitochondrial energy production in the ETC.

Electron transport between complexes I to IV is coupled to extrusion of protons from complexes I, III and IV into the intermembrane space, creating an electrochemical gradient across the inner mitochondrial membrane ($\Delta\psi_m$). Protons then flow through complex V (ATP synthase), which utilizes the energy to produce ATP from ADP. Some common mitochondrial respiratory chain inhibitors are shown. C, cytochrome c; Q, ubiquinone. From Bayir and Kagan, 2008.

1.2.2. Generation of reactive oxygen species

Oxidative stress is among the major causes of toxicity due to interaction of ROS with cellular macromolecules and structures and interference with signal transduction pathways (Lenaz, 2012). ROS are thought to be byproducts of aerobic respiration with damaging effects on DNA, protein, and lipid. The mitochondrial respiratory chain, specially from Complexes I and III, is considered the main origin of ROS (Figure 1.2.5), particularly under conditions of high membrane potential, but several other sources may be important for ROS generation, such as mitochondrial 66-kilodalton isoform of the growth factor adapter Shc (p66Shc), monoamine oxidase, α -ketoglutarate dehydrogenase, enzymatic activation of cytochrome p450, and NADPH oxidases, further suggesting involvement in a complex array of cellular processes (Bae et al., 2011; Lenaz, 2012). A growing body of evidence indicates that ROS are involved in the maintenance of redox

homeostasis and various cellular signaling pathways (Bae et al., 2011), as depicted in Figure 1.2.6.

Oxidative stress is at the basis of ageing and many pathological disorders, such as ischemic diseases, neurodegenerative diseases, diabetes, and cancer, although the underlying mechanisms are not always completely understood (Lenaz, 2012). Concerning environmental pollutants, it is recognized that the production of toxic ROS is one of the major effects responsible for a variety of toxicity phenotypes caused by environmental pollutants, leading to adverse health effects and diseases (Valavanidis et al., 2006; Yoshioka et al., 2011).

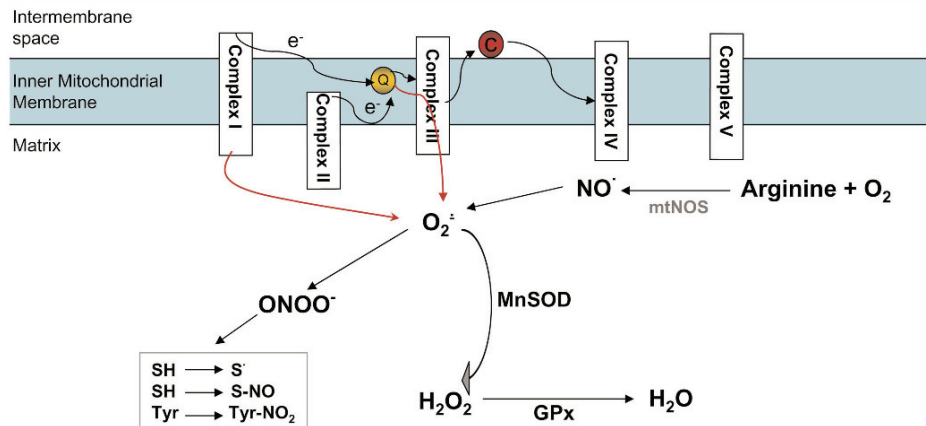


Figure 1.2.5 - Mitochondrial oxidative stress.

In the mitochondria, superoxide can be produced by respiratory complexes. Complex I in the brain and complex III in the heart and lung seem to be the primary sources of mitochondrial superoxide production. Superoxide is detoxified by manganese superoxide dismutase (MnSOD) to hydrogen peroxide (H_2O_2) in the mitochondria. Glutathione peroxidases (GPxs) convert hydrogen peroxide to water. Nitric oxide (NO) generated from (mitochondrial) nitric oxide synthase (mt)NOS can compete with MnSOD and form peroxynitrite ($ONOO^-$). Peroxynitrite in turn initiates thiol oxidation or nitrosylation and tyrosine nitration. C, cytochrome c; $O_2^{\cdot-}$, superoxide; Q, ubiquinone. From Bayir and Kagan, 2008.

Almost all O_2 consumed in mitochondria is reduced to water at Complex IV. Nevertheless, reactive oxygen species (ROS) are produced as an inevitable byproduct of respiration in mitochondria, and also but in lesser amounts at other sites in a cell. The major reactive oxygen species (ROS) are the superoxide radical ($O_2^{\cdot-}$), hydrogen peroxide (H_2O_2), and the hydroxyl radical (OH^{\cdot}). When protonated, the superoxide radical becomes a hydroperoxyl radical. In fact, the only very reactive species among them is the hydroxyl radical, which is believed to be responsible for most of the actual damage done to biological macromolecules. The risk posed by the other two species comes primarily from their spread and subsequent reactions, which ultimately lead to the formation of the hydroxyl radical.

Oxygen is a true substrate of complex IV of the mitochondrial electron transport chain, and it may be assumed that is the site in a cell where oxygen can be activated to the superoxide radical. Instead, it is widely accepted that electrons “leaking” from the electron transport chain to oxygen at high potential upstream sites are responsible for the majority of ROS produced in mitochondria. Thus, complexes I and III, and more recently complex II, have been implicated in the generation of ROS. The proposed mechanism has mutated over the years. In consideration of the small size and zero charge of the oxygen molecule, it can potentially penetrate deeply into protein domains of these complexes. The leaking electrons may come from the free radical semiquinone intermediate of ubiquinone (coenzyme Q) and the free radical intermediates formed by the flavin moieties in complex I (and II). Alternatively, it has been proposed that electrons may escape from the reduced [Fe–S] center N2. It is quite likely that a semiquinone intermediate of the Q cycle is the source of electrons in ROS production by complex III. Recent experiments and arguments in favor of complex I as a major source of ROS tend to favor the flavin intermediate as the donor.

The superoxide radical is also generated “accidentally” by reactions of oxygen at microsomal cytochromes P450, as well as by less well defined or understood reactions (auto-oxidation reactions) involving catecholamines, ascorbic acid, and reduced flavins, often with the participation of a metal ion. The toxicity of such compounds has been exploited in some physiologically useful reactions. The best-known example is the generation of superoxide,

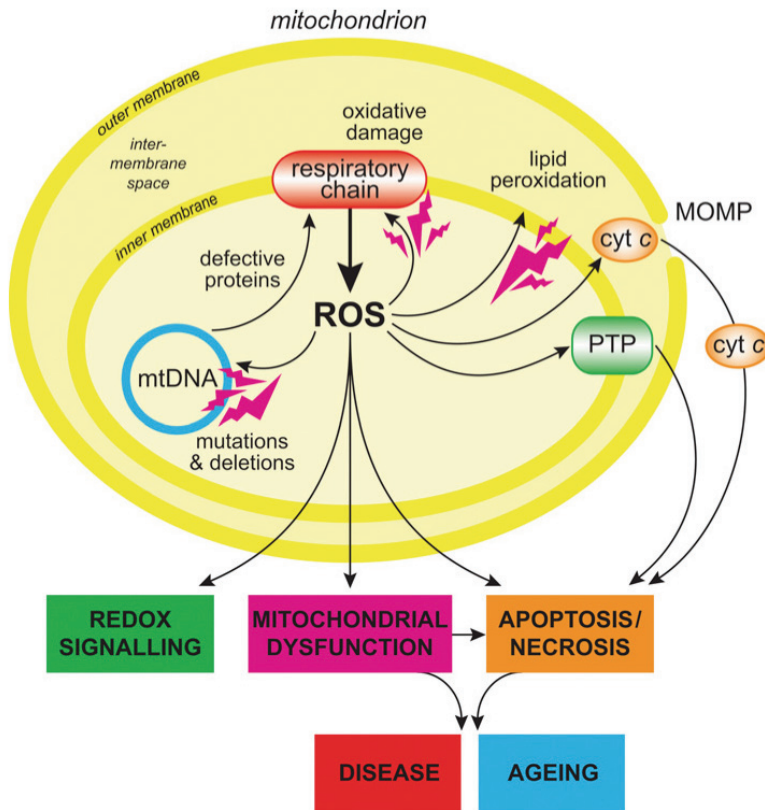


Figure 1.2.6 - Overview of mitochondrial ROS production.

ROS production by mitochondria can lead to oxidative damage to mitochondrial proteins, membranes and DNA, impairing the ability of mitochondria to synthesize ATP and to carry out their wide range of metabolic functions. Mitochondrial oxidative damage can also increase the tendency of mitochondria to release intermembrane space proteins such as cytochrome c (cyt c) to the cytosol by mitochondrial outer membrane permeabilization (MOMP) and thereby activate the cell's apoptotic machinery. In addition, mitochondrial ROS production leads to induction of the mitochondrial permeability transition pore (PTP), which renders the inner membrane permeable to small molecules in situations such as ischaemia/reperfusion injury. Consequently, it is unsurprising that mitochondrial oxidative damage contributes to a wide range of pathologies. In addition, mitochondrial ROS may act as a modulatable redox signal, reversibly affecting the activity of a range of functions in the mitochondria, cytosol and nucleus. From Murphy, 2009.

radicals, hydrogen peroxide, and HOCl by activated macrophages, presumably to kill their target cells (bacteria, fungi, etc.) before phagocytosis. Several peroxisomal oxidases generate hydrogen peroxide — for example, d-amino acid oxidase, xanthine oxidase, and the dehydrogenase in the first step of very long chain fatty acid oxidation. In some systems the superoxide radical has been proposed as an intercellular signal. In a more indirect way, the $O_2^{\cdot-}$ ion can remove nitric oxide, another free radical, and an intercellular messenger in neurotransmission, in the immune response, and in the regulation of smooth muscle contraction.

ROS are able to oxidatively modify lipids, proteins, carbohydrates and nucleic acids in mitochondria and to activate/inactivate signaling pathways by oxidative modification of redox-active factors. Cells are endowed with several defense mechanisms including repair or removal of damaged molecules, and antioxidant systems, either enzymatic or non-enzymatic (Lenaz, 2012). Reactive oxygen species have also been assigned a central role in the mechanisms of apoptosis, still with some uncertainties about whether they are responsible for signaling and cell killing or whether their increased generation is the consequence of another damaging event affecting mitochondria.

1.2.3. Mitochondrial permeability transition (MPT)

The mitochondrial permeability transition (MPT) was originally defined as sudden increase in the inner membrane permeability to solutes of molecular mass less than 1500 Da. An increase in mitochondrial membrane permeability is one of the key events in apoptotic and necrotic death, although the details of the mechanisms involved remain to be fully elucidated. Unlike the resting potentials of neurons and cardiomyocytes, which are largely governed by basal K^+ conductance of their plasma membranes, the value of the mitochondrial resting potential is controlled by the very high resistance of the inner membrane, i.e., low permeability to all ions. While the inner membrane contains several channels (Figure 1.2.7), their opening is tightly regulated in order to prevent dissipation of the membrane potential and proton

gradient that is the electrochemical energy reservoir for ATP-synthesis and transport (Kinnally et al., 2011).

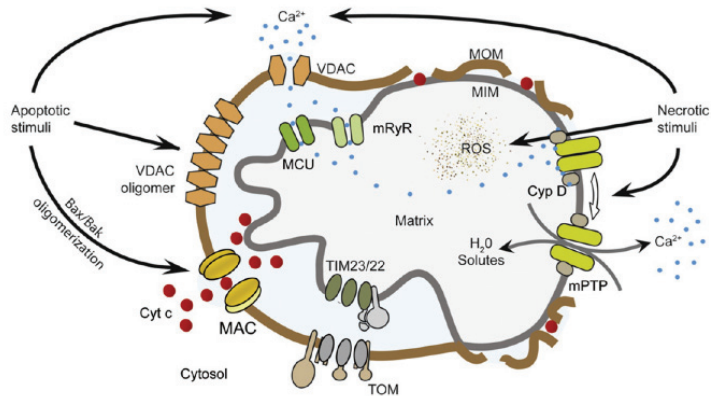


Figure 1.2.7 - Mitochondrial ion channels in apoptosis and necrosis.

Left, apoptotic stimuli induce relocation of Bax from the cytosol into the mitochondrial outer membrane (MOM). Bax, Bak, and possibly other unidentified protein(s) oligomerize and form mitochondrial apoptosis-induced channels (MAC) to release cytochrome *c*. VDAC oligomerization upon apoptotic stimuli was also reported to be involved in cytochrome *c* release. Right, necrotic stimuli lead to exacerbated calcium uptake and reactive oxygen species (ROS) generation by mitochondria. High levels of calcium and ROS induce a cyclophilin-D (CypD)-sensitive opening of mPTP that leads to swelling of the matrix and release of calcium. Swelling disrupts the outer membrane, while released calcium activates proteases, phosphatases, and nucleases that lead to necrotic degradation. TIM23/22, translocases of the inner membrane; mRyR, mitochondrial ryanodine receptor; TOM, translocase of the outer membrane; MCU, mitochondrial calcium uniporter; MIM, mitochondrial inner membrane. From Kinnally et al., 2011.

The mitochondrial permeability is now believed to be due to the opening of a voltage- and Ca^{2+} -dependent, cyclosporine A (CsA)-sensitive, high-conductance channel, which is referred to as the mitochondrial permeability transition pore (mPTP) (Bernardi et al., 1992; Bernardi, 1992; Di Lisa and Bernardi, 2009). The mPTP is the most notorious of all the inner membrane channels; it has not only been linked to a rupture of mitochondrial

outer membrane during cell death (Figure 1.2.7) but also to a myriad of pathologies, including neurodegenerative disorders such as Alzheimer's disease and multiple sclerosis (Singh et al., 2009; Su et al., 2009; Kinnally et al., 2011) and ischemia/reperfusion injury (Halestrap and Pasdois, 2009; Varela et al., 2010; Pasdois et al., 2011). mPTP is considered to be a channel with a large conductance that is activated by Ca^{2+} overloading and other factors including oxidative stress (Zoratti and Szabò, 1995; Bernardi, 1999; Chinopoulos and Adam-Vizi, 2012) and to be regulated by the transmembrane voltage (Bernardi et al., 1992; Bernardi, 1992).

A variety of potential functions are credited to mPTP, which may not be exclusive: (1) a voltage sensor, (2) a matrix pH sensor, (3) a divalent cation sensor (role in calcium homeostasis), (4) a sensor of adenine nucleotide concentrations, (5) a sensor of the redox state of the pyridine nucleotide pool, and (6) a thiol sensor (redox status of glutathione). However, it has received the most particular attention because pore opening has been implicated in the regulation of apoptosis and necrosis (Zorov et al., 2009; Rasola et al., 2010a; Rasola et al., 2010b).

1.2.3.1. Molecular composition of the mitochondrial permeability transition pore (mPTP)

Although the molecular identity of the mPTP remains unclear, several proteins have been implicated in either its structure or regulation. The original model for the pore based upon biochemical and pharmacological studies had three components: the voltage-dependent anion channel (VDAC) in the outer membrane, the adenine nucleotide translocase (ANT) in the inner membrane, plus cyclophilin D (CypD) in the matrix (Figure 1.2.8).

Currently, this model is discussed and other proteins are suggested as mPTP components or regulators, such as mitochondrial creatine kinase (CK), cytosolic hexokinase (HK), the inner membrane phospholipid cardiolipin (CL), adenylate cyclase in the intermembrane space and the peripheral benzodiazepine receptor protein of the MIM. HK, VDAC and ANT all occur as

isoforms and it remains to be determined whether there is specificity of these different forms for the mPTP.

Voltage-dependent anion channel (VDAC)

VDAC, also known as mitochondrial porin, is the most abundant protein of the MOM and the major channel for the exchange of metabolites and ions between the mitochondria and other cellular compartments (Lee et al., 1996; Rostovtseva et al., 2002). The VDAC family of proteins consists of three isoforms from three separate genes (VDAC1, VDAC2, and VDAC3) (McCommis and Baines, 2012).

As a consequence of its location at the boundary between mitochondria and cytosol, VDAC is also a binding partner for proteins that mediate and regulate the integration of mitochondrial functions with other cellular activities. Notably, VDAC has been reported to bind pro- and anti-apoptotic proteins of the Bcl-2 family that regulate the permeability of the outer membrane (Azoulay-Zohar et al., 2004); it may interact with mitochondrial proteins that form contact sites between the inner and outer membranes (Brdiczka et al., 1998) and that may generate the mPTP complex (Crompton et al., 2002); and it binds to cytosolic proteins, such as hexokinase I and hexokinase II (Pedersen et al., 2002) which influences not only its metabolic function, but also its capacity to respond to Bcl-2 family proteins and its role in apoptosis (Pastorino and Hoek, 2003; Pastorino and Hoek, 2008).

Although VDAC has long been considered a key component of the mPTP, the evidence supporting its involvement is largely circumstantial. Initial support for a role for VDAC in MPT came from Crompton's laboratory, which demonstrated that a GST–CypD fusion protein was able to pull down VDAC along with the adenine nucleotide translocase (ANT), another putative mPTP component from mitochondrial lysates (Crompton et al., 1998). Additional supporting evidence for VDAC's involvement in MPT came from experiments using putative VDAC inhibitors and anti-VDAC antibodies. Monoclonal antibodies purported to block VDAC's channel activity were reported to prevent MPT in isolated mitochondria (Shimizu et al., 2001; Zheng et al.,

2004). Yet the specificity of these antibodies for VDAC has been cast into doubt (Rostovtseva et al., 2005).

Conversely, several studies have been made demonstrating that VDAC is not an essential component of the MPT. In this regard, an intact MPT response was reported in isolated mouse mitochondria and cells essentially deficient for all three VDAC isoforms, suggesting that VDACS are dispensable for MPT and are not an essential component of the mPTP (Baines et al., 2007). Other group has also reported a maintained MPT response in VDAC1^{-/-} (Krauskopf et al., 2006) and VDAC1/3^{-/-} mitochondria (Chiara et al., 2008). Thus, in light of both the nonspecific VDAC “blocking” agents used in previous studies and the more recent findings of maintained MPT responses in VDAC-deficient null mitochondria, we must conclude that VDAC is not an essential component of the mPTP. We found that mitochondria and cells lacking VDAC have an exacerbated MPT and death response (Baines et al., 2007), suggesting that, if anything, VDAC appears to protect against rather than contribute to MPT (McCommis and Baines, 2012).

Adenine nucleotide translocase (ANT)

ANT is a reversible transporter of ATP and ADP. During oxidative phosphorylation (OXPHOS) the protein exchanges ATP out for ADP in; however, in the absence of OXPHOS ANT works in reverse to maintain mitochondrial membrane potential. Patients with heart-related diseases have been shown to harbor mutations in the ANT gene or to develop an autoimmune reaction against the protein. The ANT is the most abundant protein in mitochondria. The ANT family mediates the exchange of ATP and ADP across the inner mitochondrial membrane. There are three isoforms of ANT: ANT1, ANT2 and ANT3, being ANT1 the most abundant protein in the MIM.

A former general agreement indicated that the ANT was a participant in channel formation, perhaps by forming complexes with outer membrane proteins to create contact sites and hence to stabilize and/or enlarge the channel. Some evidences suggest that ANT1 or ANT3 is a component of the mPTP. ANT functions as a pore between two extreme conformations, in which the binding sites of the substrate are on cytosolic side of the inner membrane

- *c conformation* - or on the matrix side - *m conformation*. The conformation *c* is likely to change with the binding of Ca^{2+} , thus inducing MPT; while this does not apply for the conformation *m* of ANT.

Classically, the ANT was suggested to be the membrane component of the MPT and to exert its pore-forming function by interacting with VDAC at mitochondrial contact sites, a scheme originally proposed by the group of Halestrap (Halestrap and Davidson, 1990). However, this model has come under doubt as a result of studies demonstrating that cyclosporin-sensitive mPTP formation could occur in the absence of ANT (Bauer et al., 1999). The ANT has been ruled out as an assembling component of the pore (Kokoszka et al., 2004); using mice in which ANT is not expressed, it has been shown that it does not significantly alter MPT, thus raising doubts about ANT's identity and if it is a necessary component of the mPTP. However, the same group has demonstrated that even though ANT1 might not be a component of the mPTP *per se*, it can control susceptibility to MPT induction. Nevertheless, the ANT2 isoform has been shown to be expressed in cancer cells that display enhanced glycolysis and in such cells a large proportion of hexokinase II is bound to the mitochondria (Chevrollier et al., 2005). A hypothesis that could account for these effects proposes that CypD stabilizes the interaction between ANT and the oligomeric form of VDAC that is enhanced by hexokinase II binding (Pastorino and Hoek, 2008).

Attention to ANT and its implication in MPT has been renewed due to recent and unrelated findings: i) the polyclonal antibody used to identify a protein that binds CypD was originally deemed as ANT1, but in fact was the phosphate carrier (Leung et al., 2008; Leung and Halestrap, 2008), and ii) the ANT of the embryos of a crustacean in which mitochondrial mPTP is absent, is refractory to bongkreic acid (Konr d et al., 2011), a well-established ANT inhibitor, also known to suppress PTP (Klingenberg, 2008). Regardless of the fact that liver mitochondria isolated from mice lacking ANT1 and ANT2 isoforms still exhibited the mPTP (Kokoszka et al., 2004), evidence that the ANT may be regulating mPTP opening through interactions with the phosphate carrier and perhaps the F₀-F₁-ATP synthase, are likely to emerge (Chinopoulos and Adam-Vizi, 2012).

Cyclophilin D (CypD)

Cyclophilins are a family of proteins that catalyze the *cis/trans* isomerization of peptidic bonds. CypD is a water-soluble protein (18kDa) that is ubiquitously located predominantly in the mitochondrial matrix. Its association facilitates a conformational change in the ANT, probably promoting MPT. Indeed, CypD is a known activator of the mPTP as its inhibition by CsA leads to closure of the pore (Broekemeier and Pfeiffer, 1989; Broekemeier et al., 1992). Therefore, it is classically assumed that suppression of the ANT-CypD interaction may contribute to the elevation of the threshold for MPT induction.

Nevertheless, CypD has already been shown dispensable for mPTP assembly (Baines et al., 2005; Nakagawa et al., 2005; Schinzel et al., 2005; Basso et al., 2005), but is involved in open/closed mPTP probability (Giorgio et al., 2010; Azzolin et al., 2010; Doczi et al., 2011). CypD is a member of the cyclophilins family encoded by the *ppif* gene (Wang and Heitman, 2005), that exhibit peptidyl-prolyl *cis/trans* isomerase activity. Inhibition of *cypD* by cyclosporin A (CsA), or genetic ablation of the *ppif* gene (Baines et al., 2005; Nakagawa et al., 2005; Schinzel et al., 2005; Basso et al., 2005; Basso et al., 2008) negatively affect mPTP opening probability. However, it is not clear if the *cis/trans* peptidyl prolyl isomerase activity is a prerequisite for promoting MPT (Lin and Lechleiter, 2002). Furthermore, CypD knockout mice do not exhibit a severe phenotype; instead, these mice exhibit enhanced anxiety, facilitation of avoidance behavior, occurrence of adult-onset obesity (Luvisetto et al., 2008) and a defect in platelet activation and thrombosis (Jobe et al., 2008). These mice also exhibit limited metabolic flexibilities in the heart, due to alterations in mPTP-mediated Ca^{2+} efflux mechanisms during cardiovascular stress (Elrod et al., 2010).

Cyclophilin-D-depleted mitochondria still undergo a calcium-induced permeability transition, but this phenomenon requires higher calcium concentrations and is insensitive to CsA (Basso et al., 2005). These observations reinforce the notion that CypD is an important regulator of the mPTP but also refute the notion that this protein might be a structural component of the pore (Kinnally et al., 2011).

Yet it was recently postulated that CypD favors the open conformation

of mPTP by masking a specific site for inorganic phosphate (Pi); the occupancy of this site by Pi leads to a desensitization of the mPTP to calcium (Basso et al., 2008). In the absence of CypD, the mPTP still forms and opens in response to some challenges, but is not responsive to Ca^{2+} or inhibition by CsA. Additionally, the effects of knockout of CypD established that opening of the mPTP was essential for mitochondrial injury in necrotic cell death but dispensable for mitochondrial mediation of apoptosis (Pastorino and Hoek, 2008).

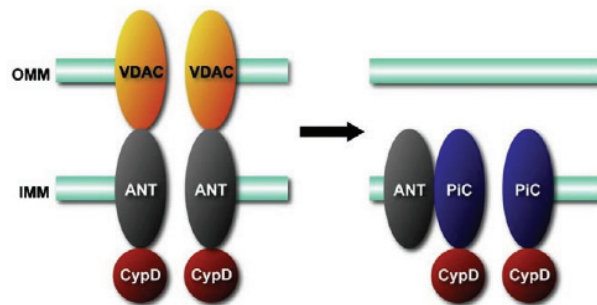


Figure 1.2.8 – Molecular models for the mitochondrial permeability transition pore (mPTP).

Left, The original model for the mPTP, consisting of the voltage-dependent anion channel (VDAC) in the mitochondrial outer membrane (MOM), the adenine nucleotide translocase (ANT) in the mitochondrial inner membrane (MIM), and cyclophilin-D (CypD) in the matrix. Right, Revised models in light of recent findings in gene-targeted mice. VDAC is no longer part of the model and it appears that an outer membrane component may not even be necessary for this process. ANT now appears to be more of a regulatory protein, and only CypD remains as an established component. In contrast, the mitochondrial phosphate carrier (P_iC) has been added to model as a potential candidate for the pore-forming unit of the MPT pore. From Baines, 2009.

Mitochondrial phosphate carrier (P_iC)

More recently, the phosphate carrier was proposed to play a central role in the MIM pore of mPTP (Halestrap, 2009).

Functional support was provided to the role of P_iC as a MTP

component by demonstrating that agents able to inhibit mitochondrial P_i transport activity also blocked MPT in isolated mitochondria. It has also been shown that the mitochondrial phosphate transporter forms a complex with CypD. MPT-inducing agents enhance P_iC –CypD interaction, whereas MPT-blocking compounds reduce it. Halestrap's group proposed a new MPT model consisting of P_iC and ANT, of which Ca^{2+} sensitivity is regulated by CypD binding to P_iC and by oxidant stress-induced dithiol cross-links within P_iC and ANT molecules.

While intriguing, the role of the P_iC in the elusive mPTP awaits more conclusive molecular studies in which the effects of eliminating the various isoforms of this carrier on the mPTP characteristics are determined.

1.2.3.2. Regulation of mPTP

Studies from different groups have questioned the molecular identity of the mPTP. A number of genetic studies have excluded VDAC (Baines et al., 2007) and ANT (Kokoszka et al., 2004) as essential structural components of the mPTP complex. As portrayed above, a new model of the mPTP consisting of phosphate carrier and ANT has been proposed where Ca^{2+} sensitivity of the pore is regulated by CypD binding to a phosphate carrier (Leung et al., 2008) (Figure 1.2.9). Many studies have provided strong evidence that CypD plays a major regulatory role in mPTP formation (Basso et al., 2005; Baines et al., 2005; Nakagawa et al., 2005). Although cytoplasmic cyclophilins such as CypA are involved in cell signaling and protein folding as chaperones (Min et al., 2005), the role of mitochondrial CypD under normal conditions remains unclear. One of the functions of CypD may be formation of the mPTP with a low conductance to regulate the ion homeostasis in the mitochondrial matrix under physiological conditions. Mitochondria isolated from CypD knockout mice were desensitized to onset of the MPT, and required much higher concentrations of Ca^{2+} to induce pore opening compared to wild type animals, which is consistent with the role of CypD to regulate Ca^{2+} -mPTP interactions. High matrix phosphate levels that compete for the nucleotide-binding site of ANT favor pore opening. The conformational state of the ANT is affected by

specific ligands of the exchanger such as carboxyatractyloside (CAT) and bongkreikic acid (BKA), that respectively decrease and increase matrix ADP binding affinity, thereby leading to the opening and closing of the mPTP. mPTP opening is inhibited by H^+ and divalent cations (Mg^{2+} , Mn^{2+} , Sr^{2+}) that antagonize Ca^{2+} binding to ANT (Bernardi et al., 1992). The conformational state and pore forming activity of mPTP compounds are also regulated by hexokinase (HK), the peripheral benzodiazepine receptor (PBR) and Bcl2 proteins on the MOM where they bind to VDAC, and creatine kinase (CK) in the intermembrane space interacting with ANT (Azarashvili et al., 2010; Ricchelli et al., 2011; Javadov et al., 2011; Sileikytė et al., 2011; Bernardi and Stockum, 2012).

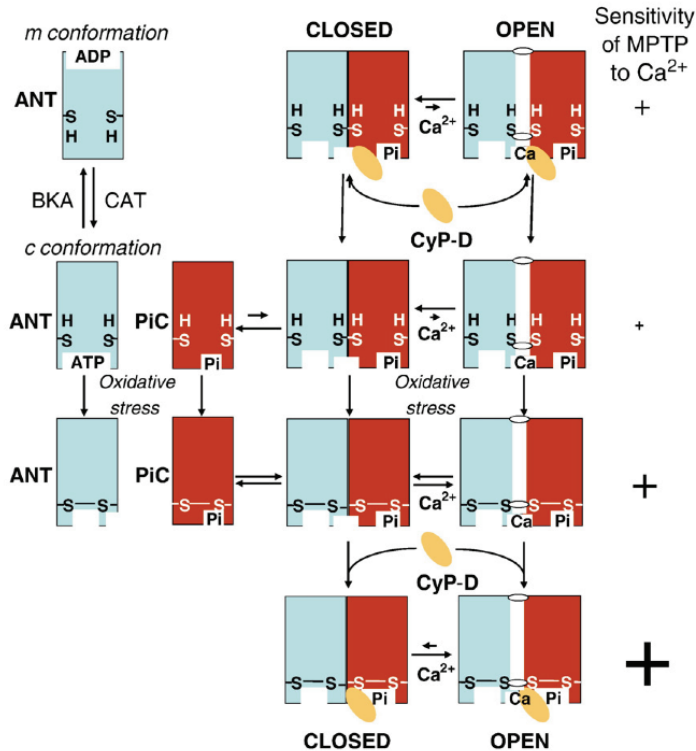


Figure 1.2.9 – Working model for mPTP opening modulation.

A scheme representing how the PiC, ANT and CypD may interact to form the mPTP and account for the effects of Ca^{2+} , oxidative stress and ligands of the ANT on mPTP opening. From Halestrap, 2009.

1.2.3.3. Physiological role of mPTP

It is clear that a prolonged opening of a number of pores, or the simultaneous opening of many pores, would deenergize and inactivate mitochondria rapidly, and it may be that such an event is associated with the irreversible breakdown of $\Delta\Psi_m$ observed in the course of apoptosis (Figure 1.2.10). However, at this time it is still a matter of much speculation as to whether the MPT makes a significant contribution to mitochondrial activities under physiological conditions and the precise metabolic role of mPTP formation is still being debated. It could be imagined as a safety valve under stressful conditions (Lemasters et al., 2009); for example the low-conductance state of the pore allows fine dissipation of mitochondrial membrane potential, preventing mitochondrial ROS generation that is due to mitochondrial hyperpolarization. However, the lack of specificity for any small-molecular-weight solute prohibits any fine-tuning for specific ions or solutes.

While there is no consensus on the physiological role of the MPT, a number of feasible suggestions have been made. Among these are that the MPT provides a way of clearing the mitochondrial matrix of damaged or unneeded molecules (Gunter and Pfeiffer, 1990), that the MPT provides an important pathway for inducing apoptosis in cells in which certain types of damage have occurred (Kroemer et al., 1997), and that the MPT provides a way of getting rid of damaged mitochondria (Lemasters et al., 2002). MPT is also likely to contribute to regulation of mitochondrial matrix volume pH and redox reactions (Di Lisa and Bernardi, 2009), and to provide a pathway for the rapid exchange of pyridine nucleotides (PN) across the MIM (Bernardi et al., 1994). Through this pathway PN synthesized in the cytosol would be rapidly available for intramitochondrial steroidogenesis (Pfeiffer and Tchen, 1975), while the efflux of PN stored in the matrix would provide the necessary substrates to poly-ADP ribose polymerase for DNA repair (Di Lisa and Ziegler, 2001). In addition, it might operate as a regulator of mitochondrial Ca^{2+} ; low conductive MPT-induced matrix swelling and increased mitochondrial Ca^{2+} can regulate ATP synthesis through the tricarboxylic acid cycle, electron transport chain and oxidative phosphorylation (Javadov et al., 2011).

Induction of MPT in response to pathological stresses can also be regulated with the signaling protein kinases PKA, PKC and GSK-3 β which interact with VDAC (Baines et al., 2003; Javadov et al., 2009). Expression of the major components (ANT, VDAC, CypD) and regulatory proteins (HK, PBR, Bcl2, CK) of the mPTP complex are presumed to play, along with metabolic and signaling factors, a key role under continuous pathological conditions such as carcinogenesis. Furthermore, unlike cardiac I/R, induction of MPT can differ among various cancer diseases in a tissue/organ/cell-specific manner (Javadov et al., 2011).

Undoubtedly, in the cardiovascular field the major focus has been mPTP involvement in myocardial I/R injury, a topic that has been covered by numerous studies (Halestrap et al., 2004; Baines et al., 2005; Di Lisa and Bernardi, 2006; Murphy and Steenbergen, 2008). The mPTP is now generally considered as the common target of different pathways set in motion by insufficient oxygen availability. In particular, the intracellular milieu created by post-ischemic reperfusion appears optimal for mPTP opening, especially because of intracellular [Ca²⁺] elevation concomitant with accumulation of ROS (Halestrap et al., 2007; Di Lisa et al., 2007). These notions were established based upon direct evidence of mPTP opening in isolated cells and intact hearts (Griffiths and Halestrap, 1995; Petronilli et al., 1999; Di Lisa et al., 2001). In addition, pharmacological and genetic approaches were successfully exploited to demonstrate that mPTP inhibition results in cardioprotection (Hausenloy and Yellon, 2003; Piot et al., 2008; Di Lisa and Bernardi, 2009). Decreased susceptibility to mPTP opening appears to be also involved in endogenous mechanisms of cardioprotection, such as those elicited by ischemic pre- and post-conditioning (Hausenloy et al., 2004; Argaud et al., 2005; Meier et al., 2005). Of note, so far mPTP-dependent cardioprotection has been obtained exclusively by targeting CypD (Basso et al., 2005; Bernardi et al., 2006). Given that the modulatory power of CypD (and therefore of CsA) is limited; and that the mPTP can open in the presence of CsA (and in the absence of CypD), it is likely that further insights into the role of mPTP in myocardial I/R injury will be provided when direct inhibitors of the mPTP will become available. Yet, and most importantly, mPTP desensitization by CsA has been reported to afford cardioprotection in clinical

settings (Piot et al., 2008; Gomez et al., 2009). Not only do these reports highlight the relevance of mPTP as a therapeutic target; they also provide clinical demonstration of the cardioprotective efficacy of pharmacological interventions aimed at preventing mitochondrial dysfunction caused by I/R.

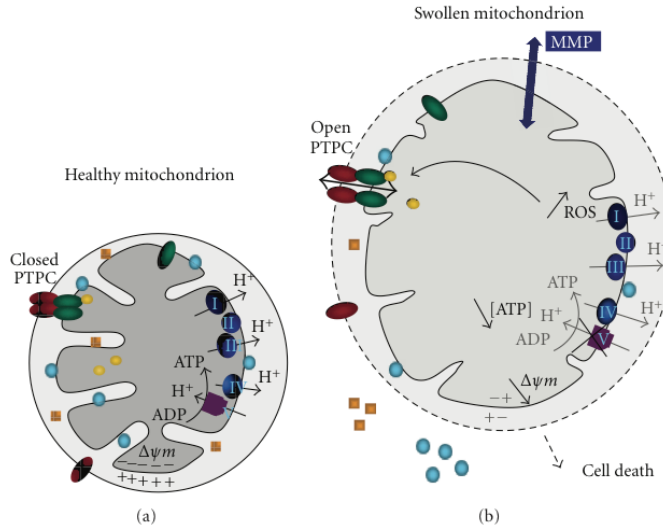


Figure 1.2.10 – Scheme of mitochondrial alterations following mitochondrial membrane permeabilization (MMP).

In response to the opening of the mPTP (green and red ellipses, corresponding to ANT and VDAC respectively in this model), swollen mitochondria exhibit an increase in volume, a more translucent matrix with less cristae and a permeabilized outer membrane. Cytochrome *c* and apoptosis-inducing factor (AIF) (blue circles and yellow squares), normally confined into the intermembrane space, are released through ruptures in the outer membrane. The transmembrane inner potential ($\Delta\Psi_m$) is dissipated in response to the arrest of the function of the respiratory complexes, which contributes to an inhibition of ATP biosynthesis. Altogether, these alterations are lethal, irreversible and lead to cell death. From Martel et al., 2012.

1.2.4. Calcium homeostasis

Ca^{2+} has long been recognized as a fundamental second messenger involved in learning, memory, fertilization, proliferation, development, muscle

contraction and secretion. Its concentration in the cytosol varies dynamically under the tight control of coordinated homeostatic mechanisms and complex interactions among pumps, channels, exchangers and binding proteins, and relatively small and/or local changes in its concentration modulate a wide range of intracellular actions.

The main driving force for Ca^{2+} accumulation across the inner mitochondrial membrane is the electrochemical gradient established and maintained by the respiratory chain. Indeed, respiring mitochondria maintain a membrane potential which constitutes a strong driving force for Ca^{2+} influx into the matrix. Applying the Nernst equation, thermodynamic equilibrium for Ca^{2+} ($\Delta\mu_{\text{Ca}} = 0$) would be reached at Ca^{2+} concentrations 106 higher than in the cytoplasm. Conversely, experimental evidence demonstrates that, in resting conditions, $[\text{Ca}^{2+}]_m$ is similar to $[\text{Ca}^{2+}]_c$, reinforcing the idea that mitochondria do not act as a Ca^{2+} store, and that Ca^{2+} distribution is modulated by kinetic rather than simply thermodynamic parameters. In other words, Ca^{2+} concentrations in the mitochondrial matrix are controlled by low affinity uptake pathways and by efflux mechanisms that re-extrude Ca^{2+} , at the cost of a significant futile cycle across the inner membrane. Influx is mainly supported by a Ca^{2+} electrophoretic mechanism (“uniporter”) whereas the $\text{Na}^+ - \text{Ca}^{2+}$ and $\text{Na}^+ - \text{H}^+$ exchangers are responsible for Ca^{2+} efflux. While the activities of the exchangers tend to saturate when $[\text{Ca}^{2+}]_m$ increases, the uniporter is a channel and does not saturate. A direct consequence of this transport system is that, when $[\text{Ca}^{2+}]_m$ increases above a certain threshold, mitochondria have to cope with the risk of Ca^{2+} overload. Avoiding mitochondrial Ca^{2+} overload is energetically demanding for the cell, which has evolved a number of transport mechanisms to rationalize the system and adapt it to varying conditions of energy expenditure (Figure 1.2.11).

The mitochondrial Ca^{2+} uniporter (MCU) is a channel, which transports Ca^{2+} , Sr^{2+} , but not Mg^{2+} with different selectivity and very low affinity. Several modulators of the MCU have been identified, including ruthenium red, an allosteric inhibitor, and divalent cations that do not permeate through the channel, such as Mn^{2+} , Ba^{2+} and lanthanides. Several estrogen receptors ligands have also been shown to modulate the activity of the uniporter. The molecular structure of this transporter remains elusive but various hypotheses

have been proposed over the years, starting in the 1970's when purification was first attempted. A highly selective Ca^{2+} channel activity with kinetic and pharmacological characteristics of the mitochondrial uniporter has been identified and characterized from the electrophysiological point of view and recent studies have also showed an important role of UCP2 and UCP3 in mitochondrial Ca^{2+} uptake.

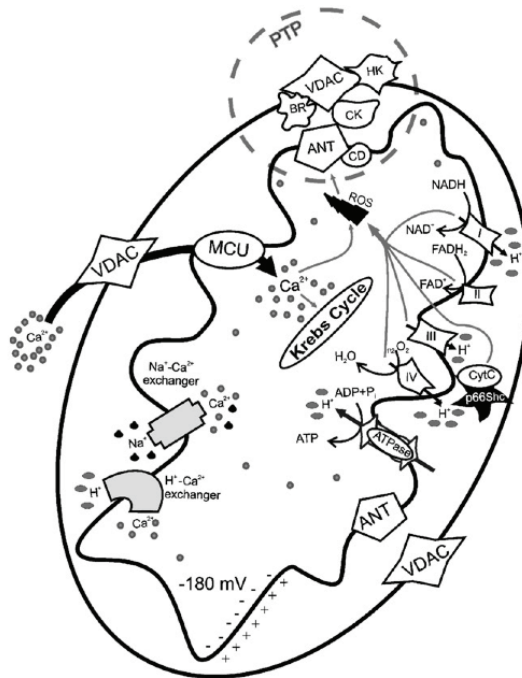


Figure 1.2.11 – Mitochondrial physiology and mitochondrial Ca^{2+} handling.

Ca^{2+} enters in the mitochondrial matrix via a low affinity uniporter (MCU) and through a high electronegative potential. Extrusion of Ca^{2+} takes two major routes, one driven by the Na^+ / Ca^{2+} exchanger, and another pathway which involves the H^+ - Ca^{2+} exchanger. In the matrix, Ca^{2+} stimulates the activity of three Ca^{2+} -sensitive dehydrogenases of the Krebs cycle. VDAC: voltage-dependent anion channel, ANT: adenine nucleotide translocase, HK: hexokinase, CD: cyclophilin D, CK: creatine kinase, BR: benzodiazepine receptor, PTP: permeability transition pore. From Giorgi et al., 2012.

1.3. Mitochondria and cell death

Mitochondria play a pivotal role in the process of cell death. It has been generally accepted that cells die by necrosis when ATP is not sufficient, or they die by the process of apoptosis when sufficient ATP is available. Apoptosis (programed cells death) is a process coordinated by a family of proteases – the caspases, which participate in the molecular control of apoptosis as triggers of cell death and as regulatory elements within this process. Excessive accumulation of Ca^{2+} leads to the formation of reactive oxygen species (ROS) and to opening of the mitochondrial permeability transition pore (mPTP), which depolarizes the mitochondria and leads to mitochondrial swelling. This may also provide a mechanism for the release of cytochrome *c* from the intermembrane space into the cytoplasm. Cytochrome *c* normally functions as a part of the respiratory chain, but when released into the cytosol it becomes a critical component of the apoptosis execution machinery, where it activates caspases and causes apoptotic cell death. Apoptosis may be triggered by extracellular signals (extrinsic pathway) or by intracellular processes (intrinsic pathway) (Figure 1.3.1). An increased mitochondrial formation of ROS triggers the intrinsic pathway by opening permeability transmission pores with increased permeability of the outer mitochondrial membrane.

1.3.1. Mitochondria in apoptosis

Two main features characterize mitochondrial involvement in apoptosis: the release of effector proteins from the IMS and the initiation of a programme of mitochondrial dysfunction, that includes loss of mitochondrial membrane potential ($\Delta\Psi_m$) (Bernardi et al., 2001). Underlying molecular mechanisms and a putative crosstalk between these two events are still under investigation.

A reservoir of proteins involved in amplification of apoptosis localizes to the IMS of mitochondria. Among them, SMAC/ DIABLO and OMI/HTRA2 enhance caspase activation through the neutralization of proteins that inhibit

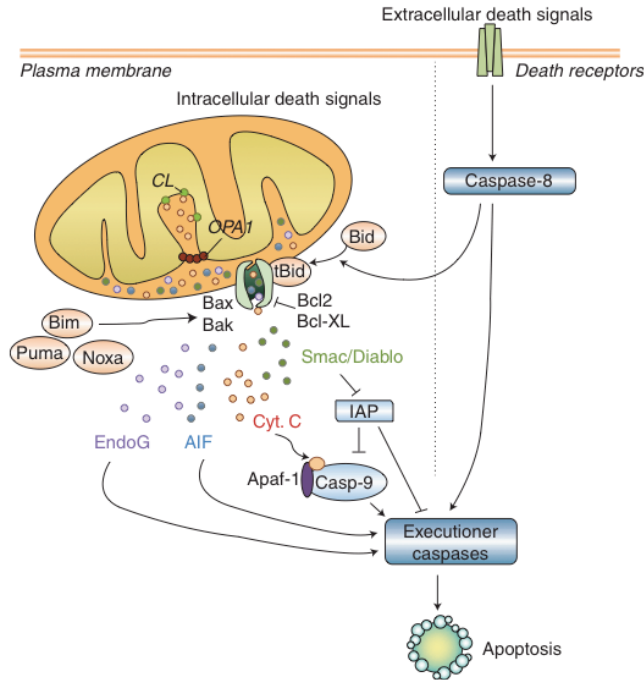


Figure 1.3.1 – Mitochondrial-dependent apoptosis.

Apoptosis can result from the activation of two distinct molecular cascades, known as the extrinsic (or death receptor) and the intrinsic (or mitochondrial) pathways. Both pathways, which can converge at the level of mitochondria, involve the activation of initiator caspases (caspase-8 and -9, respectively) that catalyze the proteolytic maturation of downstream executioner caspases, such as caspase-3, which are the final effectors of cell death. Mitochondrial outer membrane permeabilization (MOMP) represents the point-of-no-return in the mitochondrial apoptotic pathway. Following MOMP, mitochondrial apoptogenic factors such as cytochrome c, Smac/Diablo, endonuclease G, or apoptosis-inducing factor (AIF) are released to the cytosol. Once into the cytosol, these factors can initiate cell death in a caspase-dependent or a caspase-independent manner. MOMP is highly regulated by anti-apoptotic (e.g., Bcl-2 and Bcl-xL) and pro-apoptotic (e.g., Bax and Bak) protein members of the Bcl-2 family. AIF, apoptosis-inducing factor; Casp-9, caspase-9; CL, cardiolipin; OPA1, optic atrophy type 1; Cyt. c, cytochrome c; EndoG, endonuclease G; IAP, inhibitor of apoptosis; tBid, truncated Bid. From Perier and Vila, 2012.

caspses (Du et al., 2000; Verhagen et al., 2000); and Endonuclease G (Li et al., 2001; van Loo et al., 2001) and apoptosis-inducing factor (AIF) (Susin et al., 1999) have been proposed to play a role in caspase-independent cell death. A central player in caspase activation released by mitochondria upon an apoptotic stimulus is cytochrome *c* (Liu et al., 1996). The MOM was shown to be impermeable to cytochrome *c* (Wojtczak et al., 1972); thus, in order to release cytochrome *c*, the MOM must change its permeability properties. This process is named MOM permeabilization and could explain the egress of cytochrome *c* from mitochondria. Although the precise mechanism of this event is still a matter of debate, it appears clear that Bcl2 family proteins are critical regulators. In addition to MOM permeabilization, complete release of cytochrome *c* during apoptosis requires cristae remodeling (Scorrano, 2009).

Once released, cytosolic cytochrome *c* in a complex together with APAF1, dATP and ADP forms the apoptosome, which recruits procaspase-9, facilitating its auto-activation. Caspase-9 activates downstream executioner caspases (Zou et al., 1997; Thornberry and Lazebnik, 1998) that cleave other intracellular substrates leading to the characteristic morphological changes in apoptosis such as chromatin condensation, nucleosomal DNA fragmentation, nuclear membrane breakdown, externalization of phosphatidylserine (PS) and formation of apoptotic bodies (Hengartner, 2000).

1.4. Mitochondrial shape and dynamics

Mitochondrial shape is very heterogeneous, ranging from small spheres to interconnected tubules (Bereiter-Hahn and Vöth, 1994). For example, the mitochondria of rat cardiac muscle and diaphragm skeletal muscle appear as isolated ellipses or tubules in embryonic stages but then reorganize into reticular networks in the adult (Bakeeva et al., 1978). The name of the organelle, “mitochondrion”, reflects their heterogeneous morphology, a combination of the Greek words for “thread” and “grain”. During cell life, mitochondria undergo continuous cycles of fusion and fission (Figure 1.4.1). Therefore, mitochondria are now recognized as highly dynamic organelles that move throughout a cell and constantly fuse and divide (Chen

and Chan, 2010). Studies over the last several years indicate that these membrane remodeling processes promote homogenization of the mitochondrial population by content mixing and thereby preserve mitochondrial function (Detmer and Chan, 2007; Chen and Chan, 2009). Mitochondrial fusion is clearly an important physiological activity; mutations in fusion genes in humans cause neurodegenerative diseases, and mice with reduced mitochondrial fusion show severe defects in multiple cell types (Chen and Chan, 2009; Chen and Chan, 2010).

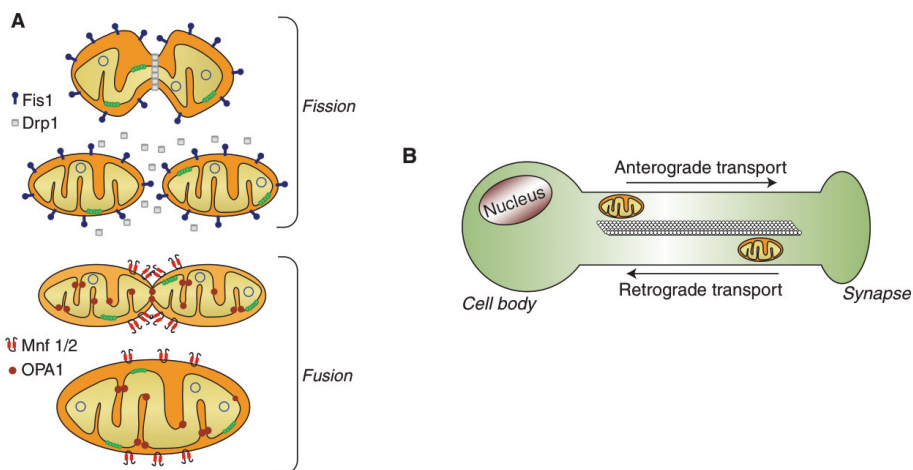


Figure 1.4.1 – Mitochondrial dynamics.

(A) Mitochondrial fusion and fission control mitochondrial number and size. Fission is mediated by dynamin-related protein 1 (Drp1) and mitochondrial fission-1 protein (Fis1). Mitofusins (Mnf) 1 and 2 are involved in the fusion of the MOM, whereas protein optic atrophy type 1 (OPA1) regulates the fusion of the MIM. **(B)** In neurons, mitochondria are recruited to subcellular compartments distant from the cell body, such as axons and dendrites, by active transport along microtubules and actin filaments. Distinct molecular motors transport the mitochondria in anterograde or retrograde directions. From Perier and Vila, 2012.

Real-time imaging reveals that individual mitochondrial tubules continually move back and forth along their long axes on radial tracks. Occasionally, two mitochondrial tubules encounter each other and fuse (Chen

et al., 2003). On the other hand, these tubules can also undergo fission events, giving rise to two or more mitochondrial units. It was reported, in pancreatic β -cells, that fusion and fission events are paired. Fusion triggers fission, but fission has no effect on the following fusion event (Twig et al., 2008)

In addition to complete fusion, a transient form of fusion was recently identified in which two mitochondria come into close apposition, exchange soluble IMS and matrix proteins, and separate, maintaining the original morphology. Transient fusion, called “kiss-and-run”, has been shown to support mitochondrial motility and metabolism; the phenomenon of transient fusion provides an efficient recharging mechanism by allowing rapid equilibration of the soluble IMS and matrix proteins and probably, smaller molecules including mRNA between the organelles. Since a short-term decrease in the $\Delta\Psi_m$ does not seem to prevent transient or complete fusion, these processes may provide a means to rescue the function of organelles that ran short in some components (Liu et al., 2009).

Research on mitochondrial fusion and fission (collectively termed mitochondrial dynamics) gained much attention in recent years, as it is important for our understanding of many biological processes, including the maintenance of mitochondrial functions, apoptosis and ageing (Detmer and Chan, 2007; Westermann, 2010) (Figure 1.4.2). Being the mitochondria bordered by two membranes, any mechanism of fusion and fission must take into account that the coordinate fusion/ division of four lipid bilayers is required. Thus, mitochondrial fusion and fission are complicated processes that are controlled by a growing number of mitochondrial-shaping proteins. The core components of the fusion machinery in mammals are mitofusin 1 and mitofusin 2 (MFN1 and MFN2), responsible for outer membrane fusion (Koshiba et al., 2004; Meeusen et al., 2004), and also optic atrophy protein 1 (OPA1), involved in inner membrane fusion (Olichon et al., 2003; Landes et al., 2010). Regarding mitochondrial fission machinery, the core components are dynamin-related protein 1 (DRP1/DLP1), involved in outer membrane division (Smirnova et al., 1998; Westermann, 2010), and mitochondrial fission 1 (Fis1), the outer membrane receptor for recruitment of DRP1 (James et al., 2003; Zhang and Chan, 2007). Mutations in two of the mitochondria shaping

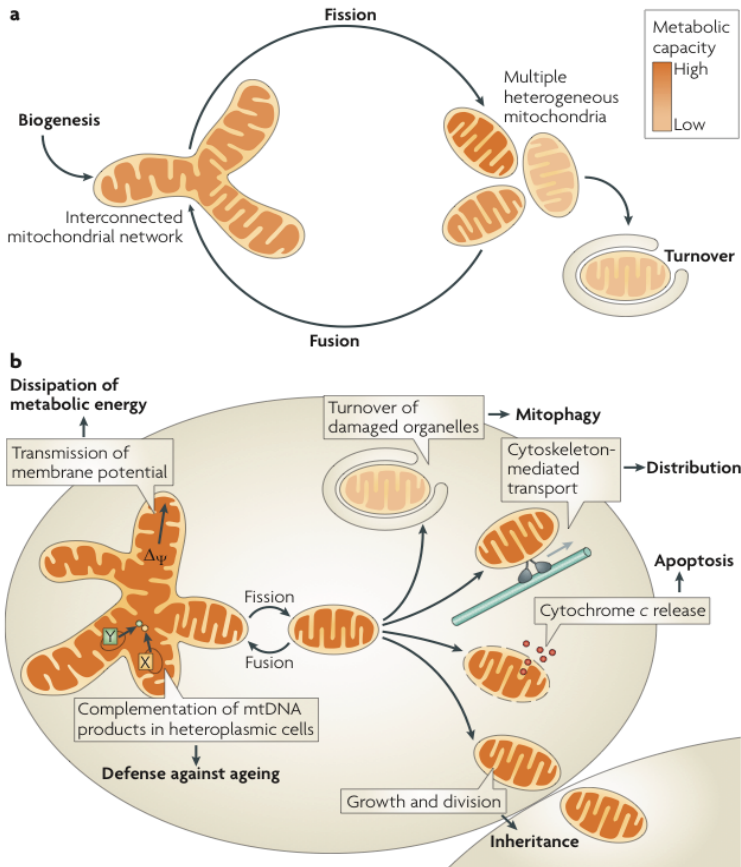


Figure 1.4.2 – Biological functions of mitochondrial dynamics.

a - The mitochondrial life cycle starts with growth and division of pre-existing organelles (biogenesis) and ends with degradation of impaired or surplus organelles by mitophagy (turnover). In between, mitochondria undergo frequent cycles of fusion and fission that allow the cell to generate multiple heterogeneous mitochondria or interconnected mitochondrial networks, depending on the physiological conditions.

b - Fusion and fission of mitochondria are important for many biological functions. Division is required for inheritance and partitioning of organelles during cell division, for the release of pro-apoptotic factors from the intermembrane space, for intracellular distribution by cytoskeleton-mediated transport and for turnover of damaged organelles by mitophagy. Fused mitochondrial networks are important for the dissipation of metabolic energy through transmission of membrane potential along mitochondrial filaments and for the complementation of mtDNA gene products in heteroplasmic cells to counteract decline of respiratory functions in ageing (X and Y depict alleles of different mitochondrial genes). Westermann, 2010.

proteins have been causally linked to familial neurodegenerative diseases. Whereas autosomal-dominant MFN2 mutations pathogenically underlie Charcot-Marie-Tooth Disease type 2A (CMT2A) (Züchner et al., 2004; Oettinghaus et al., 2011), a peripheral axonal neuropathy, OPA1 mutations lead to autosomal-dominant optic atrophy (ADOA) (Alexander et al., 2000; Delettre et al., 2000). In addition, the mitochondrial fission protein Drp1 can sporadically be affected by mutations in humans, as exemplified by the report of a lethal syndromic birth defect attributable to a heterozygous Drp1 mutation (Waterham et al., 2007). The dysregulation of mitochondrial dynamics (fusion and fission) has also been linked to other neurodegenerative conditions, including Alzheimer's, Huntington's and Parkinson's disease, as well as ischemic brain damage (Westermann, 2010; Reddy et al., 2011; Oettinghaus et al., 2011).

1.5. Autophagy

Autophagy, deriving from the Greek meaning “self-eating”, was first described by Christian de Duve in 1963 as a lysosome-mediated degradation process for non-essential or damaged cellular constituents (de Duve, 1963; de Duve and Wattiaux, 1966). It was mainly based on ultrastructural changes observed in rat liver after injection with glucagon. Glucagon results in an increase in cAMP levels, and, consequently, activation of PKA, that triggers autophagy in liver cells by a mechanism that is not yet fully understood.

Physiologically, autophagy serves to preserve the balance between organelle biogenesis, protein synthesis and their clearance. Autophagy is emerging as an important mediator of pathological responses and engages in cross-talk with ROS (reactive oxygen species) and RNS (reactive nitrogen species) in both cell signaling and protein damage (Lee et al., 2012).

Autophagy, a catabolic process conserved from lower to higher eukaryotes, is essential for recycling energy sources when cells have to deal with demanding conditions, as nutrient depletion and hypoxia, or during development. Cells increase the level of autophagy in response to other

environmental stresses, such as toxicants exposure, oxidative stress, pathogen infection, radiation or anticancer drug treatment. Additionally, a basal, constitutive level of autophagy plays a key role in the quality control maintenance inside the cell, being essential for the degradation of superfluous or damaged/old organelles as well as long-lived proteins and protein aggregates. Impaired mitochondrial function, oxidative stress, accumulation of protein aggregates and autophagic stress are common in many pathologies, including neurodegenerative diseases (Shacka et al., 2008; Schapira and Gegg, 2011).

Autophagy refers to any process of degradation of cytosolic components at the lysosome, embracing diverse pathways. Three autophagic pathways have been characterized based on the apparent differences observed in cargo delivery to the lysosome – macroautophagy, microautophagy and chaperone-mediated autophagy (CMA) (Figure 1.5.1). Summarily, during macroautophagy, a phagophore forms in the cytosol and expands into a double-membrane, engulfing cytosolic components, including proteins, lipid droplets, ribosomes and organelles and giving rise to the autophagosome. The external membrane of the autophagosome fuses with the lysosomal membrane, being the inner vesicle together with its cargo degraded. Resulting nutrients are recycled back to the cytosol, through membrane permeases.

Microautophagy differs from macroautophagy since cytosolic components are directly sequestered by the lysosome through an invagination of the lysosomal membrane. Degradation of soluble proteins and entire organelles by microautophagy has been described in yeast, where a group of proteins involved in microautophagy have been identified, some of which are in common with macroautophagy. On the other hand, our understanding of microautophagy in mammalian cells is poor.

CMA, a form of autophagy just described in mammals, mediates the translocation of soluble proteins from the cytosol to the lysosome, across a translocon-like complex in the lysosomal membrane. Proteins to be degraded by CMA are recognized by a chaperone of the HSP70 family in the cytosol. The complex chaperone-substrate binds to a receptor protein in the lysosomal

membrane, which moves the substrate into the translocation complex. Once in the lysosomal lumen, the substrates are rapidly degraded.

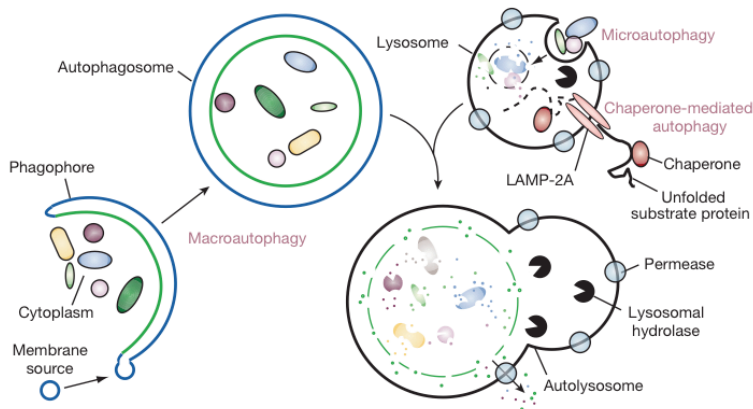


Figure 1.5.1 – Different types of autophagy.

Microautophagy refers to the sequestration of cytosolic components directly by lysosomes through invaginations in their limiting membrane. In the case of macroautophagy, the cargoes are sequestered within a unique double-membrane cytosolic vesicle, an autophagosome. Sequestration can be either nonspecific, involving the engulfment of bulk cytoplasm, or selective, targeting specific cargoes such as organelles or invasive microbes. Fusion of the autophagosome with a lysosome provides hydrolases. Lysis of the autophagosome inner membrane and breakdown of the contents occurs in the autolysosome, and the resulting macromolecules are released back into the cytosol through membrane permeases. CMA involves direct translocation of unfolded substrate proteins across the lysosome membrane through the action of a cytosolic and lysosomal chaperone hsc70, and the integral membrane receptor LAMP-2A (lysosome-associated membrane protein type 2A). From Mizushima et al., 2008.

Defining the stages of autophagy and its progress in a tissue or cell is important for understanding its function and regulation (Figure 1.5.2). Ultrastructural analysis by EM (electron microscopy) of autophagosomes at different stages of maturation has been the classic approach for confirming autophagic activities. EM can distinguish early autophagosomes or

phagopores, and amphisomes, from autolysosomes generated by fusion of amphisomes or autophagosomes fusing lysosomes (de Duve and Wattiaux, 1966).

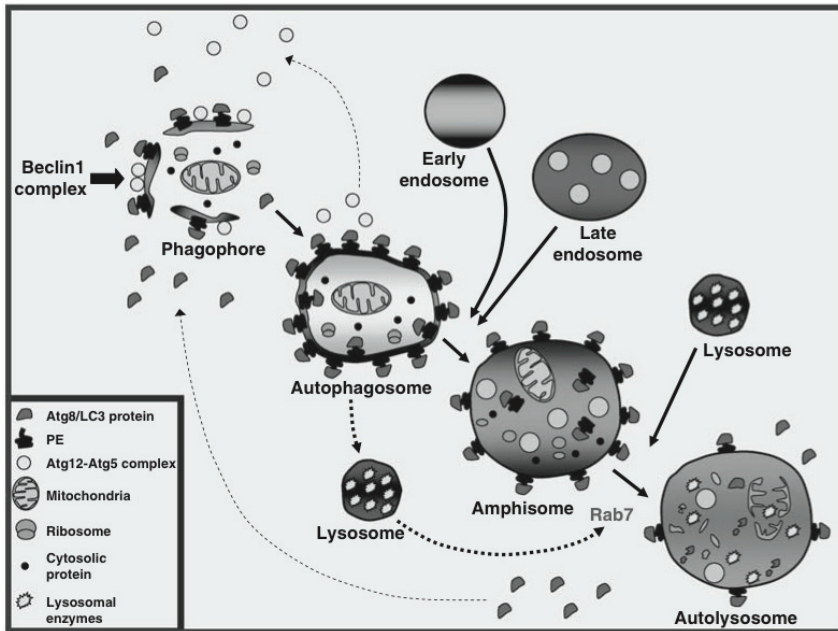


Figure 1.5.2 – The autophagic pathway.

The production of PI3P by the Beclin 1 complex is an early event in autophagosome formation that is necessary for the recruitment of certain Atg proteins to the phagophore or isolation membrane. Subsequently, the sequential recruitment of Atg12-Atg5 complex and Atg8-LC3 protein to the phagophore takes place. The cytosolic form of LC3, LC3-I, is covalently bound to phosphatidylethanolamine (PE), generating LC3-II, which binds to the autophagosomal membrane. The phagophore, a cup-shaped structure, encapsulates cytosolic proteins and organelles, forming a double-membraned structure termed autophagosome. At this point, most of the Atg proteins, except LC3-II, are recycled from the autophagosomal membrane back to the cytosol. Then, the autophagosome can fuse with endosomal compartments, generating the amphisome. The sequestered material is finally degraded by fusion of the amphisome with the lysosomal compartment, forming the autolysosome. Fusion of autophagosomes and amphisomes with the lysosomal compartment depends on an active Rab7. From Fader and Colombo, 2009.

Measuring the long-lived protein degradation rate by pulse–chase methods is also a commonly used complementary approach (Klionsky et al., 2008). These two methods have helped to determine autophagic pathways and time lapses during autophagy.

Another widely used tool for measuring autophagy is based on Atg8/LC3. Generation of the pre-autophagosomal structure requires the beclin-1–class III PI3K (phosphoinositide 3-kinase) complex, as well as generation and insertion of LC3 (light chain 3)-II into the autophagosomal membrane (Chen and Klionsky, 2011). Atg8/LC3 is a ubiquitin-like protein and it undergoes post-translational modifications when LC3-I becomes LC3-II (Kabeya et al., 2004; Tanida et al., 2004); this allows to discriminate the proteins by their difference in mobility on gel electrophoresis. LC3-II insertion into the autophagosomal membrane is a consistent key step in autophagosomal formation, and its level reflects the relative amount of autophagosomes in the cell. LC3-II protein can also be visualized by immunocytochemistry as vesicular puncta when associated with autophagosomes (Tanida et al., 2008).

1.5.1. Physiological functions of autophagy / Autophagy and disease

Autophagy is crucial for cell life. Indeed, autophagy is essential to maintain tissue homeostasis, due to its role in defending against metabolic stress, like, for instances, growth factor depletion, nutrient deprivation, hypoxia, ER stress and microbial infections.

In mammals, autophagy is indispensable for development and differentiation, at least at three different steps – pre-implantation development, survival to neonatal starvation and differentiation of erythrocytes, lymphocytes and adipocytes. Indeed, mouse models knockout for core Atg genes revealed embryonic or perinatal lethality.

A defect in autophagy can be retrieved in diverse pathological conditions (Figure 1.5.3). In particular, impairment of the autophagic activity

has been reported in neurodegenerative diseases, like Parkinson's disease, Huntington's disease and Alzheimer's disease. Decreased autophagic activity results in accumulation of aggregates formed by the mutated toxic proteins, a key feature of these diseases. Indeed, activation of autophagy was proven to be beneficial in animal models of Huntington's disease. In addition, defective activation of the autophagic programme has been recently reported to be pathogenic also in congenital muscular dystrophies linked to collagen VI deficiency. Again, forced activation of autophagy improved the dystrophic phenotype.

In addition, autophagy plays an important role in innate and adaptive immunity, probably having a major role in degradation of pathogens, for subsequent antigen presentation.

Autophagy and differentiation

Autophagy may help the cell to rapidly and efficiently change its cytosolic composition, accelerating routine protein and organelle turnover and modifying the cell's appearance in terms of exposed receptors, transcriptional factors present in the nucleus, and cytoskeletal dynamics. Likewise, autophagy can significantly influence cell-autonomous and/or regulated differentiation (Cecconi and Levine, 2008).

In the case of *becn1*^{-/-} mutant embryos, visceral endoderm development occurs, although cells seem to have an abnormal morphology and development is blocked after visceral endoderm formation (Yue et al., 2003). In specific stage of embryogenesis, the autophagosomes may selectively destroy subcellular structures or clusters of proteins, allowing a fast replacement by the protein synthesis apparatus that involves translation or translational control of mature mRNAs (Cecconi and Levine, 2008). Similarly, the brain patterning of *Ambra1* mutant embryos is dysregulated during neural tube differentiation at e10.5 (Fimia et al., 2007), with the morphogen sonic hedgehog (Shh) diffused in the area of the neural tube floor plate rather than concentrated in the notochord, which is related to impaired autophagosome formation mediated by *Ambra1*.

Autophagy genes could also play a role in the specification of the left-right axis. In vertebrates, left-right symmetry is determined in part by a flow of

Shh in the left cells of the node during gastrulation, inducing left-gene expression in the left part of the primitive streak. Interestingly, the factor UVRAG (another component of the dynamic Beclin 1/Vps34 complex) is mutated in a human case of abnormal left-right axis formation, resulting in heterotaxy and multiple malformations (Iida et al., 2000). This phenotype could also be related to an impairment of Shh distribution in the node, caused by a decreased rate of autophagosome formation and a defective cell makeover in those cells (Cecconi and Levine, 2008).

Autophagy and neurodegenerative disease

Early reports demonstrating that autophagosomes accumulate in the brains of patients with diverse neurodegenerative diseases, including Alzheimer's disease, transmissible spongiform encephalopathies, Parkinson's disease, and Huntington's disease (Rubinsztein et al., 2007; Levine and Kroemer, 2008), led to the initial hypothesis that autophagy contributed to the pathogenesis of these disorders. In mice with cerebellar degeneration due to mutations in glutamate receptor, autophagy was also postulated to be a mechanism of non-apoptotic cell death (Yue et al., 2002). In contrast, other studies provide compelling evidence that at least in model organisms autophagy protects against diverse neurodegenerative diseases and that the accumulation of autophagosomes primarily represents the activation of autophagy as a beneficial physiological response or, in the case of Alzheimer's disease, the consequence of a defect in autophagosomal maturation (Martinez-Vicente and Cuervo, 2007; Rubinsztein et al., 2007).

The development of neurodegenerative disease in patients with proteinopathies implies that the autophagy may reach a saturation point in which its capacity to degrade the mutant aggregate-prone proteins is exceeded, or that concurrent defects may occur in the autophagy pathway. Acquired defects in autophagosome formation may result from the sequestration of autophagy proteins in aggregates formed by mutant proteins, the age-related decline that occurs in Beclin 1 and potentially other autophagy protein expression in human brain, and other unidentified factors (Shibata et al., 2006). In addition to defects that result in decreased autophagic activity, genetic or functional alterations may occur that impair delivery of

autophagosomes to the lysosome. For example, mutations that affect the dynein motor machinery impair autophagosome-lysosome fusion, leading to decreased autophagic clearance of aggregate proteins and enhanced toxicity of the huntingtin mutant protein in *Drosophila* and mouse models (Ravikumar et al., 2005). Of long-term interest, both for the treatment of neurodegenerative diseases and, potentially, the prevention of aging, would be drugs that can reverse age-dependent declines that occur in CNS autophagy protein expression and lysosomal clearance of autophagosomes (Levine and Kroemer, 2008).

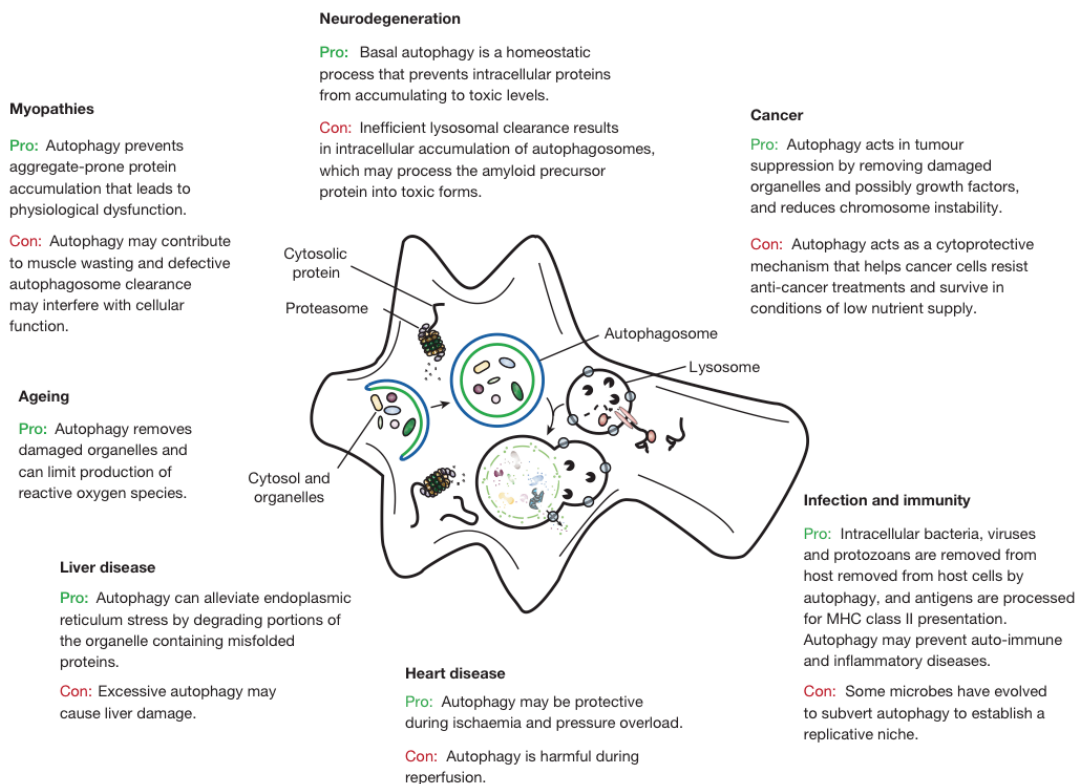


Figure 1.5.3 - The role of autophagy in human disease.

Degradation, in particular through autophagy and the proteasome, is important in cellular physiology. Autophagy can act as a cytoprotective mechanism to prevent various diseases, and dysfunctional autophagy leads to pathology. In some cases, however, autophagy can be deleterious; for example, some microbes subvert autophagy for replication, and the cytoprotective action can allow cancer cells to resist anti-cancer treatments. From Mizushima et al., 2008.

Autophagy and Liver Disease

Tissue-specific knockout studies in mice indicate an important role for basal hepatocyte autophagy in intracellular protein and organelle quality control. The protein quality-control function may be important in the pathogenesis of the most common genetic cause of human liver disease, α -1-antitrypsin deficiency, which is associated with chronic inflammation and carcinogenesis (Perlmutter, 2006). Perhaps, similar to neurodegenerative disorders caused by aggregate-prone proteins, pharmacological activation of autophagy may be helpful in these conditions. A toxic gain-of-function point mutation in α -1-antitrypsin Z (α -1-ATZ) impairs proper protein folding and renders a normally secreted hepatic protein prone to form aggregated polymers within the hepatocyte ER. Whereas wild-type α -1-antitrypsin is degraded primarily by the proteasome, mutant α -1-ATZ is thought to be degraded primarily by autophagy (Yorimitsu and Klionsky, 2007). In cell lines depleted of atg5, there is decreased degradation of the mutant α -1-ATZ, especially insoluble forms, and increased accumulation of cytoplasmic inclusion bodies (Kamimoto et al., 2006). A broader question of biomedical relevance is whether the protein quality-control function of autophagy plays a more general role in protecting the liver against alcohol and other hepatotoxic agents.

Autophagy and Muscle Disease

Similar to neurodegenerative diseases, the pathogenesis of myodegenerative diseases may involve either the failure of autophagosomes to fuse with lysosomes or the aggregation of misfolded proteins that exceed the autophagic clearance capacity of the myocyte. Danon disease, a genetic disease characterized by cardiomyopathy, myopathy, and variable mental retardation, results from a mutation in the lysosomal protein LAMP-2 and is associated with extensive accumulation of autophagosomes in the muscles of LAMP-2-deficient mice and patients (Levine and Kroemer, 2008). The concept that failure of lysosomes to fuse with autophagosomes contributes to myopathy is further supported by evidence that pharmacological inhibition of

this fusion step (e.g., with chloroquine or hydroxy-chloroquine) causes severe vacuolar myopathies in rats and humans (Bolaños-Meade et al., 2005).

There are several other histologically related diseases, such as X-linked myopathy with excessive autophagy, infantile autophagic vacuolar myopathy, adult-onset vacuolar myopathy with multiorgan involvement, and X-linked congenital autophagic vacuolar myopathy (Nishino, 2006); the prediction is that these disorders may be due, at least in part, to an impairment in autophagosome-lysosome fusion. Thus, a general theme seems to be emerging in diseases associated with aggregate-prone proteins not only in the brain but also in the liver and muscle; the autophagy pathway plays a central role in the clearance of such proteins, and pharmacologic upregulation of autophagy may protect against aggregate accumulation.

Autophagy and Cardiac Disease

Defective autophagy (due to impaired autophagosome-lysosome fusion) may play a role in relatively rare forms of inherited diseases of the heart (e.g., Danon disease, Pompe disease) (Levine and Kroemer, 2008). Of greater medical significance is the possibility that autophagy may constitute an important physiological or pathophysiological response to cardiac stresses such as ischemia or pressure overload, which are frequently encountered in patients with coronary artery disease, hypertension, aortic valvular disease, and congestive heart failure. The accumulation of autophagosomes has been noted in cardiac biopsy tissues of patients with these disorders, rodent models of these cardiac diseases, and isolated stressed cardiomyocytes (Terman and Brunk, 2005). Prior to genetic studies, it was largely assumed that autophagy invariably contributed to myocyte degeneration in such settings. However, more recent data challenge this view; the cytoprotective effects of autophagy (either via ATP production, protein and organelle quality control, or other mechanisms) may predominate in certain settings.

The cardiomyocyte, similar to the neuron, is a postmitotic cell in which basal autophagy may be important in protein and organelle quality control. Heart-specific knockout of *atg5* in adult mice results in cardiac hypertrophy and contractile dysfunction that is accompanied by increased levels of ubiquitinated proteins and ultrastructural evidence of sarcomere and

mitochondrial structural abnormalities (Levine and Kroemer, 2008). Beyond this need for autophagy under basal conditions, the heart may uniquely rely on stress- induced upregulation of autophagy to ensure the availability of energy substrates and to promote cellular remodeling.

Autophagy and Cancer

Several genetic links have emerged between autophagy defects and cancer, providing increasing support for the concept that autophagy is a bona fide tumor suppressor pathway (Mathew et al., 2007). The regulation of autophagy overlaps closely with signaling pathways that regulate tumorigenesis. Several tumor suppressor genes involved in the upstream inhibition of TOR signaling, including PTEN, TSC1, and TSC2, stimulate autophagy and, conversely, TOR-activating oncogene products such as class I PI3K and Akt inhibit autophagy (Levine and Kroemer, 2008). P53, the most commonly mutated tumor suppressor gene in human cancers, positively regulates autophagy in DNA-damaged cells, perhaps through AMPK activation of the TSC1/TSC2 complex and subsequent TOR inhibition or perhaps via upregulation of DRAM (damage-regulated autophagy modulator), a lysosomal protein that may induce autophagy (Feng et al., 2005; Crighton et al., 2006). The death-associated protein kinase (DAPk) also induces autophagy and apoptosis, is commonly silenced in human cancers by methylation, and has tumor and metastasis suppressor properties (Gozuacik and Kimchi, 2006). The cellular proto-oncoproteins, Bcl-2 and Bcl-XL, which are often overexpressed in human cancers, are generally thought to mediate oncogenesis by suppressing mitochondrial membrane permeabilization, one of the rate-limiting steps of apoptosis. In addition, ER-localized Bcl-2 and Bcl-XL inhibit autophagy by binding to the Beclin 1 autophagy protein (Maiuri et al., 2007). Thus, there is a strong correlation between molecules that are involved in autophagy induction and tumor suppression and between molecules that are involved in autophagy inhibition and oncogenesis.

Although it is presently unclear whether cell survival/cell death effects are relevant to the tumor suppressor role of autophagy, such effects are likely important in cancer therapeutics. A large series of clinically approved and experimental anticancer therapies induce the accumulation of

autophagosomes in tumor cell lines in vitro (Maiuri et al., 2007). For many years, it was thought that these therapies kill cells through autophagy (i.e., induce “autophagic cell death”). However, specific inhibition of autophagy with siRNAs targeted against ATG genes usually accelerates, rather than prevents, cell death in these settings, indicating that autophagy activation represents a cellular attempt to cope with stress induced by cytotoxic agents. This suggests that inhibition of autophagy (rather than stimulation of autophagy) might be beneficial in cancer treatment.

1.5.2. Selective autophagy

Initially, autophagy was believed to be a non-selective process, meaning that cytosolic components would be randomly surrounded by the autophagosome and broken down. However, it was observed in different studies that, under specific conditions, certain macromolecular components were preferentially delivered to the lysosome. Along the years, several examples of selective degradation have been revealed, as specific breakdown of aggregated proteins (Ravikumar et al., 2002), selective removal of superfluous or damaged organelles – like mitochondria (mitophagy) (Elmore et al., 2001), peroxisomes (pexophagy) (Sakai et al., 2006) and endoplasmic reticulum (ER-phagy) (Bernales et al., 2006) - and specific degradation of invading bacteria (Zheng et al., 2009).

Molecular mechanisms of selective autophagy have just started to be unveiled. Generally, a receptor protein, that is part or binds the cargo to be engulfed, interacts also with the autophagosomal membrane protein Atg8/LC3 and/ or an adaptor protein, as Atg11 in yeast, mediating the selective targeting of the cargo to the autophagosome. Receptor proteins for different cargoes have been revealed – for instances, Atg19, which acts as a receptor protein for the yeast Cvt pathway; Atg32, which functions as a receptor in yeast mitochondria; PpAtg30, in yeast peroxisomes; NIX, in mammalian mitochondria and p62, NBR1, two mammalian proteins that bind ubiquitinated substrates (Komatsu and Ichimura, 2010).

1.5.2.1. Mitophagy - Selective degradation of mitochondria

The term “mitophagy” was first introduced in 2005 (Lemasters, 2005), even if the first descriptions of mitochondria inside lysosomes date from about 40 years before. Engulfment of mitochondria together with other organelles by lysosomes in rat hepatocytes exposed to glucagon have been described in 1962 (Ashford and Porter, 1962).

Concomitant with energy production through oxidative phosphorylation in the mitochondria, this organelle generates ROS, causing protein, lipid and DNA oxidation and often inducing cell death. Therefore, quality control of mitochondria is essential for cellular homeostasis, and it is thought that such process is achieved through autophagy based on occasional identification of mitochondria surrounded by autophagosome and the presence of deformed mitochondria in autophagy-deficient cells.

Being crucial organelles for energy production, regulation of cell signaling and amplification of apoptosis (Rizzuto et al., 2000; Green and Kroemer, 2004), and simultaneously the major source of reactive oxygen species (ROS), that may cause oxidative damage to their own lipids, proteins and DNA (Scherz-Shouval and Elazar, 2011), mitochondrial quality control is crucial for the fitness of the cell. Mitophagy is believed to play a key role, being the prime mechanism to eliminate superfluous or damaged mitochondria (Michel et al., 2012). The critical role that autophagy plays in the maintenance of a “healthy” cohort of mitochondria was showed both in yeast (Zhang et al., 2007) and mammals (Twig et al., 2008). Yeast strains with ATG (autophagy-related) genes deletions are unable to degrade mitochondria during stationary phase, present growth defects in a non-fermentable carbon source and accumulate dysfunctional mitochondria. In accordance, ATG mutants present lower oxygen consumption rates, decreased mitochondrial membrane potential and higher ROS levels (Zhang et al., 2007). Similarly, mammalian cells deficient for ATG5 or treated with an inhibitor of autophagy – 3-MA – presented a reduction in maximal respiration (Twig et al., 2008).

In the last few years, mitophagy has been intensively studied. The accumulating evidences indicate that mitochondria can be selectively removed by autophagy and the signals that specifically target mitochondria to autophagy have started to be unraveled (Figure 1.5.4).

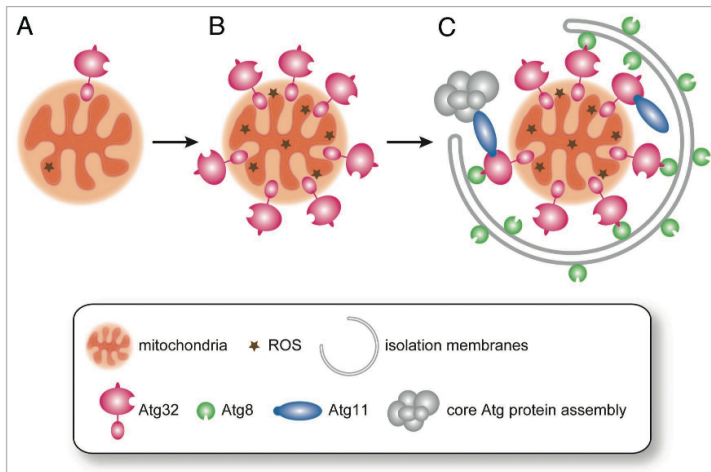


Figure 1.5.4 – A working model of Atg32-mediated mitophagy.

(A) Mitochondria in growing cells contain low levels of Atg32 and ROS, and mitophagy is hardly seen. (B) When cells accumulate high levels of ROS, Atg32 is strongly expressed in the cytosol, targeted to mitochondria, and inserted into the outer membrane. (C) Atg32 recruits Atg8 and Atg11 to the mitochondrial surface. Atg11 acts as a scaffold to facilitate assembly of core Atg proteins essential for autophagosome formation. Atg8, Atg11, and the assembled core Atg proteins cooperatively generate isolation membranes/phagophores enclosing mitochondria. From Okamoto et al., 2009.

1.6. Mitochondrial biogenesis and mitophagy: quality control and mitochondrial abundance regulation

The definition of “mitochondrial biogenesis” refers to both the formation of mitochondria during the cell cycle, the genesis of the organelle for normal turnover, as well as the phylogenesis and ontogenesis of mitochondria

(Michel et al., 2012). Some authors have classified the proposed theories on the biogenesis of mitochondria into three categories: (i) de novo synthesis of the organelle from sub-microscopic precursors present in the cytoplasm; (ii) formation from other membranous structures of the cell; (iii) growth and division of pre-existing mitochondria. The bulk of experimental evidences performed on mitochondrial biogenesis process is in favor of the concept that pre-existing mitochondria may grow and divide. However, the other two possibilities have not been ruled out conclusively yet.

When dealing with the biogenesis of mitochondria, at least three coordinated aspects related to the composition, structure, and function of the organelle require special attention: (i) the transcription, the import, targeting, and potential assembly of nuclear genes-encoded proteins within mitochondria; (ii) the maintenance, replication, and the transcription of mitochondrial genome; and (iii) the biogenesis of mitochondrial membranes. To be coordinated, all these aspects need to be tightly orchestrated at the transcriptional level in response to various external stimuli and downstream signaling pathways.

The abundance of mitochondrial population in cells does not only result from the biogenesis of the organelle but is also dependent on its turnover that involves the degradation of internal mitochondrial components as well as the autophagic digestion of the entire organelle by mitophagy (Figure 1.6.1).

The basal turnover of mitochondria can gradually be enhanced in response to different stresses of various intensities such as the accumulation of unfolded or aggregated proteins that induce a specific and adaptive mitochondrial unfolded protein response (mtUPR) (Haynes and Ron, 2010). However, severe mitochondrial dysfunction such as activity impairment caused by defective oxidative phosphorylation will lead to the entire organelle degradation. The response to increasing mitochondrial stress is crucial in a cell attempt to recover proper mitochondrial homeostasis, which, if not, would lead to cell dysfunction or even cell death by apoptosis (Tatsuta and Langer, 2008; Luce et al., 2010).

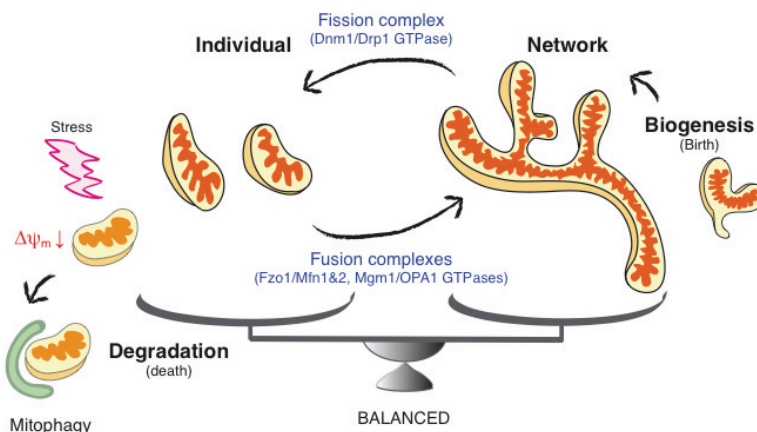


Figure 1.6.1 – The mitochondrial life cycle.

Fission and fusion are two opposing processes that control mitochondrial number, size, shape, and distribution. In addition, these events allow mitochondria to shuttle between two distinct states — “individual state” and “network state”. Additional processes that define the life of mitochondria are biogenesis (birth) and degradation (death). Since mitochondria cannot be synthesized *de novo*, they must be proliferated from pre-existing ones. Their biogenesis seems to be regulated through multiple processes including protein and lipid import, oxidative phosphorylation, and mtDNA replication. From Okamoto and Kondo-Okamoto, 2012.

1.7. Aims / Objectives

It is recognized that the effects caused by environmental toxicants are mainly mediated through the binding of noxious agents to the AhR. All major human cell types express AhR, including pulmonary tissue. The liver, adipose tissue, and skin are the major storage sites of AhR ligands in humans. These AhR ligands are also concentrated in bronchial epithelial cells, suggesting that the respiratory system is very sensitive to AhR ligands. However, the mitochondria are crucial organelles in cell homeostasis and in cell life/death. Direct effects of chemical toxicants on mitochondria, causing its dysfunction, could be the cause to further cellular damage induced by pollutants and to the development of pollutants-associated diseases.

In this work we aim to explore the effects of Dibenzofuran on isolated mitochondria. Since DBF is an environmental pollutant to which we are exposed mainly through air (inhalation), we aim to evaluate lung mitochondrial function upon exposure to DBF. Nevertheless, we will also assess mitochondrial function using isolated mitochondria from liver, the main detoxifying organ and the organ that accumulates the most of the xenobiotics in the organism. Furthermore, we aim to evaluate the effects of DBF on lung cells. Mitochondrial damage can further induce cellular damage, yet cells have more complex rescue mechanisms, such as autophagy. We aim to evaluate DBF-induced damage in lung cells and the triggering of autophagy. The triggering and the enhancement of the defense/rescue mechanisms of the cell can help to prevent some of the damage and, ultimately, some of the diseases caused by the exposure to environmental pollutants.

Chapter 2

Materials and methods

2.1 Materials

Except when noted, all compounds were purchased from Sigma-Aldrich (St. Louis, MO). Dibenzofuran was purchased from Supelco, USA (4-0261).

All reagents and chemicals used were of the highest grade of purity commercially available.

2.2 List of antibodies used

<i>Antibody</i>	<i>Specie</i>	<i>Dilution</i>	<i>Supplier</i>	<i>Reference</i>
Actin	Mouse	1 : 5000	Sigma	A5441
ANT	Mouse	1 : 500	Mitosciences	MSA02
CypD	Mouse	1 : 1000	Mitosciences	MSA04
Cyt c	Mouse	1 : 1000	BD Pharmingen	556433
LC3	Mouse	1 : 500	NanoTools	0260- 100/2G6
p-62	Guinea-pig	1 : 10000	Progen	GP62-C
VDAC	rabbit	1 : 5000	AbCam	Ab3434

Goat anti-rabbit immunoglobulin G (IgG)-AP conjugated was purchased from Santa Cruz Biotechnology (Santa Cruz, CA) (sc-2007); goat anti-mouse IgG + IgM-AP conjugated antibody from Amersham Biosciences (NIF 1316); HRP-conjugated rabbit anti-guinea-pig antibody from Zymed (61-4620). ECF Western blotting reagent was purchased from Amersham Biosciences (Piscataway, NJ) (RPN 3685).

2.3 Animals

Pig lungs were used to obtain isolated mitochondria. Lungs were obtained from a local supplier, collected each day of experiments immediately after animals sacrifice and kept on ice during transport and isolation procedure.

For liver mitochondria isolation, Wistar male rats were used, obtained from Charles River (France). Upon arrival, animals were allowed 7 days to acclimatize (room temperature was 22-24° C) and housed under controlled

light (12h-light cycle) and humidity (moisture 50-60%) conditions with free access to food and water (pH 4.5). All animals received care according to institutional guidelines.

2.4 Isolation of mitochondria

Mitochondria were isolated from lung or liver by conventional methods with slight modifications, as previously described (Gomes et al., 2012; Rolo et al., 2009). All isolation material was kept on ice during the isolation procedure. The lung or the liver tissue was finely minced in an ice-cold homogenization medium (250mM sucrose, 0.5mM EGTA, 0.5% bovine serum albumin (BSA) and 10 mM HEPES, pH 7.4) and the minced blood-free tissue was then homogenized with a “Potter-Elvehjem” type glass homogenizer and a Teflon piston. The homogenate was then centrifuged in a refrigerated centrifuge (Sorvall, Thermo Scientific), at 800x *g*. Supernatant was collected and centrifuged at 10.000x *g* to pellet mitochondria, which were resuspended in washing medium (250mM sucrose and 10 mM HEPES, pH 7.4). When using lung tissue, an additional centrifugation at 800x *g* was performed; supernatant was again collected and centrifuged at 10.000x *g* to pellet mitochondria. The pellet was resuspended and finally centrifuged at 10.000x *g*. Mitochondria in the pellet were resuspended in a final washing medium and immediately used.

Protein content was determined by the biuret method (Gornall et al., 1949), calibrated with BSA.

2.5 Mitochondrial transmembrane potential ($\Delta\Psi_m$) measurements

The mitochondrial transmembrane potential ($\Delta\Psi_m$) was estimated using an ion-selective electrode to measure the distribution of tetraphenylphosphonium (TPP^+) according to previously established methods (Kamo et al., 1979; Palmeira et al., 1994). The reference electrode was Ag/AgCl₂ (model MI 402, Microelectrodes Inc, Bedford, NH). Both electrodes were connected to an adequate potentiometer (Jenway pH meter 3305); the signal was delivered to a Kipp and Zonen recorder (model BD 121, Kipp & Zonen B.V.) via a manufactured potential compensatory box (Madeira, 1975).

Mitochondria (lung: 2mg; liver: 1mg) were suspended with constant stirring, at 25°C, in 1 ml of standard respiratory medium (130mM sucrose, 50mM KCl, 5mM MgCl₂, 5mM KH₂PO₄, 50µM EDTA, 5mM HEPES, pH 7,4) supplemented with 3µM TPP⁺ and 3µM rotenone, and were energized with 10mM succinate. A matrix volume of 1.1µl/mg protein was assumed (Masini et al., 1984). Control assays were done in order to exclude the possibility of interference with the electrode.

2.6 Mitochondrial respiration / Oxygen consumption

Oxygen consumption of isolated mitochondria was polarographically determined with a Clark oxygen electrode (Estabrook, 1967; Rolo et al., 2009) connected to a suitable recorder, through an oxygen electrode control system. Mitochondria (lung: 2mg; liver: 1mg) were suspended under constant stirring, at 25°C, in 1 ml of standard respiratory medium described above with rotenone (3µM) as inhibitor of complex I, and energized by adding succinate to a final concentration of 10mM. ADP (50, 100 or 250 nmol) was added to induce state 3 respiration. The respiration control ratio (RCR) was calculated taking into account oxygen consumption rates during state 3 (following ADP phosphorylation) and subsequent state 4 respiration. The ADP/O ratio was calculated as the nmol of ADP phosphorylated by nanomoles oxygen consumed (Chance and Williams, 1956).

2.7 ATPase activity

ATPase activity was determined spectrophotometrically at 660 nm, in association with ATP hydrolysis (Madeira et al., 1974). The reaction was carried out at 37°C, in 2ml reaction medium (100 mM NaCl, 25 mM KCl, 5 mM MgCl₂, and 50 mM HEPES, pH 7,4). After the addition of freeze-thawed mitochondria (0,25 mg), DBF was added and allowed to incubate for 3 min before the initiation of the reaction by adding 2mM Mg²⁺-ATP, in the presence or absence of oligomycin (1µg/mg protein). After 10 minutes, the reaction was stopped by adding 1ml of 40% trichloroacetic acid and the samples centrifuged (5min, 3.000x g). 2ml of ammonium molybdate (1%) plus 2ml of

deionized H₂O were then added to 1ml of supernatant and reacted for 5min at room temperature. ATPase activity was calculated as the difference in total absorbance and absorbance in the presence of oligomycin.

2.8 Cytochrome c oxidase (COX) activity

COX activity was polarographically determined with a Clark oxygen electrode, as previously described (Brautigan et al., 1978; Varela et al., 2008). The reaction was carried out at 25 °C in 1.4 ml of standard respiratory medium (as in mitochondrial respiration) supplemented with 2µM rotenone, 10µM oxidized cytochrome c and 0.3 mg Triton X-100. After the addition of freeze-thawed mitochondria (0.5 mg), DBF was added and allowed to incubate for 3 min before the initiation of the reaction by adding 5mM ascorbate plus 0.25mM tetramethylphenylene-diamine (TMPD).

2.9 Mitochondrial permeability transition (MPT)

MPT was assessed estimating mitochondrial swelling through changes in light scattering as monitored spectrophotometrically (Jasco V-560 spectrophotometer) at 540 nm (Palmeira and Wallace, 1997; Teodoro et al., 2011). The experiments were started by the addition of 1 mg of mitochondria to a final volume of 2 ml of the standard incubation medium (200mM sucrose, 10mM HEPES (pH 7,4), 1mM KH₂PO₄ and 10µM EGTA), supplemented with 3µM rotenone and 5mM succinate. The medium was stirred continuously and temperature maintained at 25°C. After a brief incubation period to establish a baseline absorbance, different calcium (CaCl₂) concentrations were added as indicated by the arrows in the figures, to induce permeability transition. In selected assays, cyclosporine A (a known MPT inhibitor) or, in lung mitochondria experiments, ADP (100µM) plus oligomycin (1µM), were used as a negative control to prevent MPT (Palmeira and Wallace, 1997).

2.10 Measurement of mitochondrial calcium fluxes / calcium retention capacity

The accumulation and release of calcium by isolated mitochondria was determined using a calcium-sensitive fluorescent dye, Calcium Green-5N, as previously described (Varela et al., 2010). Briefly, the reactions were carried out at 25 °C in 2 ml of the MPT buffer (as above), supplemented with rotenone (3 µM), oligomycin (0.5 µg/ml) and Calcium Green-5N (200nM). Mitochondria (1 mg) were loaded and fluorescence was recorded continuously using a Victor3 plate reader (Perkin–Elmer), with excitation and emission wavelengths of 485 and 535nm, respectively. Energization was obtained with 5 mM succinate. Calcium fluxes are expressed as relative fluorescence units (RFUs).

2.11 Immunoprecipitation of ANT and western blot detection of cyclophilin D

ANT was immunocaptured from mitochondrial extracts using monoclonal antibodies to ANT crosslinked to agarose beads (MitoSciences Cat#MSA01). Mitochondria (1mg) collected after calcium-induced MPT were resuspended in 300µl of the extraction buffer for immunoprecipitation (250mM sucrose, 20mM MOPS, 10mM Tris, 0.5% Triton, protease Inhibitor cocktail, pH 7.2) and frozen in liquid nitrogen. Samples were incubated overnight at 4°C with the antibody/agarose beads. Beads were washed four times with ice-cold buffer. Elution of immunocomplexes with Laemmli sample buffer and heat-denaturation were performed immediately prior to one-dimensional gel electrophoresis. Proteins were separated on 15% SDS-polyacrylamide gels and electroblotted onto PVDF membranes. The western blots were then probed with antibodies against ANT and CypD. Western blot membranes were blocked with 5% nonfat milk and incubated with antibodies anti-ANT or anti-CypD overnight at 4°C. Immunodetection was performed with WesternDot 625 (Invitrogen) goat anti-mouse western blot kits and the membranes were imaged using a Gel Doc instrument (Biorad).

2.12 Carboxyatractyloside (CAT) titration

CAT is a highly selective inhibitor of cytosolic side-specific ANT that causes stabilization of the *c* conformation of ANT leading to MPT induction and loss of mitochondrial membrane potential.

The mitochondrial transmembrane potential was estimated as described before. Energized mitochondria were titrated with 0.02 nmol CAT. Successive additions of CAT aliquots before ADP addition, progressively block a higher number of ANT units contributing to the observed decreased number of phosphorylation cycles induced by successive ADP additions.

2.13 Western blotting analysis with lung mitochondria

Mitochondrial pellets were obtained after mitochondrial permeability induction experiments described above and kept frozen. After thawing pellets were homogenized in lysis buffer (1M urea, 10mM Tris, 2% SDS, pH 7.5, 60°C). Aliquots were fractionated in 8–15% polyacrylamide gels, transferred to polyvinylidene difluoride (PVDF) membranes, and blotted with anti-cytochrome *c* or anti-VDAC antibodies. The immunoreactive proteins were visualized with goat anti-mouse and anti-rabbit antibodies, membranes were reacted with the ECF detection system and read with the Versa Doc imaging system (series 1300, Bio-Rad). VDAC content was used as mitochondrial loading control for the total protein content.

2.14 Cell line

A549 human lung carcinoma cell line was purchased from American Type Culture Collection, USA (ATCC catalog no. CCL-185).

2.15 Cell culture

A549 cells were cultured in Minimum Essential Medium (MEM) Eagle (with 1.5 g/l sodium bicarbonate and 0.11 g/l pyruvate), containing 10% foetal bovine serum (FBS). Cells were maintained in a humidified CO₂ (5%) incubator at 37°C, and passaged and harvested for experiments by detachment with a recombinant enzyme trypsin, TrypLE Express (Invitrogen,

Cat. No. 12605). ~80% confluent cells were used for DBF treatment. Control cells received an equivalent amount of vehicle (ethanol 0.1%).

2.16 Cell death/viability

For analysis of cell death 2.5×10^4 A549 cells were grown in 12-well plates and treated as indicated 24h after seeding. When indicated, cells were collected and stained with propidium iodide and annexin-V-FLUOS (BenderMedSystems) according to the manufacturer's protocol. Cell viability was then measured by flow cytometry (FACSCalibur, BD Biosciences) as the percentage of annexin-V- and propidium iodide-negative events.

2.17 LDH leakage

Cell viability and membrane integrity was evaluated by measuring the amount of cytoplasmic Lactate Dehydrogenase released into the medium, using an assay based on the reduction of NAD by the action of LDH. LDH based kit (TOX-7) was purchased from Sigma. The resulting reduced NAD (NADH) is utilized in the stoichiometric conversion of a tetrazolium dye. The resulting coloured compound is measured spectrophotometrically at 490nm. A549 cells were seeded in 12-well plates at 1.25×10^4 cells/ml and allowed to attach and recover for 1 day prior to drug treatment. Medium from each well (each experimental sample) was centrifuged to pellet cells and aliquots were transferred to clean flat-bottom plate to proceed with enzymatic analysis accordingly to the in vitro toxicology assay kit.

2.18 Cell proliferation

Cell proliferation and in vitro cytotoxicity were measured with Sulforhodamine B method (Skehan et al., 1990). Sulforhodamine B (TOX-6) was purchased from Sigma. The cells were seeded in 12-well plates at 1.25×10^4 cells/ml (in a total medium volume of 2ml per well) and allowed to attach and recover for 1 day prior to drug treatment. After addition of DBF cells were cultured for up 2 days (24h and 48h). After the treatment, cells were briefly washed, fixed and stained with the dye. The incorporated dye was then

liberated from the cells in a Tris-base solution. Absorbance of the solubilized dye was measured at 540 nm in a Victor³ plate reader (Perkin–Elmer), indicating the degree of cytotoxicity caused by test compound.

2.19 MTT reduction assay

Mitochondrial dehydrogenases activity was evaluated by measuring the amount of formazan formed after cleavage of the 3-[4,5-dimethylthiazol-2-yl]-2,5-diphenyl tetrazolium bromide (MTT) ring. MTT assay kit (TOX-1) was purchased from Sigma. A549 cells were seeded in 12-well plates at 1.25×10^4 cells/ml (final volume of 2ml) and allowed to attach and recover for 1 day prior to drug treatment. After addition of DBF, cells were cultured for up to 2 days (24h and 48h). At the end of the treatment, 1mg of MTT (from a recently prepared stock of 5 mg/ml in PBS) was added to each well and the plates returned to the incubator for 3h to allow MTT reduction. After the incubation media was dumped off and purple formazan crystals were dissolved in 1ml isopropanol during 30 minutes on a shaking table. The resulting purple solution was spectrophotometrically measured at 540nm.

2.20 Adenine nucleotides content

A549 cells were cultured in flasks and treated for 24 and 48h with DBF 150 μ M and 250 μ M. At the end of the treatment cells were harvested by detachment with trypsin; adenine nucleotides were extracted using an acid extraction (HClO₄) procedure, final pH 7 achieved with aliquots from stock 2.5M KOH in 1.5M K₂HPO₄, maintaining samples on ice. Adenine nucleotides were separated by reverse-phase high-performance liquid chromatography, HPLC (Stocchi et al., 1985). The chromatographic apparatus was a Beckman-System Gold, consisting of a 126 Binary Pump Model and a 166 Variable UV detector, controlled by a computer. The detection wavelength was 254 nm, and the column was a 5-m Lichrospher 100RP-18 from Merck (Darmstadt, Germany). An isocratic elution with 100mM phosphate buffer (KH₂PO₄, pH 6.5) and 1.2% methanol was performed with a flow rate of 1 ml/min. The time required for each analysis was 5 minutes.

2.21 Measurement of mitochondrial membrane potential ($\Delta\Psi_m$) in A549 cells

$\Delta\Psi_m$ in A549 cells was measured with a fluorescent probe, tetramethylrhodamine methyl ester (TMRM), as described before (Rolo et al., 2003) with slight modifications. TMRM was purchased from Invitrogen (T668). Briefly, to monitor mitochondrial $\Delta\Psi$, cells grown in 12-well plates were loaded with 6.6 μM TMRM for 15 min at 37 °C. Cells were then washed and culture medium without FBS or phenol red was added. TMRM is a cell-permeant, cationic fluorescent dye that is readily sequestered by active mitochondria, accumulating electrophoretically in proportion to their $\Delta\Psi$ (Ehrenberg et al., 1988). Fluorescence was measured using excitation and emission wavelengths of 485 and 590 nm, respectively. After recording basal fluorescence, mitochondrial $\Delta\Psi$ was estimated taking into account the complete depolarization caused by 2,4-dinitrophenol (DNP), normalizing the data to protein content in each well.

2.22 Oxygen consumption in A549 cells

Cells were cultured as described before and exposed to DBF. Cells were then harvested by trypsinization and washed with PBS. The whole cell pellets were then suspended in DMEM and 0.2×10^6 cells were added to individual wells of a 96-well BD Oxygen Biosensor System plate (BD Biosciences), followed by cell culture medium (without phenol red) to a final volume of 200 μl per well. The plates were then maintained for 30min at 37 °C in a humidified incubator with 5% CO_2 . Plates were scanned in a temperature-controlled (37°C) plate reader (Perkin-Elmer Victor3) with an excitation wavelength of 485nm and an emission wavelength of 630 nm. Measurements were taken 1 min apart for a total of 40 min and the time profiles of fluorescence intensity in each well were analyzed using Excel software (Microsoft). The fluorescence traces in each well were normalized to the signal in air-saturated buffer. Slopes of fluorescence signal were calculated in the dynamic range of the measurements to compare respiratory rates of different samples.

2.23 Measurement of ROS production

ROS production was determined fluorometrically, as described before (Palmeira et al., 2007). 2',7'-Dichlorodihydrofluorescein diacetate (H₂DCF-DA) (D6883) was purchased from Sigma. Briefly, cells were collected by trypsinization and centrifugation, and resuspended at 1×10^6 cells per ml in culture medium without FBS or phenol red. Cells were loaded with 50 μ M H₂DCF-DA for 30 min at 37 °C, washed and 200 μ l containing 2×10^5 cells were loaded into a 96-well plate. The fluorescence coming from the formation of oxidized derivatives was monitored at an excitation wavelength 485 nm and an emission wavelength 538 nm, for 30 min, to calculate the rate of ROS formation.

2.24 Nuclear morphology (apoptosis)

Cells were seeded on glass cover slips in 6-well plates at 1.25×10^4 cells/ml, as previously described (in a total medium volume of 5ml per well). At 24h or 48h treatment (250 μ M DBF), plates were rinsed twice with PBS. Cover slips were fixed in solution (1ml) of paraformaldehyde 4% and sucrose 4% during 15min at room temperature. Cells were then washed two times with PBS. The cells were stained with 5 μ g/ml Hoechst 33342 in PBS during 10 minutes to evaluate nuclear morphology. Hoechst 33342 (H1399) was purchased from Invitrogen. Cover slips were mounted in a fluorescent mounting medium (Dako) and images were recorded using a Zeiss Axioskop 2 Plus fluorescence microscope (Carl Zeiss) with a Zeiss AxioCam MRC (Carl Zeiss). Apoptotic cells were identified as those whose nuclei exhibited brightly staining condensed chromatin, nuclear fragmentation or apoptotic bodies.

2.25 LysoTracker accumulation

Cells were seeded on glass cover slips in 6-well plates as described above. After DBF treatment they were gently washed with PBS and incubated for 30 minutes with LysoTracker Red 100nM in culture medium without phenol red. LysoTracker Red DND-99 (L7528) was purchased from Invitrogen. Cells were then inspected and photographed using a Zeiss Axioskop 2 Plus

fluorescence microscope (Carl Zeiss) with a Zeiss AxioCam MRC (Carl Zeiss).

2.26 LC3 subcellular distribution

A549 cells were seeded on glass cover slips in 6-well plates as described above, and transfected with YFP-LC3 plasmid (kindly provided by Dr. M. Sandri in the Venetian Institute of Molecular Medicine, Padua, Italy) using Lipofectamine 2000 Transfection Reagent (Invitrogen) accordingly to manufacturer's instructions. Cells were allowed to express the protein and incubated with DBF 24h after transfection. As a positive control for autophagy induction cells were incubated in "starvation" medium (Hank's Balanced Salt Solution supplemented with 10mM Hepes, pH 7.4). After treatment cells were fixed with formaldehyde 3,7% and images recorded using a Zeiss Axioskop 2 Plus fluorescence microscope (Carl Zeiss) with a Zeiss AxioCam MRC (Carl Zeiss). Cells were blindly classified as autophagy-negative cells (presenting a predominantly diffuse YFP-LC3 fluorescence) or autophagy-positive cells (cells with a punctuate YFP-LC3 pattern).

2.27 Western blotting analysis with A549 cell extracts

A549 cells were collected from culture flasks after exposure to DBF, homogenized in lysis buffer (1M urea, 10mM Tris, 2% SDS, pH 7.5, 60°C) and cell lysates aliquots were fractionated in 8–15% polyacrylamide gels, transferred to PVDF membranes, and probed with anti-LC3 antibody, anti- β -actin antibody, anti-p62 antibody, anti-mouse antibody (dilution 1:10000) or anti-guinea-pig antibody (dilution 1:5000). Membranes were reacted with the ECF or ECL Plus (GE Healthcare) detection system. The fraction prepared from starved cells was used as a positive control. β -actin content was used as loading control for the total protein content and showed no differences between groups.

2.28 DNA isolation and real-time qPCR

DNA was isolated from control and DBF-treated samples with resource to a specialized kit (Qiagen GmbH). Total DNA yield was quantified in a

Nanodrop instrument (Thermo Scientific). Mitochondrial copy number was assessed using real-time PCR, by quantifying the number of DNA copies of a mitochondrial encoded mitochondrial gene (Cytochrome B) normalized against a nuclear encoded mitochondrial gene (Pyruvate kinase). For mitochondrial copy number assays, the values represent the cycle at which the gene's Ct was obtained; thus, a lower value represents a higher content of the same gene. Gene expression was evaluated by real-time qPCR, in a MiniOpticon equipment (Bio-Rad). Primers used were the following:

Cyt B human antisense: 5' TGT TGT TTG GAT ATA TGG AGG ATG 3'

Cyt B human sense: 5' TGA TAT TTC CTA TTC GCC TAC ACA 3'

Pyruvate kinase human antisense: 5' CTC CTA GTT TTC ACC CTC ATT TTC 3'

Pyruvate kinase human sense: 5' GTC GAT CCA GGA GAA CAT ATC AT 3'

2.29 Statistical analysis

Results are presented as means \pm S.E.M. of the number of different experiments (3-5 independent experiments). Solvent controls were included within each experimental determination. Statistical significance was determined using the two-tailed Student's t test. A *P* value < 0.05 was considered statistically significant.

Chapter 3

Exposure to Dibenzofuran affects lung mitochondrial function *in vitro*

3.1 – Introduction

In humans, exposure to dioxins and dioxin-like pollutants, such as fuel constituents, is associated with chronic obstructive pulmonary disease development and with lung cancer (Patel and Homnick, 2000; Matsumoto et al., 2007; Billet et al., 2008). Moreover, chronic respiratory diseases are one of the major problems concerning public health subjects. Dibenzofuran (DBF) is an aromatic ether with properties and chemical structure similar to dioxins. Potential exposure to DBF may occur through inhalation and dermal contact, particularly at sites engaged in combustion/carbonization processes (coal tar and coal gasification) where DBF is released to the ambient air (Aristizábal et al., 2008; Hu et al., 2009; Chang et al., 2010). This pollutant has also been identified in tobacco smoke and listed as a pollutant of concern due to its persistence in the environment, potential for bioaccumulation and toxicity to humans and the environment (Mennear and Lee, 1994; Iida et al., 2007; Nadal et al., 2009; Li et al., 2010). Nevertheless and although the lung is a primary site of exposure for many inhaled chemical contaminants, studies about pollutants-induced toxic effects in lung function are scarce.

Mitochondria play a central role in cell life and cell death (Kushnareva and Newmeyer, 2010). Mitochondria are the energy suppliers for eukaryotic cells and a proper mitochondrial function is therefore essential in the fulfilment of the tissues energy-demand. Therefore, alterations of mitochondrial bioenergetic features by toxicants reduce energetic charge and may result in cell death. Previous studies have identified mitochondrial targets of environmental pollutants, namely ROS production and decreased ATP content (Senft et al., 2002; Shertzer et al., 2006). Consequently, maintenance of cell function is strictly dependent on the existence of a healthy population of mitochondria.

The main objectives of this work concerned DBF effects on lung mitochondrial function. Due to the central role of mitochondria in cell function, isolated pig lung mitochondria were used to analyse effects of DBF at the level of mitochondrial function (membrane potential, respiration, MPT induction and cytochrome *c* release). Clarifying the role of pollutants in some

mechanisms of toxicity, such as unbalance of bioenergetics status or cell death induction, may help explain the progressive and chronic evolution of lung diseases.

3.2 – Results

3.2.1 – Mitochondrial transmembrane potential

Transmembrane potential ($\Delta\Psi_m$) sustained by mitochondria upon energization is essential for mitochondrial function. Since this parameter reflects the differences on electric potential and represents the greater component of the electrochemical gradient of protons in the membrane, contributing for the majority of the energy used in the oxidative phosphorylation, mitochondrial transmembrane potential was evaluated after incubation with DBF. Mitochondria transmembrane potential was not significantly altered upon exposure to DBF, when compared to control, as well as repolarization potential (Table 3.2.1; Figure 3.2.1).

Table 3.2.1 – Effects of DBF in mitochondrial transmembrane potential ($\Delta\Psi_m$) and lag phase.

Mitochondria were incubated with DBF prior to succinate energization and $\Delta\Psi$ was evaluated using a TPP⁺-electrode as described in Chapter 2.

	Control	DBF 50 μ M	DBF 100 μ M	DBF 150 μ M	DBF 250 μ M
Initial potential $\Delta\Psi$	186.60 \pm	190.50 \pm	189.80 \pm	183.80 \pm	185.10 \pm
(-mV)	2.56	2.61	2.79	6.42	0.20
$\Delta\Psi$ Depolarization	17.50 \pm	17.13 \pm	18.47 \pm	17.03 \pm	14.27 \pm
(-mV)	0.26	0.32	0.26	0.70	1.50
$\Delta\Psi$ Repolarization	177.80 \pm	180.90 \pm	178.60 \pm	173.30 \pm	175.70 \pm
(-mV)	2.72	3.69	3.22	7.00	1.27
Lag phase (s)	27.00 \pm	34.00 \pm	41.00 \pm	82.00 \pm	73.50 \pm
	5.20	7.21	6.08	17.78 *	16.50 *

Data are means \pm SEM of different experiments. * indicates statistically significant difference versus control (P < 0.05).

Depolarization induced by the addition of ADP didn't show statistical significant variations in lung mitochondria exposed to DBF when compared to control, despite the slight decrease tendency in depolarization of mitochondria incubated with the highest concentration of DBF (Table 3.2.1; Figure 3.2.1).

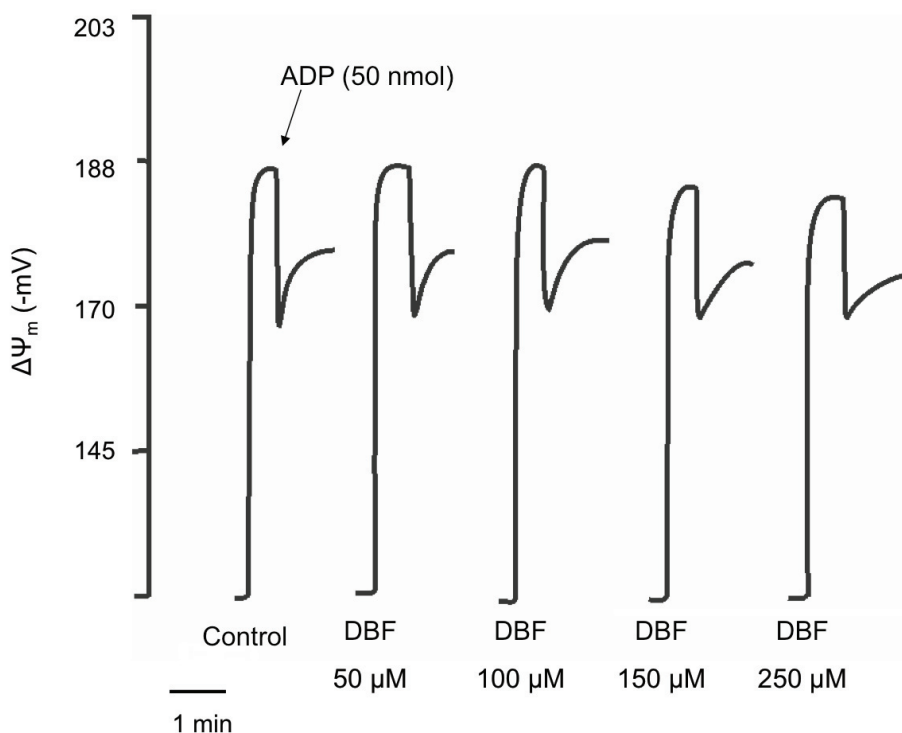


Figure 3.2.1 - Mitochondrial transmembrane potential ($\Delta\Psi_m$) and lag phase.

Transmembrane potential measurements were performed with the TPP^+ -electrode using freshly isolated mitochondria (2mg), as described in Chapter 2. DBF was added to mitochondria 3min prior to energization with succinate. The traces are representative of different experiments performed with independent mitochondrial preparations.

Conversely, the lag phase that occurs before repolarization was significantly increased in lung mitochondria incubated with DBF at concentrations of 150 and 250 μM (Table 3.2.1; Figures 3.2.1 and 3.2.2).

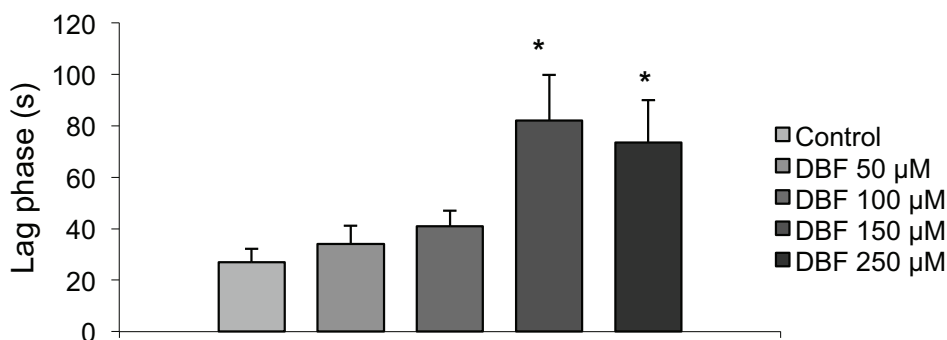


Figure 3.2.2 – Effects of DBF in the lag phase preceding the mitochondrial repolarization.

Measurements were performed with the TPP^+ -electrode as described in Chapter 2. Data are means \pm SEM of different experiments. * indicates statistically significant difference versus control ($P < 0.05$).

3.2.2 – Mitochondrial respiration / oxygen consumption

Oxidative phosphorylation and respiratory chain competence of lung mitochondria was investigated by following oxygen consumption after succinate oxidation, upon exposure to DBF. The results showed no significant variation for all of the parameters evaluated in mitochondria exposed to DBF as compared with control: state 3 and state 4 respiration; respiratory control ratio (RCR); and oxidative phosphorylation efficiency, expressed as ADP/O ratio (Table 3.2.2).

Table 3.2.2 – Oxygen consumption measurements.

Mitochondria were incubated with DBF and O₂ consumption was evaluated with use of a Clark-type electrode, as described in Chapter 2.

	Control	DBF 50 µM	DBF 100 µM	DBF 150 µM	DBF 250 µM
State 3 (<i>natoms O/min/mg protein</i>)	31,68 ± 10,56	38,35 ± 4,1	32,52 ± 3,04	33,99 ± 5,12	32,52 ± 10,56
State 4 (<i>natoms O/min/mg protein</i>)	19,43 ± 8,45	23,65 ± 2,74	22,39 ± 3,91	24,99 ± 3,4	20,28 ± 8,45
R.C.R.	1,72 ± 0,2	1,44 ± 0,13	1,35 ± 0,13	1,36 ± 0,08	1,68 ± 0,18
ADP/O	0,63 ± 0,055	0,62 ± 0,086	0,63 ± 0,05	0,5 ± 0,046	0,8 ± 0,06

Data are means ± SEM of different experiments. No statistically significant differences were found ($P < 0.05$).

3.2.3 – ATPase activity

The enlarged lag phase in mitochondria exposed to DBF suggested that exposure to the pollutant could affect mitochondrial phosphorylative system. In order to clarify this alteration, mitochondrial ATPase (ATPsynthase) activity, one of the components of the mitochondrial phosphorylative sub-system, was evaluated through phosphate (P_i) production from ATP hydrolysis. No significant differences were found between lung mitochondria incubated with DBF and control (Figure 3.2.3), showing that the decreased performance of phosphorylation in lung mitochondria upon DBF exposure (as reflected by an increased lag phase) was not clearly correlated with a less efficient ATPase.

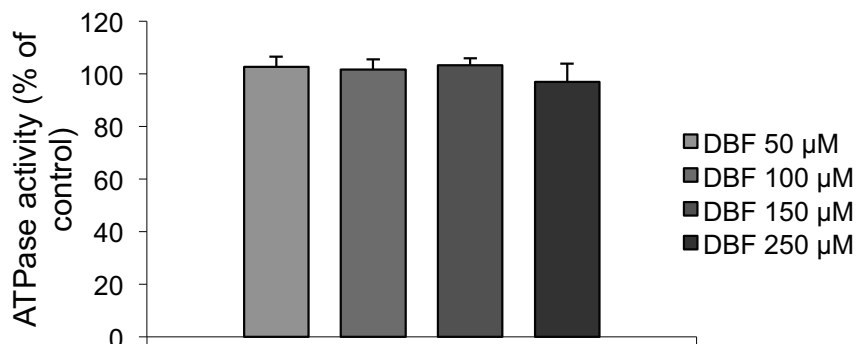


Fig. 3.2.3 – ATPase activity in lung mitochondria.

Mitochondria were incubated with different concentrations of DBF and ATPase activity was measured spectrophotometrically (660nm) in association with ATP hydrolysis, as described in Chapter 2. Data are presented as means \pm S.E.M. No statistically significant differences were found ($P < 0.05$).

3.2.4 – Mitochondrial permeability transition

Mitochondria show a finite capacity of accumulating calcium before undergoing the calcium-dependent MPT. Mitochondrial swelling induced by calcium was used as an indicator of lung mitochondria susceptibility to MPT induction (Figure 3.2.4). Lung mitochondria exposed to DBF showed greater capacity of calcium accumulation before undergoing permeability transition. ADP and oligomycin together were used as inhibitors of MPT induction, allowing lung mitochondria to accumulate and keep hold of added calcium for a longer period.

3.2.5 – Cytochrome c content

Mitochondrial content in cytochrome c was assessed in lung mitochondria after MPT induction (Figure 3.2.5), in order to estimate cytochrome c release from mitochondria undergoing MPT.

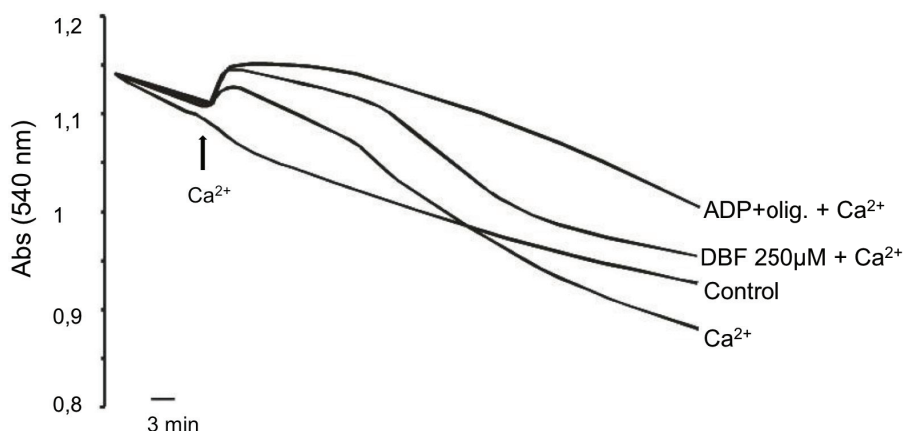


Figure 3.2.4 – Susceptibility to mitochondrial permeability transition induction. Mitochondria were incubated with DBF and MPT was induced with the addition of Ca^{2+} . MPT was evaluated spectrophotometrically (540nm) as described in Chapter 2. The traces are representative of different independent experiments.

Cytochrome c content was more preserved in mitochondria incubated with DBF, after calcium addition, in comparison to mitochondria incubated only with calcium (Figure 3.2.5). This indicates that DBF may slightly prevent mitochondria from undergoing mitochondrial permeability transition, consequently showing minor cytochrome c release than mitochondria exposed only to calcium.

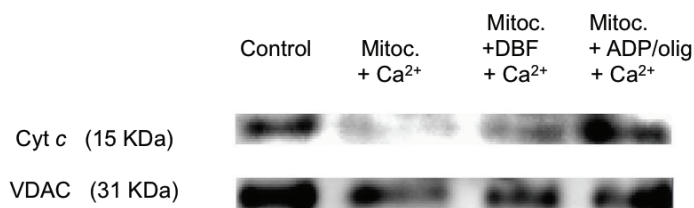


Figure 3.2.5 – Cytochrome c content in lung mitochondria exposed to DBF. Western blot evaluations were conducted as described in Chapter 2, using mitochondrial samples collected after MPT induction experiments. Images are representative bands of protein content.

Again, as in mitochondrial swelling, mitochondria incubated with ADP and oligomycin together, showed cytochrome c content similar to that in control (Figure 3.2.5).

3.3 – Discussion

Exposure to dioxins and other environmental pollutants, such as fuel constituents and incineration products, is associated in humans with obstructive pulmonary disease and lung cancer (Boffetta, 2006). DBF is a widespread environmental contaminant that results from chemical and combustion processes, and exposure to it brings out several dreadful effects. Although some work has been conducted on pollutants-induced liver toxicity using liver cells in culture and animal models (Bunger et al., 2003; Niittynen et al., 2008; Weinstein et al., 2008), the evaluation of lung cell function after exposure to this kind of toxicants is scarce. In this study we report that DBF affects mitochondria isolated from lungs.

Previous studies on mitochondrial dysfunction induced by exposure to pollutants, such as TCDD or arsenic, have been carried out in liver (Mildaziene et al., 2002; Lee and Sokol, 2007), blood cells (Banerjee et al., 2008) or in brain (Coburn et al., 2008). In both hepatic mitochondria isolated from TCDD-treated mice and mitochondria incubated in vitro with TCDD, a number of functional alterations have been observed, including a defect in ATP synthesis and increased ROS production (Senft et al., 2002; Shen et al., 2005; Shertzer et al., 2006). Experiments with isolated mitochondria from lungs showed that the generation of mitochondrial membrane potential was not compromised by exposure to DBF. Nevertheless, the time that elapses from ADP-induced depolarization until total repolarization – lag phase – was significantly enlarged in mitochondria exposed to DBF, suggesting that DBF may impair mitochondrial phosphorylative efficiency. No significant differences were observed on mitochondrial respiration, unlike the effects of other pollutants in hepatic mitochondrial respiratory chain function (Shertzer et al., 2006). Additionally, Shertzer and collaborators have also shown a decrease in hepatic ATP levels related to a defect in the mitochondrial ATP synthase in

rats treated with TCDD for 1 week. Thus, the mitochondrial phosphorylative system is probably a target for pollutant-induced mitochondrial dysfunction.

MPT induction is associated with pathological conditions and is triggered by high Ca^{2+} , oxidative stress, ATP depletion, high inorganic phosphate and mitochondrial depolarization. In this work, MPT induction in mitochondria incubated with DBF was evaluated. Results show that this pollutant seems to slightly prevent MPT induction. In one week TCDD-exposed mice, it has been shown that TCDD induces an increase in mitochondrial ROS and membrane potential though a mechanism involving an elevated reduction state of glutathione, which then prevents MPT induction (Shen et al., 2005). Thus, although the impairment of ATP synthesis induced by pollutants in both lung and hepatic mitochondria, data suggest that dioxins and DBF in a certain extent inhibit induction of the MPT.

Although we have reported a limited toxicity of DBF affecting isolated mitochondria function, which could be due to very short time exposure of mitochondria to the pollutant *in vitro*, our results indicate that mitochondria are probably a target in DBF-induced lung toxicity. A decrease in the mitochondrial phosphorylative efficiency elicited by DBF is a damaging result from exposure to this toxicant and further studies are needed to better evaluate DBF-induced impairment of pulmonary function.

Chapter 4

Dibenzofuran-induced mitochondrial dysfunction: Interaction with ANT carrier

4.1 – Introduction

Environmental pollution has been challenging human health and healthcare practitioners more and more in the last decades. As a consequence of a wide range of industrial applications, several toxic compounds are produced, environmental release occurs and exposure becomes inevitable. Moreover, several diseases and clinical conditions have been linked to environmental pollutants exposure, such as lung inflammatory diseases (Jung et al., 2007; Lecureur et al., 2012), asthma (McGwin et al., 2010) and cancer (Brody et al., 2007; Raaschou-Nielsen et al., 2011).

Exposure to environmental contaminants such as polycyclic aromatic hydrocarbons (PAH) and halogenated aromatic hydrocarbons (HAH), including dioxins (Yoshioka et al., 2011), plays an important role in the development of several types of human cancers. PAH and HAH are wide spread environmental contaminants that are present in cigarette smoke, coal tar and automobile exhaust. The carcinogenic effects of several PAH and HAH are initiated after their binding and activation of the aryl hydrocarbon receptor (AhR) (Mandal, 2005).

Dibenzofuran (DBF) is a ubiquitous dioxin-like compound, considered to be an environmental pollutant. However, little is known about its effects, namely on primary targets such as the lung. We have previously reported detrimental effects of DBF in lung mitochondria (Duarte et al., 2011) and in lung cells (Duarte et al., 2012). Although some studies reported that environmental toxicants induce mitochondrial damage (Palmeira and Madeira, 1997; Duarte et al., 2011), more systematic studies have not yet been carried out in order to uncover toxic effects of some pollutants harming mitochondria directly.

Mitochondria are the key organelles for energy production and many other cellular processes, including signaling pathways regulating several biologic processes in the cell. Oxidative phosphorylation (OXPHOS) in mitochondria produces more than 95% of a cell's energy in the form of ATP under normal physiological conditions and this process involves five different protein complexes (complex I-V). Mitochondrial respiration generates most of the cellular energy (ATP) and yields several intermediate compounds involved

in cellular metabolism. Therefore, perturbation of mitochondrial functions may result in severe consequences for general metabolism and all the energy transducing processes that require ATP.

Besides energy production, mitochondria also participate in several signaling pathways regulating, for example, cell death/survival (Westermann, 2010; Kinnally et al., 2011). An increase in mitochondrial membrane permeability is one of the key events in apoptotic and necrotic death, although the mechanisms involved are yet to be fully elucidated. It is accepted that mitochondrial permeability transition is caused by the permeability transition pore (PTP), a voltage- and Ca^{2+} -dependent, cyclosporine A (CsA)-sensitive, high conductance channel, whose opening leads to permeabilization of the inner mitochondrial membrane (IMM) to solutes with molecular masses up to 1.5 kDa (Rasola et al., 2010). Activation of mitochondrial permeability transition (MPT) is considered to be a major cause of cell death under a variety of pathophysiological conditions, including ischemia/reperfusion injury, neurodegenerative disease, traumatic brain injury (TBI), muscular dystrophy and drug toxicity (Kroemer et al., 2007; Millay et al., 2008; Varela et al., 2008; Halestrap and Pasdois, 2009; Mbye et al., 2009; Nicholls, 2009; Russmann et al., 2009; Varela et al., 2010).

Despite major efforts, the molecular nature of the mPTP remains undefined. Earlier candidates such as the IMM adenine nucleotide translocase (ANT) and the outer mitochondrial membrane (OMM) voltage-dependent anion channel (VDAC) are now considered to be regulators rather than constituents of the mPTP (Rasola et al., 2010), and new putative regulators have been proposed in the recent years. Indeed, it has been proposed that the mPTP is regulated by proteins that interact with the OMM such as hexokinase (Chiara et al., 2008; Pastorino and Hoek, 2008) and by ligands of the OMM translocator protein of 18 kDa, TSPO, formerly known as the peripheral benzodiazepine receptor (Krestinina et al., 2009; Azarashvili et al., 2010; Sileikytė et al., 2011).

In the past, extensive analyses have dissected the factors that regulate the mPTP *in situ* (Bernardi et al., 2006). Nonetheless, extreme caution must be exerted when these data are extrapolated to mPTP modulation in the living cell. The continuous crosstalk between mitochondria and other cell

compartments suggests that several proteins can play regulatory roles on the pore, connecting signaling cascades known to control the apoptotic process with the mPTP, as this is a key switch in the cell commitment to death (Rasola et al., 2010).

In this work we evaluated the toxic effects of the pollutant DBF *in vitro*, using isolated mitochondria from rat liver. We assessed mitochondrial function (transmembrane potential generation, oxygen consumption), mitochondrial susceptibility to MPT induction and permeability of mitochondrial membrane to protons, exposing mitochondria to the pollutant.

4.2 – Results

4.2.1 – Mitochondrial membrane potential

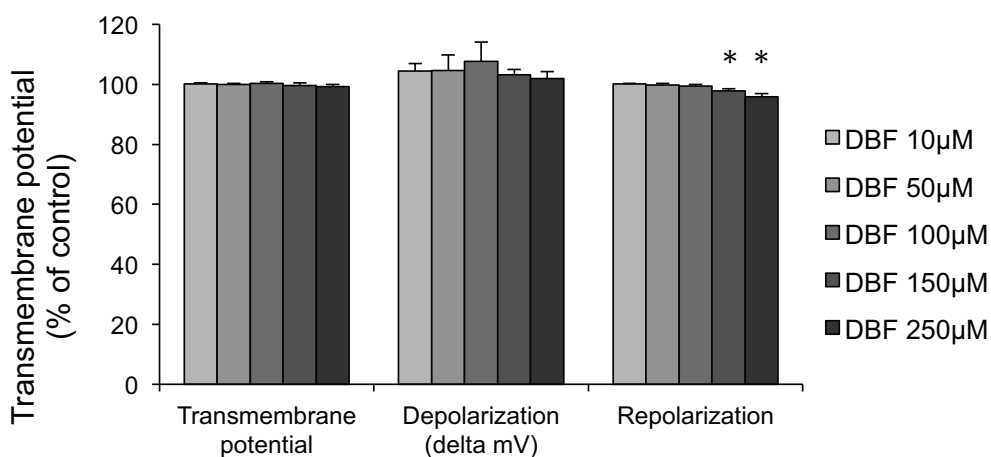
In order to better understand the effects of the environmental pollutant DBF on mitochondria and its function, we assessed the mitochondrial transmembrane potential ($\Delta\Psi_m$) which, upon energization, is essential for mitochondrial function; this parameter reflects the differences on electric potential and represents the greater component of the electrochemical gradient of protons in the membrane, contributing to the majority of the energy used in the oxidative phosphorylation. We found that the $\Delta\Psi_m$ generated by mitochondria isolated from rat liver was not affected by DBF exposure, comparing to control (Table 4.2.1; Figure 4.2.1); similarly, there were no differences in the depolarization induced when ADP was added to mitochondria (Table 4.2.1). However, some differences were found for the repolarization potential of mitochondria after the phosphorylative cycle, which is decreased in mitochondria exposed to the higher concentrations of DBF that were tested, 150 μM and 250 μM (Table 4.2.1).

Table 4.2.1 – Effects of DBF in mitochondrial membrane potential ($\Delta\Psi_m$) and lag phase.

Mitochondria were incubated with DBF prior to succinate energization and $\Delta\Psi_m$ was evaluated using a TPP⁺-electrode as described in Chapter 2.

	Control	DBF 10 μ M	DBF 50 μ M	DBF 100 μ M	DBF 150 μ M	DBF 250 μ M
$\Delta\Psi_m$		100.2 \pm	100 \pm	100.4 \pm	99.7 \pm	99.2 \pm
(% of control)	100	0.25	0.42	0.46	0.75	0.74
$\Delta\Psi_{ADP}$		104.4 \pm	104.7 \pm	107.7 \pm	103.2 \pm	101.9 \pm
(% of control)	100	2.59	5.08	6.44	1.84	2.42
Repolarization		100.1 \pm	99.8 \pm	99.4 \pm	97.8 \pm	95.8 \pm
(% of control)	100	0.3	0.46	0.51	0.75 *	1.07 *
Lag phase		111.4 \pm	122.4 \pm	120.3 \pm	145.0 \pm	167.2 \pm
(% of control)	100	1.17 *	6.43 *	7.71 *	8.15 *	10.49 *

Data are means \pm SEM of different experiments. * indicates statistically significant difference versus control ($P < 0.05$).

**Figure 4.2.1 - Mitochondrial transmembrane potential ($\Delta\Psi_m$) in succinate-energized liver mitochondria.**

Reactions were carried out using 1 mg of freshly isolated mitochondria, as described in Chapter 2. $\Delta\Psi_m$ was measured using a TPP⁺-electrode. DBF was added prior to energization with succinate (3 min incubation). Data are means \pm SEM of different experiments. Values statistically different from control: * $P < 0.05$.

We also measured the period of time during which mitochondria phosphorylate all the ADP that is added, known as lag phase. We found that the lag phase preceding repolarization was significantly increased in mitochondria exposed to DBF, when comparing to control (Table 4.2.1; Figure 4.2.2), suggesting an impairment in the phosphorylative system, considering that the energization induced by the substrate was not impaired. Still, we could see that the increase in the lag phase was greater for the higher concentrations of DBF, showing some kind of “dose-dependent” correlation.

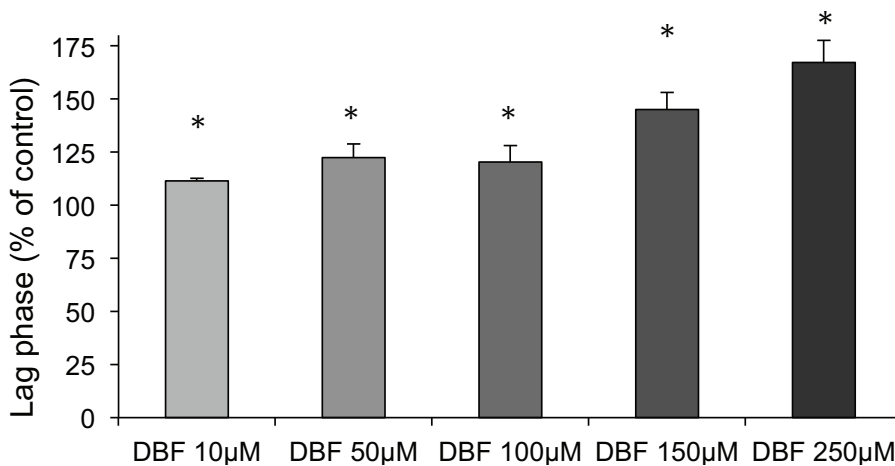


Figure 4.2.2 – Effects of DBF in the lag phase preceding the mitochondrial repolarization.

Mitochondria were incubated with DBF prior to succinate energization and $\Delta\Psi_m$ was evaluated using a TPP⁺-electrode as described in Chapter 2. Data are means \pm SEM of different experiments. * indicates statistically significant difference versus control ($P < 0.05$).

4.2.2 – Mitochondrial oxygen consumption

Oxidative phosphorylation and respiratory chain competence of mitochondria were investigated by following oxygen consumption upon exposure to DBF. The results showed an increase in the respiratory state 2 of mitochondria exposed to DBF (Figure 4.2.3), which could suggest an increase in membrane permeability to protons and consequent increase in oxygen

consumption in the respiratory chain. However, no differences were found when we tested the mitochondrial membrane permeability to protons assessing mitochondrial osmotic behavior in a NH_4NO_3 buffer (Figure 4.2.4).

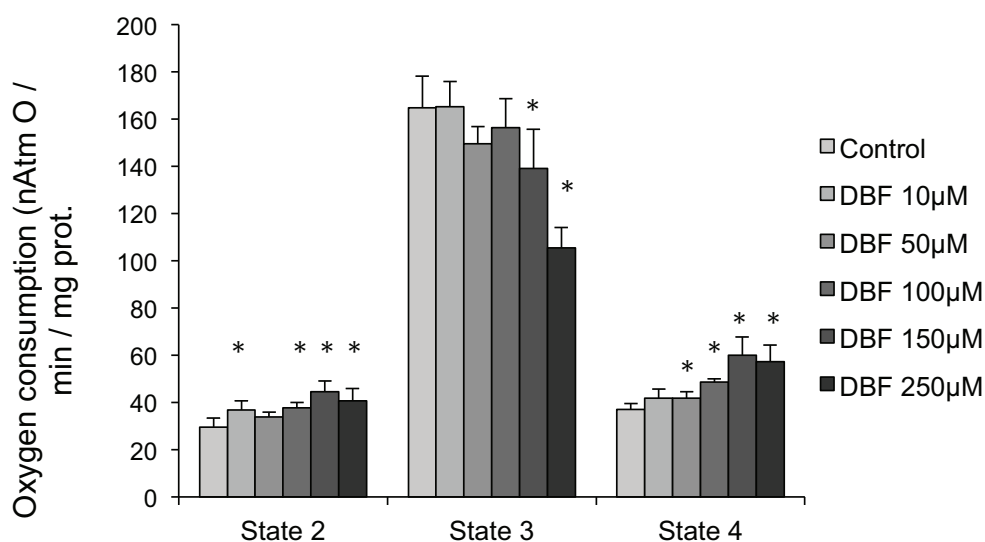


Figure 4.2.3 – Effects of DBF on mitochondrial oxygen consumption.

State 2, state 3 and state 4 respiration in liver mitochondria, upon incubation with DBF, were evaluated polarographically using a Clark oxygen electrode, as described in Chapter 2. Data are means \pm SEM of different experiments. * indicates statistically significant difference versus control ($P < 0.05$).

After addition of ADP to mitochondria, we found a decrease in respiratory state 3 (Figure 4.2.3) oxygen consumption rate when mitochondria were exposed to DBF. Still, the experiments also showed that even when state 3 was not clearly decreased phosphorylation was taking longer when DBF was present, supporting the enlarged lag phase reported previously (Figure 4.2.2) and the idea that DBF elicits some defects in the mitochondrial phosphorylative system. Additionally, respiratory state 4 was clearly increased in mitochondria exposed to DBF (Figure 4.2.3), reflecting the impairment in mitochondrial function and a possible disruption of mitochondrial membrane impermeability after phosphorylation and consequent forced respiration. Consequently, both RCR and ADP/O ratios were decreased in mitochondria

exposed to the pollutant (Figure 4.2.5), implying an impairment in the oxidative phosphorylation efficiency.

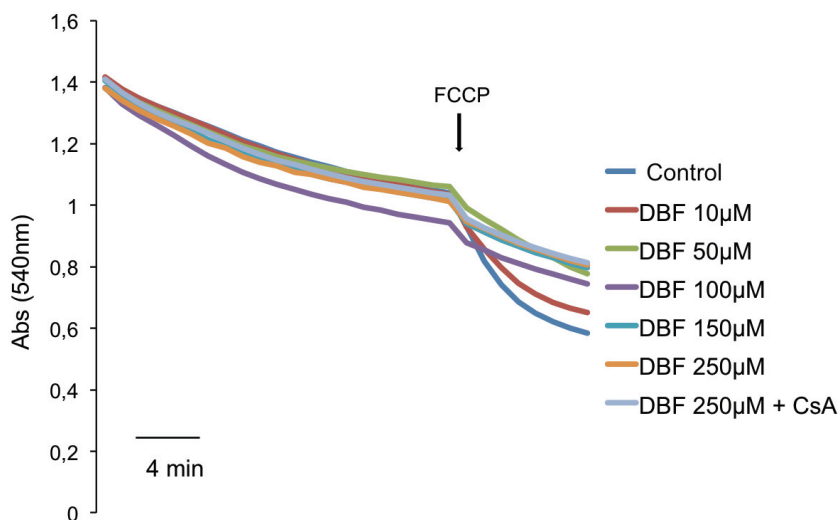


Figure 4.2.4 - Mitochondrial membrane permeability to protons after incubation with DBF.

Reactions were carried out in a NH_4NO_3 buffer using 1 mg of mitochondria. Osmotic volume changes were evaluated using spectrophotometry (540 nm) as described in Chapter 2. FCCP addition is indicated by the arrow. The traces are representative of different experiments performed with independent mitochondrial preparations.

4.2.3 – Enzymatic activities

We have also tested mitochondrial Cytochrome *c* Oxidase (COX) enzymatic activity, which showed no significant differences in mitochondria exposed to DBF, when compared to control (Figure 4.2.6), which deals with the constant state 3 respiratory rates. To try to elucidate the increased lag phase and impairment during phosphorylation, we have also assessed mitochondrial ATPase activity; the results showed that DBF caused a decrease in the ATPase activity for all the concentrations tested (Figure 4.2.7).

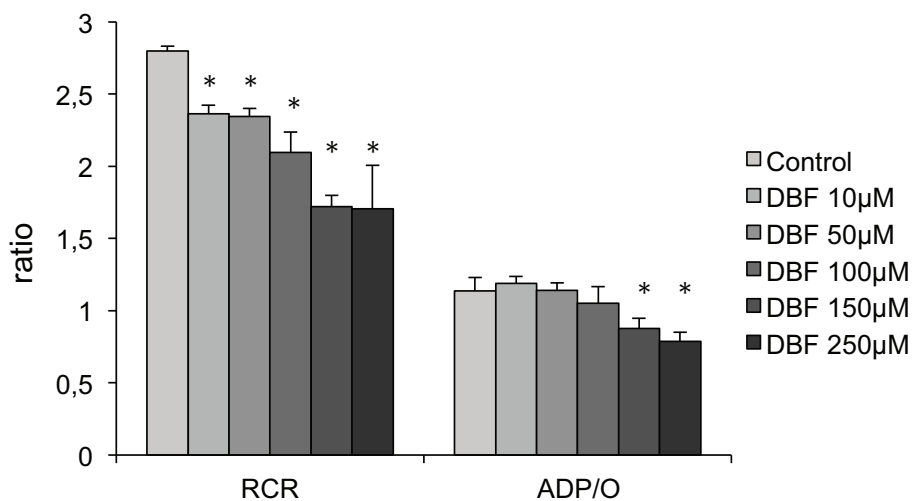


Figure 4.2.5 – Effects of DBF in mitochondrial RCR and ADP/O ratios.

Oxygen consumption was polarographically determined with a Clark oxygen electrode as described in Chapter 2. Data are means \pm SEM of different experiments. * indicates statistically significant difference versus control ($P < 0.05$).

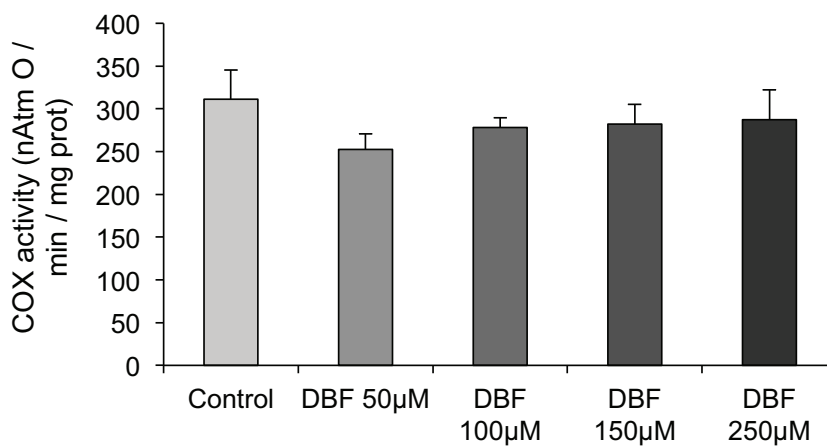


Figure 4.2.6 - Cytochrome c Oxidase activity.

Enzymatic activity was measured polarographically after incubation with DBF, using a Clark oxygen electrode as described in Chapter 2. Data is expressed in nAtoms O / min / mg protein. No statistically significant differences were found ($P < 0.05$).

Nevertheless, the defects in ATPase efficiency didn't fully match the "dose-dependent" increase in lag phase detected in the membrane potential experiments, and therefore the impairment during phosphorylative cycles was not due only to a less active mitochondrial complex V. The decrease in the ATPase activity can explain the longer lag phase but does not exclude that DBF can act on another component of the phosphorylative system (e.g. ANT).

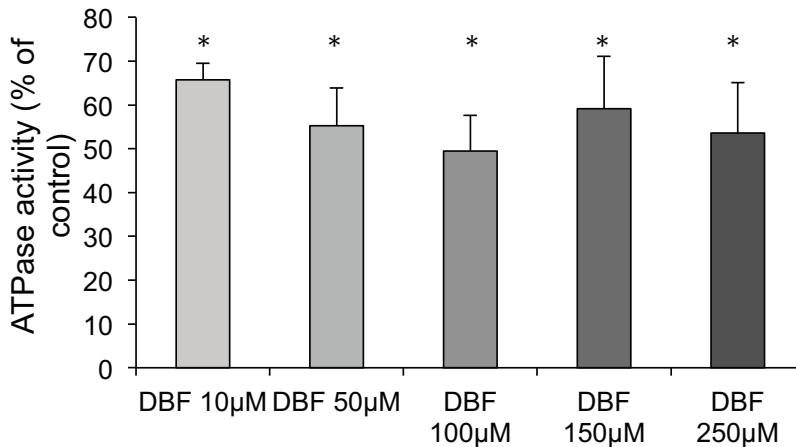


Figure 4.2.7 – Mitochondrial ATPase activity.

This activity was measured spectrophotometrically in mitochondria upon incubation with DBF, as described in Chapter 2. Data are means \pm SEM of different experiments. * indicates statistically significant difference versus control ($P < 0.05$).

4.2.4 – Mitochondrial swelling and MPT induction

The effects of DBF on mitochondrial permeability transition (MPT) were assessed using light scattering to monitor mitochondrial swelling. We found that DBF reduced mitochondrial calcium-induced and CsA-sensitive osmotic swelling (Figure 4.2.8), suggesting that the pollutant can inhibit the permeability transition to some extent. This data pointed out to an effect of DBF in one particular component of the phosphorylative system that is also enrolled in the permeability transition, the adenine nucleotide translocase (ANT).



Figure 4.2.8 – Effects of DBF on the susceptibility to the induction of mitochondrial permeability transition (MPT). Mitochondrial swelling was evaluated spectrophotometrically (540 nm) as described in Chapter 2. MPT was induced by the addition of Ca^{2+} . The traces are representative of different experiments performed with independent mitochondrial preparations.

To test the hypothesis that DBF interacts with ANT, we first performed a titration with carboxyatractyloside (CAT), a highly selective inhibitor of ANT, cytosolic side-specific, that causes stabilization of the *c* conformation of ANT leading to mPTP opening and loss of mitochondrial membrane potential. For titration with CAT, after addition of succinate, mitochondria developed a potential of about -220 mV (negative inside). With the addition of ADP, the potential dropped because ATP synthase uses $\Delta\Psi_m$ to phosphorylate ADP. After a short lag phase, when ADP phosphorylation takes place, the transmembrane potential repolarized close to the initial value. Successive additions of CAT aliquots before ADP addition, as indicated in Figure 4.2.9, progressively blocked a higher number of ANT units contributing to the observed decreased number of phosphorylation cycles induced by successive ADP additions, as well as to the observed increasing in lag phase corresponding to successive phosphorylation cycles.

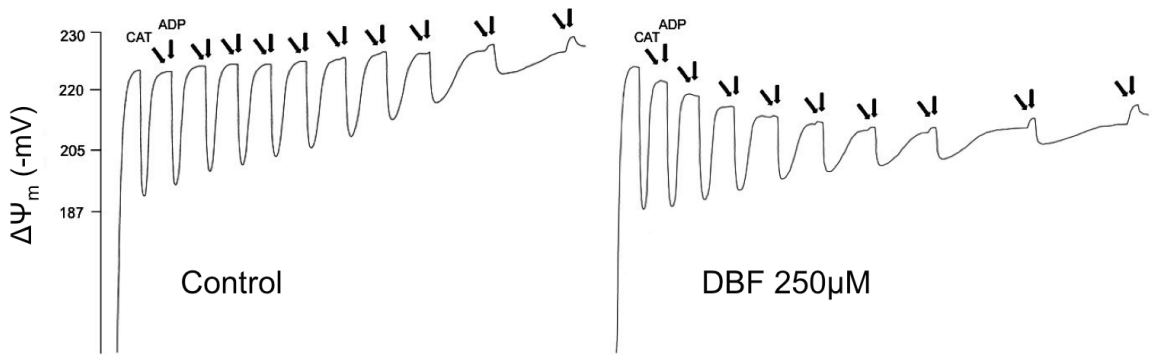


Figure 4.2.9 – Mitochondrial transmembrane potential ($\Delta\Psi_m$) and lag phase.

DBF was added to the reaction medium (1ml) with mitochondria (1mg) and allowed to incubate for 3min before the addition of succinate as substrate. Addition of ADP induces phosphorylation/depolarization. A titration with CAT was performed, adding successive amounts of 0.02 nmol, where indicated by the arrows. ADP aliquots (100 nmol) were also added to induce depolarization. The traces represent typical direct recordings from independent experiments.

Measuring mitochondrial membrane potential after ADP addition we found that, with DBF, less CAT was needed to completely abolish repolarization after phosphorylation (Figure 4.2.10), indicating that mitochondria incubated with DBF already had ANT inhibition and thus an impaired phosphorylative system. Furthermore, in Figure 4.2.11 we can see that mitochondria incubated with DBF show a higher increase in phosphorylative lag phase when CAT is added. Exposure to DBF is already causing an interference/inhibition of ANT in mitochondria, and the lag phase after ADP loading is already higher for DBF-exposed mitochondria, relatively to control. When we performed the experiments with CAT, the expected increase in lag phase is greater in DBF-exposed mitochondria. Moreover, for a little amount of CAT added to DBF-exposed mitochondria, much less than in control, depolarization/repolarization after ADP loading is abolished (effect that is also reflected on Figure 4.2.11), which is in agreement with previous experiments showing DBF inhibition of ANT in isolated mitochondria.

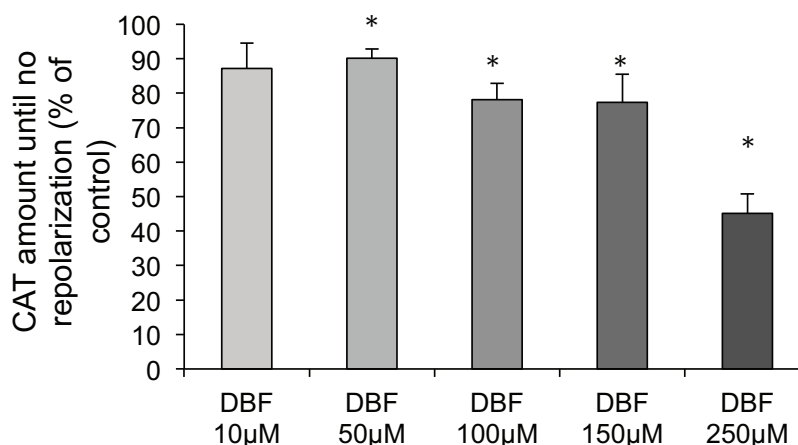


Figure 4.2.10 – Inhibition of mitochondrial ANT carrier by CAT.

Mitochondrial transmembrane potential ($\Delta\Psi_m$) was measured with a TPP⁺-electrode as previously, and a titration with CAT was performed until no depolarization/repolarization was observed when ADP was added to mitochondria. Data are means \pm SEM of different experiments. * indicates statistically significant difference versus control ($P < 0.05$).

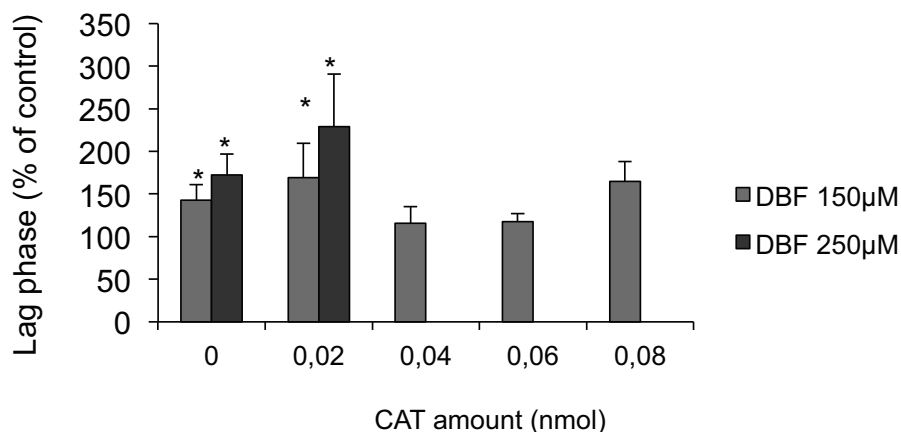


Figure 4.2.11 – Effects of DBF and CAT on mitochondrial phosphorylative lag phase (% of control).

Mitochondria were incubated with DBF as described in Chapter 2. Little amounts of CAT were progressively added before ADP addition. The experiments were the same as in Figure 4.2.9. Data are means \pm SEM of different experiments. * indicates statistically significant difference versus control ($P < 0.05$).

Using CAT also in mitochondrial swelling experiments, we could see that DBF prevents mitochondrial swelling that is induced by CAT (Figure 4.2.12), and we also compared this prevention with that provided by bongkreikic acid (BKA); both DBF and BKA inhibit MPT induction and consequent mitochondrial swelling (Figure 4.2.12).

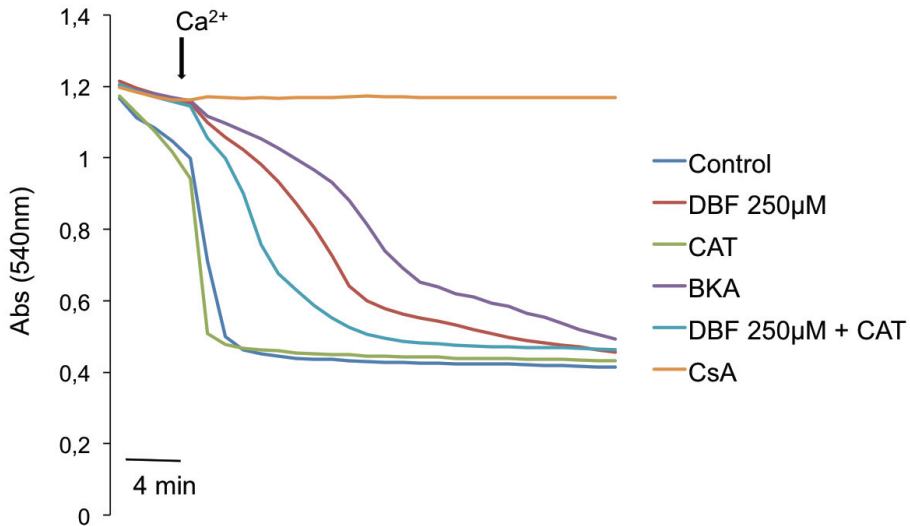


Figure 4.2.12 – Effects of DBF on the susceptibility to the induction of mitochondrial permeability transition (MPT).

Osmotic changes were evaluated spectrophotometrically (540 nm) as described in Chapter 2. DBF, CAT (0.4 nmol), BKA (3.7 nmol) or CsA were added to mitochondria before the beginning of the assay. The traces are representative of different experiments performed with independent mitochondrial preparations.

4.2.5 – Calcium retention capacity

To further analyze MPT induction and DBF effects we tested calcium retention capacity in mitochondria, using the fluorescent probe Calcium-Green

5N. These experiments showed that DBF exposure induced an increase in the calcium retention capacity after energization, when compared to control (Figure 4.2.13). DBF caused a delay in calcium release from mitochondria, that is the consequence of mPTP opening and MPT induction, a CsA-sensitive event (Figure 4.2.13).

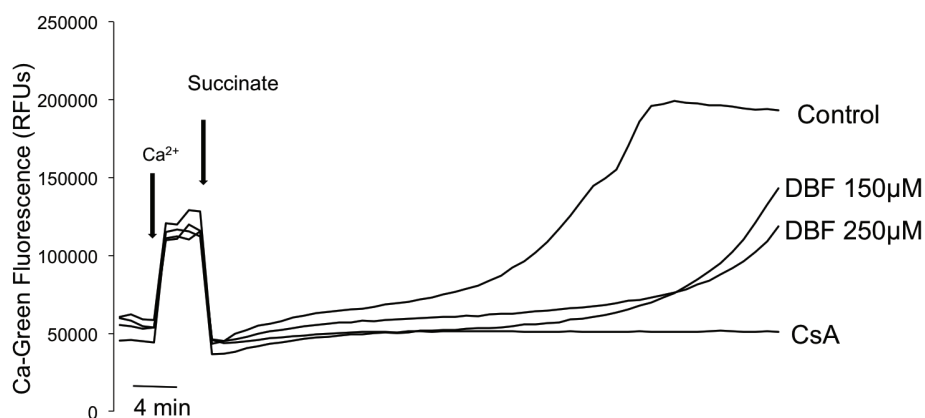


Figure 4.2.13 – Effects of DBF on mitochondrial calcium fluxes.

Calcium fluxes, expressed as relative fluorescence units (RFUs), were fluorometrically monitored using the probe Calcium-Green-5N as described in Chapter 2. DBF was added to mitochondria before beginning the assay. The traces are representative of different experiments performed with independent mitochondrial preparations.

Analyzing calcium retention capacity in mitochondria we confirmed that CAT greatly induces MPT (Figure 4.2.14); DBF exposure prevents the induction of MPT, even when CAT is present, and again it displays an effect similar to BKA, which blocks ANT in a conformation that prevents pore opening and MPT (Figure 4.2.14).

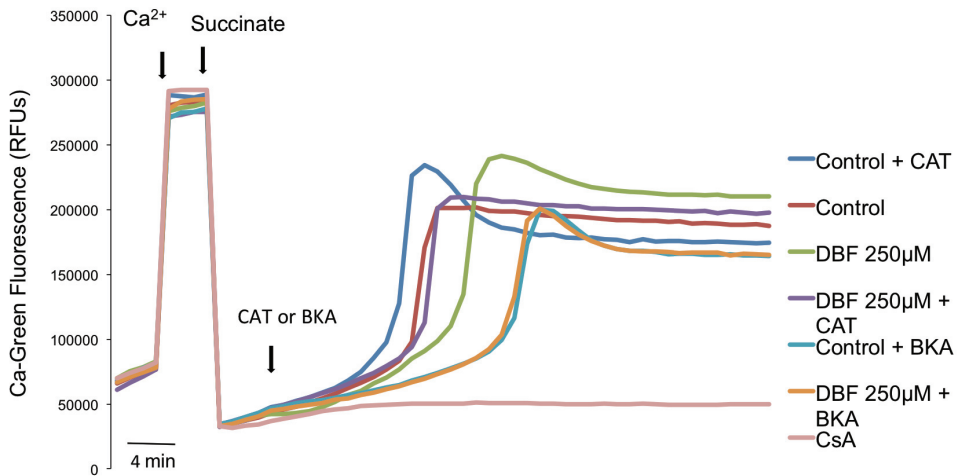


Figure 4.2.14 – Effects of DBF and ANT modulators on mitochondrial calcium fluxes.

Calcium fluxes were fluorometrically monitored using the probe Calcium-Green-5N, as described in Chapter 2. DBF or CsA were added before the beginning of the assay. CAT (0.4 nmol) or BKA (3.7 nmol) were added where indicated by the arrows. The traces are representative of different experiments performed with independent mitochondrial preparations.

4.2.6 – ANT immunoprecipitation

Keeping in mind that, during MPT induction, permeability pore opens and CypD binding to ANT regulates it, we performed immunoprecipitation assays. Using mitochondria samples that were used in MPT induction experiments, we immunoprecipitated ANT and then used western blot to evaluate CypD present in the precipitate (thus bound previously to ANT). We could see that, when MPT induction is prevented, either with CsA or DBF exposure, the ratio CypD/ANT in the sample is decreased when compared to control or CAT (Figure 4.2.15), also suggesting that DBF was interacting with ANT and so preventing CypD binding and consequent MPT induction.

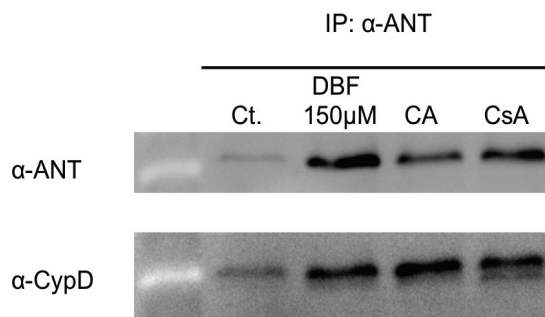


Figure 4.2.15 – Immunoprecipitation of ANT and CypD from mitochondrial extracts.

Mitochondrial samples used in MPT experiments were collected. Immunoprecipitation with an antibody α -ANT was performed using agarose beads and western blots were performed as described in Chapter 2. Images are representative bands of protein content.

4.2.7 – mPTP activation by mitochondrial outer membrane translocator protein (TSPO)

In the last years, several other proteins have been reported to modulate mPTP opening, namely the mitochondrial outer membrane translocator protein of 18 kDa, TSPO, formerly known as the peripheral benzodiazepine receptor. We wanted to check if DBF was also interacting with this receptor and this way modulating MPT induction.

We performed calcium retention capacity experiments using a ligand for TSPO, PK11195, which induces pore opening and consequent calcium release (Figure 4.2.16). However, when DBF was present, no differences were found in calcium retention capacity of mitochondria challenged with the ligand (PK11195), suggesting that DBF effects were not being exerted via TSPO binding (Figure 4.2.16).

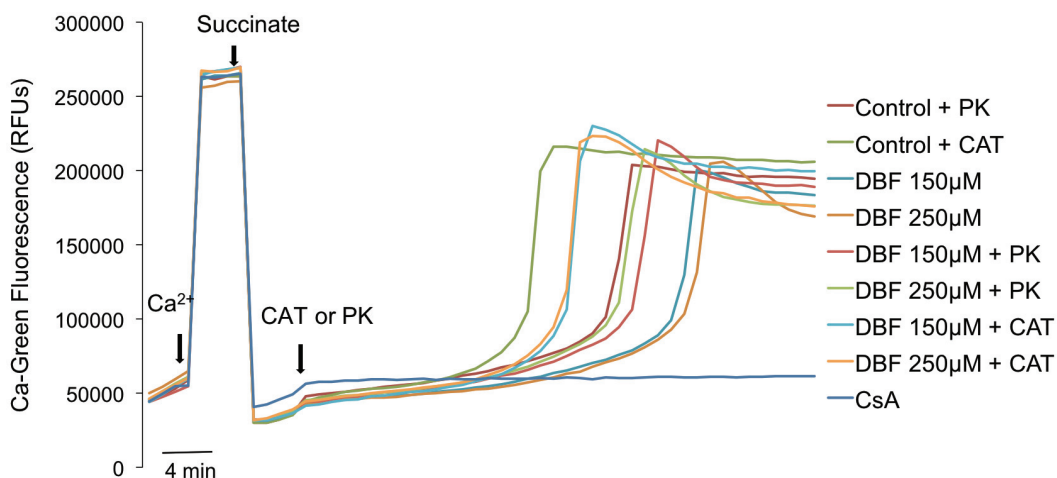


Figure 4.2.16 – Effects of DBF and mitochondrial outer membrane translocator protein (TSP0) modulation on mitochondrial calcium fluxes.

Calcium fluxes were fluorometrically monitored using the probe Calcium-Green-5N, as described in Chapter 2. DBF or CsA were added before the beginning of the assay. PK11195 (30 nmol) or CAT (0.4 nmol) were added where indicated by the arrows. The traces are representative of different experiments performed with independent mitochondrial preparations.

4.3 – Discussion

Environmental pollutants such as dioxins and furans are extremely toxic and related with several diseases, such as cancer. Some toxicology studies have addressed health effects related to exposure to chemicals, but few have described the molecular targets that cause toxicity (Yoshioka et al., 2011). Therefore, clarifying the role of pollutants in some basic mechanisms of toxicity, such as unbalance of bioenergetics, may help to explain the development of some diseases related to environmental pollutants exposure.

DBF is an aromatic ether with properties and chemical structure similar to dioxins, listed as a pollutant of concern due to its persistence in the environment, potential to bioaccumulation and toxicity to humans. Potential exposure to DBF may occur through inhalation and dermal contact, particularly at sites engaged in combustion/carbonization processes. This

work focused on the toxic effects of DBF directly on mitochondria, using an *in vitro* approach, given that not many studies have been conducted concerning mitochondrial harming by environmental pollutants. We have previously reported some of the effects caused by DBF, either for mitochondria isolated from lungs (Duarte et al., 2011) or lung cells in culture (Duarte et al., 2012).

Mitochondria are key organelles in cellular function. Their main role is to generate energy (ATP) for cellular function, but they also participate in several other processes such as calcium homeostasis, free radicals generation and apoptosis (Contreras et al., 2010; Orrenius et al., 2007). The study of drug-induced mitochondrial toxicity may elucidate distinct mechanisms by which drugs interfere with energy production by the cell. Given the importance of mitochondria for organisms, to evaluate toxic effects that impair mitochondrial function is necessary when one wants to study the toxicity of a given compound, namely an environmental pollutant. The aim of this study was to evaluate if DBF is a mitochondrial toxicant through interference with the bioenergetic features of the mitochondria.

The results indicate that mitochondria are targeted by DBF-induced toxicity. Although DBF did not affect mitochondrial capacity to generate and sustain membrane potential, created by the electron transport chain and used to drive production of ATP from ADP in the matrix, we could see a decrease in the mitochondrial phosphorylative efficiency elicited by DBF, which seems to be a critical event in DBF-induced impairment of cell function. Similar mitochondrial impairment had already been reported for exposure to other toxicants (Simões et al., 2010). Energization and phosphorylation capacities of mitochondria isolated from Wistar rats were investigated by following the transmembrane potential ($\Delta\Psi_m$) developed by mitochondria upon succinate oxidation. Although $\Delta\Psi_m$ developed after succinate energization was not affected, the lag phase that occurs in the phosphorylative cycle and precedes repolarization was increased in mitochondria incubated with DBF when compared to control. This reflects an impairment in the phosphorylative system, which causes a delay in the restoration of membrane potential after conversion of ADP to ATP. When measuring oxygen consumption rate by mitochondria, we could detect a decrease in respiratory state 3 (active phosphorylation) after exposure to DBF. Additionally, an increase in

respiratory state 2 and state 4 with mitochondria energized with succinate would suggest an increase in mitochondrial membrane permeability to protons, consequent membrane potential dissipation and activation of respiration to regenerate transmembrane potential; however, no increase in permeability to protons was found after exposure to DBF. We could see that mitochondria exposed to DBF didn't recover the state 4 respiration values after phosphorylation, showing that DBF affects mitochondrial integrity and coupling of oxidative phosphorylation. Consequently, both respiratory control ratio (RCR) and efficiency of ATP synthesis coupled to mitochondrial respiration, referred to as the ADP/O ratio, were decreased in mitochondria exposed to DBF when comparing to control.

To further explore and understand the cause for the increased lag phases induced by DBF, showing an impairment in phosphorylative system, and the oxygen consumption rates, we evaluated ATPase activity, since other component of the phosphorylative system should be impaired, in order to justify the evident increase in mitochondrial lag phase during phosphorylation. In fact, ATPase activity was decreased in mitochondria exposed to DBF. Although, the defects in ATPase efficiency didn't fully match the "dose-dependent" increase in lag phase detected in the membrane potential experiments, and this effect does not exclude action at the level of other components of the phosphorylative system.

Further studies were conducted in order to evaluate the mechanisms by which DBF affects mitochondria phosphorylative system. Having detected an inhibition of MPT elicited by DBF, we considered that a common player of both phosphorylation and MPT was a target for DBF toxicity. We performed experiments to evaluate MPT induction, a phenomenon that results from the opening of the so called mitochondrial permeability transition pore (mPTP) causing membrane potential disruption, matrix swelling and outer membrane rupture (Kinnally et al., 2011). The results showed that this toxicant prevented MPT induction, when compared with control mitochondria. Thus, although the impairment of ATP synthesis in hepatic mitochondria, data prompted us the idea that DBF was interacting with ANT; and so DBF was somehow mimicking CsA or BKA to inhibit induction of the MPT and prevent mitochondrial swelling.

With the results pointing out an interaction of DBF with ANT as the cause for the decreased efficiency of ATP production, we performed titrations with CAT to better understand DBF effects on mitochondrial transmembrane potential. CAT is a highly selective inhibitor of cytosolic side-specific mitochondrial ANT that causes stabilization of the *c* conformation of ANT leading to mPTP opening. The results showed that, in mitochondria incubated with DBF, less CAT was needed to completely inhibit repolarization after ADP addition when compared to control. On the other hand, mitochondrial lag phase during a phosphorylative cycle was larger when we added CAT to mitochondria incubated with DBF, compared to control. This showed us that, when exposed to DBF, mitochondria already had some ANT inhibition, supporting the DBF/ANT interaction and consequent impairment of the translocase's function. Using CAT also in mitochondrial swelling experiments, we could see that DBF prevented mitochondrial swelling that is induced by CAT, and we also compared this prevention with that provided by BKA, observing that both DBF and BKA inhibit MPT induction and consequent mitochondrial swelling. Additional experiments were performed using the fluorescent probe calcium-green to assess calcium retention capacity. We confirmed that DBF inhibited MPT induction, not only when compared only to control situation but also preventing CAT effect on the MPT triggering.

In order to elucidate the involvement of DBF in the mPTP opening and the role of an interaction with ANT, we performed immunoprecipitation to check this interaction. It is known that, during mPTP opening, CypD interactions with ANT promote mPTP opening and MPT induction (Rasola et al., 2010; Hansson et al., 2011). We could see that, in samples that were used in MPT induction experiments, immunoprecipitating ANT we could detect CypD (thus bound previously to ANT). When MPT induction was prevented, either with CsA or DBF exposure, the ratio CypD/ANT in the sample was decreased when compared to control or CAT, also supporting that DBF was interacting with ANT and so preventing CypD binding and MPT induction. Nonetheless, we also wanted to assess if DBF was interacting with other protein that has been reported to modulate mPTP opening, the mitochondrial outer membrane translocator protein of 18 kDa, TSPO, formerly known as the peripheral benzodiazepine receptor (Azarashvili et al., 2010;

Ricchelli et al., 2011; Sileikytė et al., 2011). We wanted to check if DBF was also interacting with this receptor and this way modulating MPT induction. We performed calcium retention capacity experiments using a ligand for TSPO, PK11195, which induces pore opening and consequent calcium release. However, when DBF was present, no differences were found in calcium retention capacity of mitochondria challenged with the ligand (PK11195), suggesting that DBF effects were not being exerted via TSPO binding and following mPTP modulation.

In summary, this work shows that DBF impairs hepatic mitochondrial function. DBF toxicity is mainly related to a decrease in phosphorylative efficiency, shown by an increase in lag phase. Also, a possible interaction of DBF with ANT carrier is supported by our results and induction of mitochondrial permeability transition is also affected by DBF exposure. Yet, further studies focused on understanding the upstream molecular mechanisms by which metabolic pathways are deregulated are needed. Those may ultimately help to develop therapeutic strategies and to prevent diseases related to pollutants exposure.

Chapter 5

Exposure to Dibenzofuran triggers autophagy in lung cells

5.1 - Introduction

Although DBF is considered an environmental toxicant, to which populations are exposed mainly through inhalation, studies about pollutants-induced toxic effects in lung function are scarce. We have studied some of the effects of DBF exposure in isolated mitochondria both from lung and liver, respectively the primary target organ and the metabolizing organ.

Mitochondrial dynamics is clearly important in cellular homeostasis. Mitochondria are the energy suppliers for eukaryotic cells and a proper mitochondrial function is therefore essential in the fulfilment of the tissues energy-demand. ATP synthesis occurs via electron transport and oxidative phosphorylation; for that reason, mitochondria are also involved in the production of ROS (Carlson et al., 2005). Therefore, alterations of mitochondrial bioenergetic features by toxicants reduce energetic charge and result in cell death. Previous studies have identified mitochondrial targets of environmental pollutants, namely ROS production and decreased ATP content (Senft et al., 2002a; Shertzer et al., 2006). Consequently, maintenance of cell function is strictly dependent on the existence of a healthy population of mitochondria. In this respect, mitochondrial degradation by autophagy (mitophagy) may play an essential role in maintaining mitochondrial functionality.

Autophagy is an evolutionarily conserved subcellular degradation process decomposing folded proteins, protein complexes and entire organelles, such as aggregates of misfolded proteins or damaged mitochondria (Gozuacik and Kimchi, 2007). Classically considered to be a pathway contributing to cellular homeostasis and adaptation to stress (e.g., during times of starvation), the autophagic machinery is now recognized to be recruited during several pathogenic conditions and diseases, and during the execution of a caspase-independent cell death (Rubinsztein et al., 2007; Levine and Kroemer, 2008).

The main objectives of this work concerned DBF effects on pulmonary cellular function. A human lung epithelial cell line (A549) exposed in culture to DBF was used to address cell death and viability, ATP content, mitochondrial membrane potential, oxygen consumption and ROS production, nuclear

morphology and autophagy induction. Clarifying the role of pollutants in some mechanisms of toxicity, such as unbalance of bioenergetics status or cell death induction, may help to explain the progressive and chronic evolution of lung diseases.

5.2 – Results

5.2.1 – Cell death / viability

A549 cell viability after incubation with DBF was a basic parameter to assess in order to understand the toxic effects of DBF on lung cells. Cell viability showed not to be affected by DBF incubation (Figure 5.2.1 - A), indicating that the effects of this pollutant in A549 cells do not induce cell death, for the concentrations and exposure periods tested. We performed flow cytometry experiments after staining of the cells with annexin V (detecting cells that have expressed phosphatidylserine on the cell surface, a feature found in apoptosis) and Propidium Iodide (PI) (a membrane impermeant dye generally excluded from viable cells, that enters the necrotic cells and is considered therefore a marker for necrotic cell death).

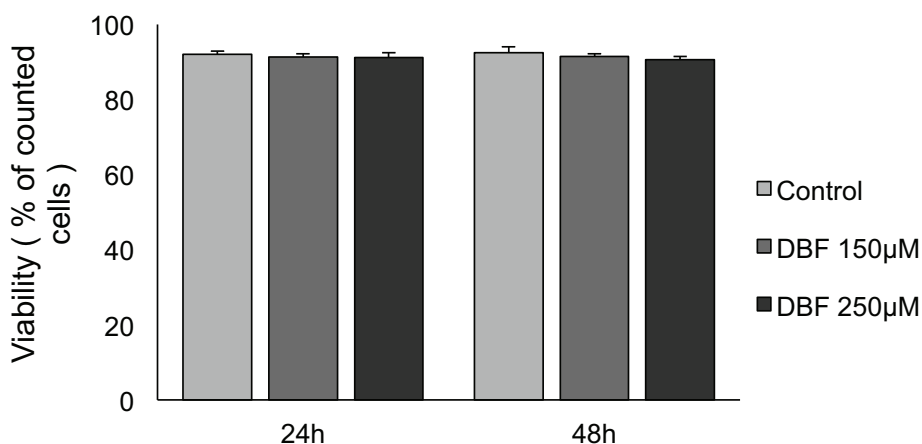


Figure 5.2.1 (A) – A549 cell death/viability after DBF exposure.

A549 cells were cultured as described in Chapter 2. DBF was added for 24h or 48h and Annexin-PI assay was performed. Data are means \pm SEM of different experiments. No statistically significant differences were found ($P < 0.05$).

A549 cells negative staining for annexin-V and propidium iodide showed that DBF didn't cause apoptosis or necrosis (respectively) in A549 cells (Fig. 5.2.1 – A).

A549 cells viability upon exposure to DBF was also correlated with the amount of LDH released into the media. DBF incubation did not increase the release of LDH (Fig. 5.2.1 – B), indicating that DBF exposure doesn't cause significant necrotic cell death at 24h of exposure.

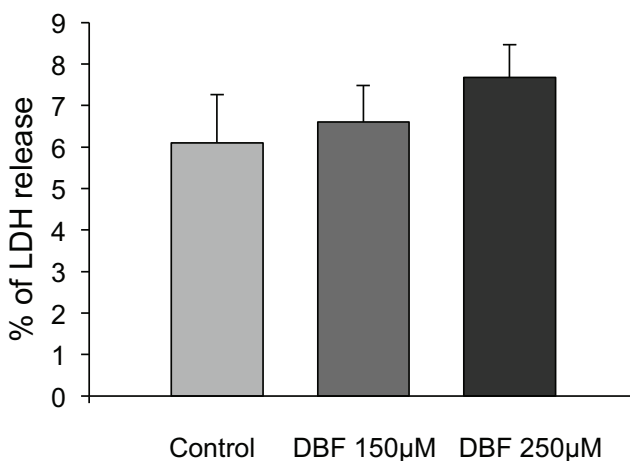


Figure 5.2.1 (B) – Effects of DBF exposure on LDH release.

A549 cells were cultured and treated for 24h with DBF. Samples were collected and assayed for LDH release into the media using spectrophotometry, as described in Chapter 2. No statistically significant differences were found ($P < 0.05$).

5.2.2 – Nuclear morphology (apoptosis)

Staining of nucleus with Hoechst 33342 was visualized in order to evaluate apoptosis induction in A549 cells exposed to DBF (Figure 5.2.2). Exposure to DBF clearly caused a decrease in cell number, which is consistent with data obtained with cell proliferation assays. However, there is no evidence of apoptotic nucleus (brightly staining condensed chromatin,

nuclear fragmentation or apoptotic bodies) indicating that DBF didn't induce apoptosis in A549 cells.

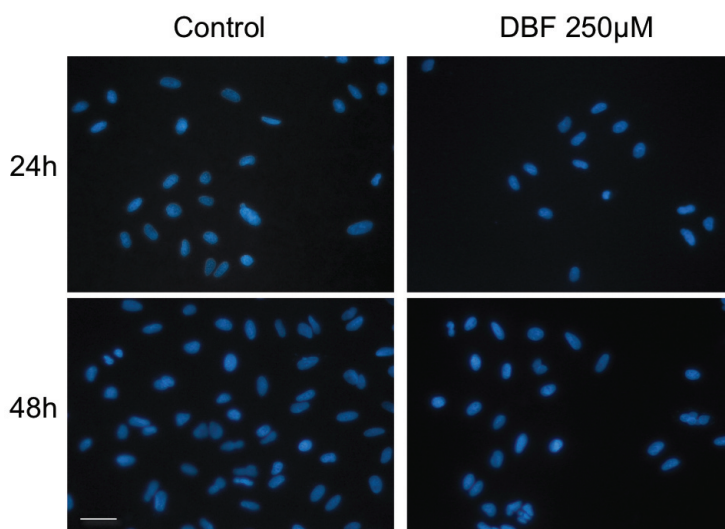


Figure 5.2.2 – Fluorescence microscopy images showing A549 cells treated for 24h and 48h with 250 µM DBF.

A549 cells were cultured on top of cover slips, exposed to DBF and stained with Hoechst 33342 as described in Chapter 2. Representative images are presented to show the nuclear morphology in A549 cells. Scale bar, 20 µm.

5.2.3 – Cell proliferation

Cell proliferation was assessed as another fundamental parameter to evaluate time- and dose-dependent effects of DBF on A549 cells. As shown in Figure 5.2.3, exposure of A549 cells to DBF resulted in inhibition of cell proliferation; this inhibition was even more accentuated at 48h. Inhibition of cell proliferation for 150 µM DBF was significant only for the 48h exposure (Figure 5.2.3). Since no cells were detached (initial indicator of acute cell damage), that suggested that inhibition of cell proliferation was due to a specific effect of DBF on cell division/cell cycle progression, rather than on cell viability.

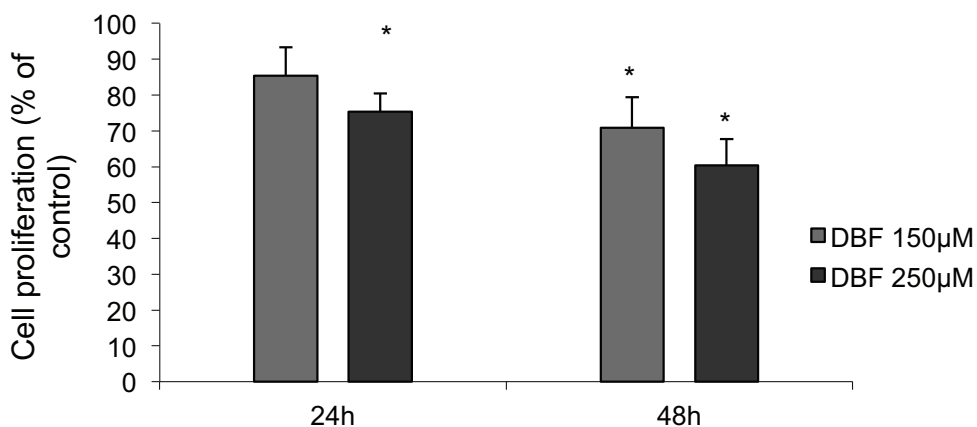


Figure 5.2.3 - Effects of DBF on cell proliferation.

After 24h and 48h treatment, cell proliferation was estimated spectrophotometrically by sulforhodamine B assay, as described in Chapter 2. Percent proliferation was calculated by comparing with control cell proliferation, considered as 100% at each time point. Data are means \pm SEM of different experiments. * indicates statistically significant difference versus control ($P < 0.05$).

5.2.4 – MTT reduction

Cell cultures exposed to 250 μ M DBF for 24 h showed a significant decrease in MTT reduction (Figure 5.2.4), indicating decreased mitochondrial activity. This effect was even more pronounced in cell cultures exposed to 250 μ M DBF for 48h, and with this treatment also 150 μ M DBF caused a decrease in MTT reduction.

5.2.5 – Adenine nucleotides content

Evaluation of adenine nucleotides content in A549 cells revealed that exposure to DBF caused a significant decrease in ATP content (Figure 5.2.5 -

A) relatively to control cells, with a consequent decrease in ATP/ADP ratio (Figure 5.2.5 - B).

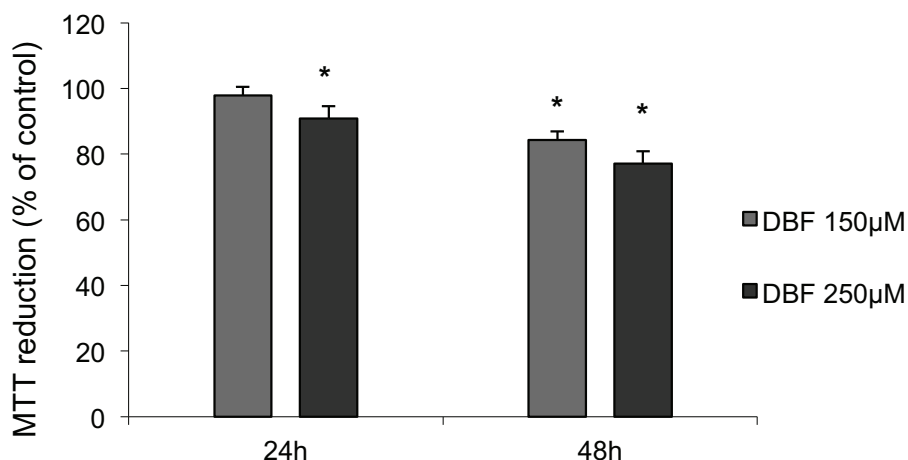


Figure 5.2.4 – Relative MTT reduction after exposure to DBF.

After 24 and 48 hours, mitochondrial activity was measured by MTT assay, using spectrophotometry to measure the amount of MTT formazan, as described in Chapter 2. Data are means \pm SEM of different experiments. * indicates statistically significant difference versus control ($P < 0.05$).

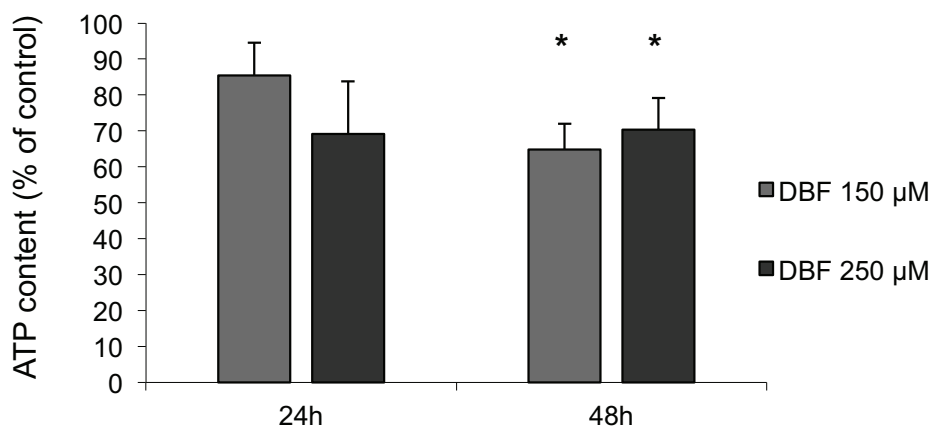


Figure 5.2.5 (A) – ATP content in lung cells exposed to DBF.

A549 cells were cultured, exposed to DBF for 24h and 48h and then collected to extract adenine nucleotides as described in Chapter 2. ATP levels were measured by reverse-phase HPLC. Data are means \pm SEM of different experiments. * indicates statistically significant difference versus control ($P < 0.05$).

The decline in ATP content in A549 cells was significant for both concentrations of the pollutant tested (150 μ M and 250 μ M) but only for 48h of exposure. The data shows an energy deficit in lung cells exposed to DBF suggesting impairment in ATP production.

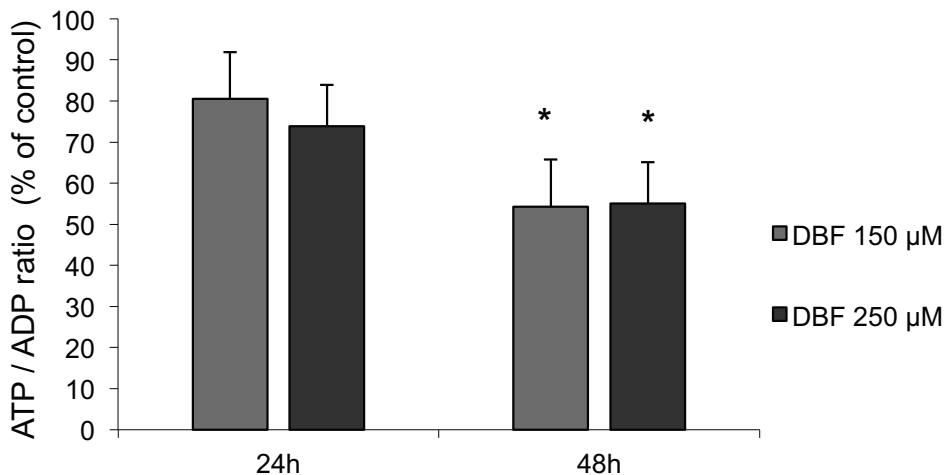


Figure 5.2.5 (B) – ATP/ADP ratio in lung cells exposed to DBF.

A549 cells were cultured, exposed to DBF for 24h and 48h and then collected to extract adenine nucleotides as described in Chapter 2. Data are means \pm SEM of different experiments. * indicates statistically significant difference versus control (P < 0.05).

5.2.6 – Measurement of mitochondrial membrane potential ($\Delta\Psi_m$)

Using A549 cells incubated for 24h with DBF, we assessed mitochondrial membrane potential with the fluorescent dye TMRM. The results showed that exposure to DBF caused a decrease in mitochondrial potential for 24h treatment (Figure 5.2.6). The decrease in mitochondrial potential was elicited by exposure to 250 μ M DBF and it was significantly lower when compared to control.

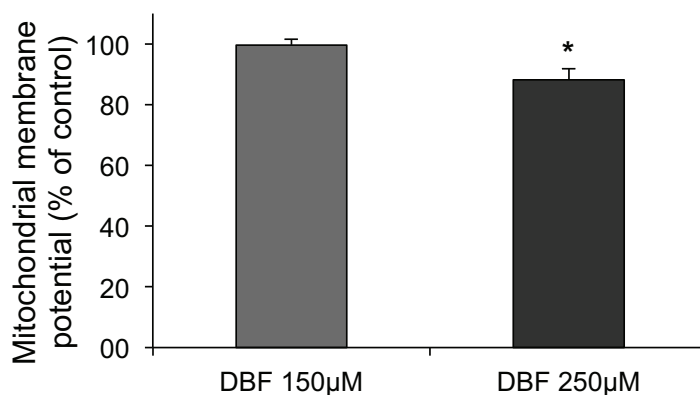


Figure 5.2.6 – Mitochondrial membrane potential ($\Delta\Psi_m$) in A549 cells exposed to DBF.

Cells exposed for 24h to DBF were used to estimate mitochondrial membrane potential ($\Delta\Psi_m$) fluorometrically with the probe TMRM, as described in Chapter 2. Data are means \pm SEM of different experiments. * indicates statistically significant difference versus control ($P < 0.05$).

5.2.7 – Measurement of mitochondrial oxygen consumption

Oxygen consumption was evaluated in A54 cells exposed to DBF for 24h. We could see that DBF exposure caused a decrease in mitochondrial oxygen consumption rate (Figure 5.2.7), when compared to control. The decreased oxygen consumption rate indicates an impairment in mitochondrial function caused by exposure to DBF, showing that the pollutant can induce damage in lung cells at the OXPHOS level.

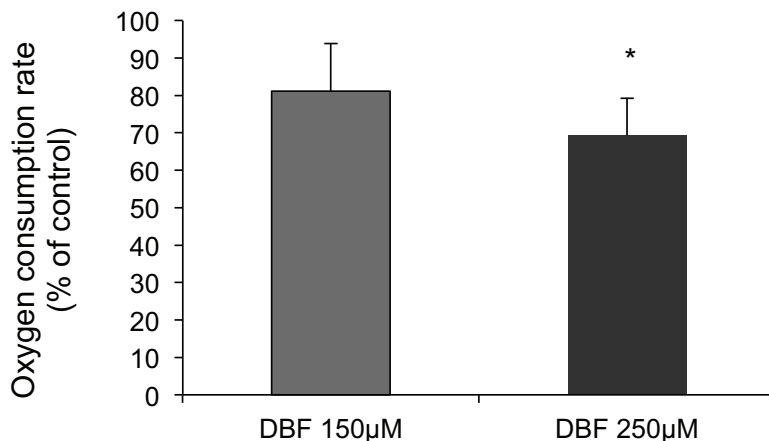


Figure 5.2.7 – Mitochondrial oxygen consumption rate in A549 cells exposed to DBF.

Cells exposed for 24h to DBF were used to estimate mitochondrial oxygen consumption rate using fluorometry, as described in Chapter 2. Data are means \pm SEM of different experiments. * indicates statistically significant difference versus control ($P < 0.05$).

5.2.8 – Measurement of ROS production

The evaluation of the ROS formation rate in cells exposed to DBF was done using a probe that is fluorescent when oxidized ($H_2DCF-DA$), giving us an estimate of the ROS production in cells after 24h of exposure to DBF.

For both concentrations tested, 150 μM and 250 μM , ROS production rate was decreased (Figure 5.2.8) when compared to control. Despite the lower rate in cells exposed to 150 μM DBF, the decreased was only significant in cells exposed to 250 μM DBF.

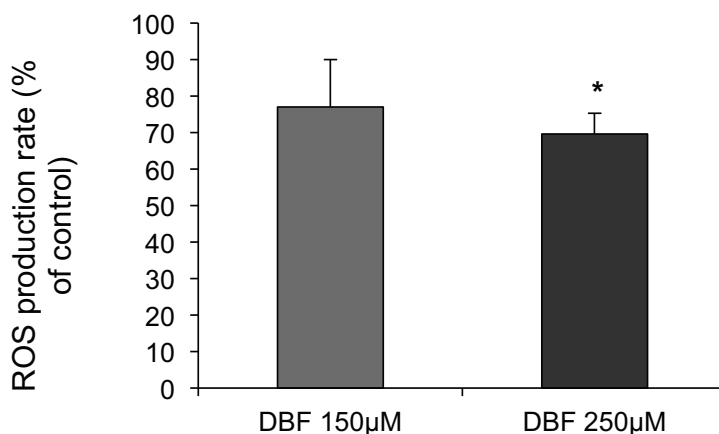


Figure 5.2.8 – ROS production rate in A549 cells after exposure to DBF.

Cells were cultured and exposed to DBF for 24h, and then assayed for ROS production fluorometrically using the probe H₂DCF-DA, as described in Chapter 2. Data are means ± SEM of different experiments. * indicates statistically significant difference versus control (P < 0.05).

5.2.9 – LC3 distribution pattern and autophagy induction

LC3 protein is mostly present in the soluble form (LC3-I) in the cytosol during basal physiological conditions. When autophagy is induced, LC3-I is processed to form LC3-II that is present in autophagosome membranes. We transfected A549 cells with YFP-LC3 plasmid and then exposed the cells to DBF (250 μM) or incubated them in starvation medium as a positive control for autophagy induction.

When we analysed the intracellular distribution of YFP-LC3 in A549 cells, we noticed that DBF exposure induced the accumulation of this marker of autophagy into punctuate, vesicular structures (Figure 6.2.9). On the contrary, control cells displayed a faint, diffuse cytoplasmic YFP-LC3 distribution. Of note, the punctuate pattern of YFP-LC3 was similar to that observed in cells that underwent starvation, the prototypical inducer of autophagy (Figure 5.2.9). A quantitative, blind analysis of YFP-LC3 distribution showed that DBF exposure caused a significant increase in the punctuate autophagy-like pattern of this fluorescent marker (Figure 5.2.9).

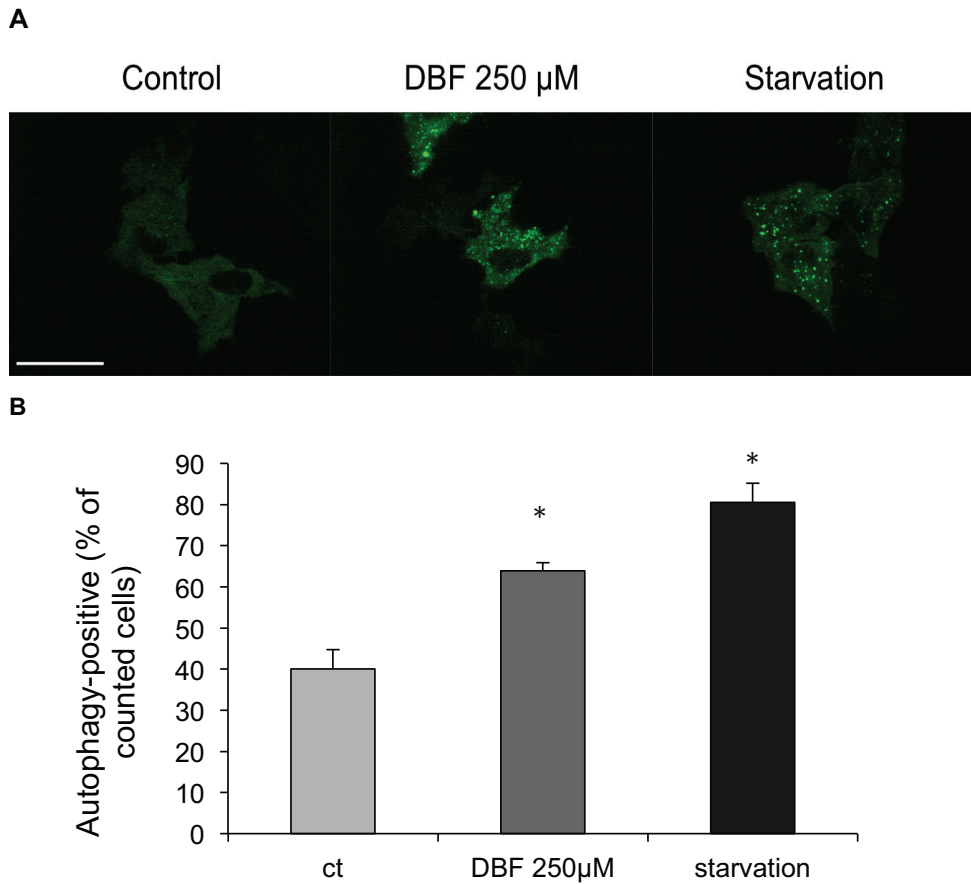


Figure 5.2.9 – Autophagy triggering in A549 cells after exposure to DBF.

A - Cellular distribution of YFP-LC3. A549 cells were transfected with YFP-LC3 and exposed to 250 μ M DBF for 24h, as described in Chapter 2. Representative images are presented. Scale bar, 20 μ m. **B** – Blind quantitative analysis of autophagy induction in A549 cells. A549 cells transfected with YFP-LC3 were inspected and imaged using the fluorescence microscope, as described in Chapter 2. Data is presented as the percentage of autophagy-positive cells in the total number of transfected cells counted. Values statistically different from control: * $P < 0,05$.

5.2.10 – LC3 and p62 accumulation by western blot analysis

A549 cells in culture exposed to DBF showed an increase in LC3 content (Figure 5.2.10), a protein involved in autophagy process. Additionally,

after 48h incubation, DBF induced an increase in LC3-I (cytosolic) to LC3-II conversion, the membrane bound protein involved in autophagosome formation and elongation. At 24h exposure there was an increase in LC3-I content, although the LC3-II content didn't change significantly when compared to control. During autophagic process, LC3-I is formed from newly synthesized LC3, followed by the conversion of a fraction of LC3-I into LC3-II. This way, the amount of LC3-II is correlated with the extent of autophagosome formation. Accordingly, DBF exposure caused an accumulation of processed LC3-II at 48h (Figure 5.2.10). After 24h we could only detect an increase in LC3-I content and we didn't see an increase in LC3-II protein band, probably due to a rapid breakdown of autophagosomes and concomitant degradation of LC3-II.

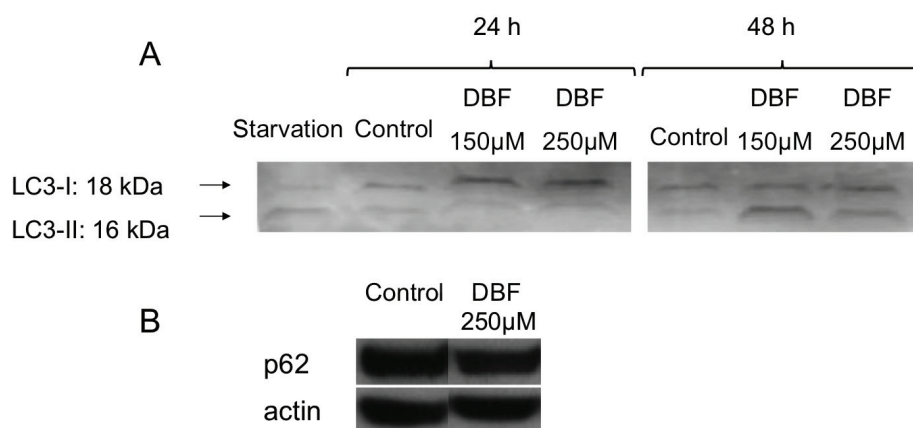


Figure 5.2.10 – Autophagy-related protein markers content in A549 cells exposed to Dibenzofuran.

Cell lysates obtained upon exposure to Dibenzofuran were used to perform Western Blot experiments and evaluate protein contents. **A** - LC3 conversion and accumulation (LC3-I and LC3-II). **B** - p62 protein content in A549 cells exposed to Dibenzofuran.

Furthermore, analysis of another autophagy marker such as p62 protein content showed that A549 cells exposed to DBF for 24h have a slight decrease in p62 protein content (Figure 5.2.10), indicating an increased rate

of degradation of this protein, and therefore an increase in autophagic degradation process.

5.2.11 – LysoTracker accumulation

A549 cells exposed to DBF showed an increased cellular staining with the lysosomal dye LysoTracker Red (Figure 5.2.11), which accumulation is proportional to lysosomal acidification and number, and has already been used to monitor activation of autophagy. LysoTracker accumulation experiments were conducted in order to evaluate the status of cellular components degradation by autophagic delivery to lysosomes. Exposure of A549 cells to DBF 250 μ M caused an increase in LysoTracker staining, when compared to control, indicating an increase in lysosomal vacuoles (Figure 5.2.11), and thus representing an increase in self-digestion mechanisms in lung cells exposed to DBF.

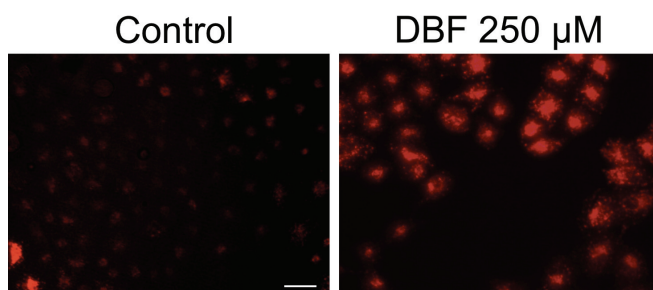


Figure 5.2.11 – Fluorescence microscopy images showing LysoTracker accumulation in A549 cells.

A549 cells were cultured in glass coverslips, exposed to DBF for 24h, and incubated with LysoTracker Red DND-99 (100nM, 30min) before images were taken in the fluorescence microscope. Representative images are presented. Scale bar, 20 μ m.

5.2.12 – Mitochondrial DNA copy number

DBF caused an increase in autophagy in A549 cells at 24h of exposure. Since autophagy can be specific and eliminate organelles rather than bulk

cytoplasm, we evaluated mtDNA copy number in cells exposed to DBF. However, no differences were found for mtDNA copy number per cell (Figure 5.2.12), indicating that at this time of exposure no mitochondria-specific autophagy (mitophagy) was confirmed.

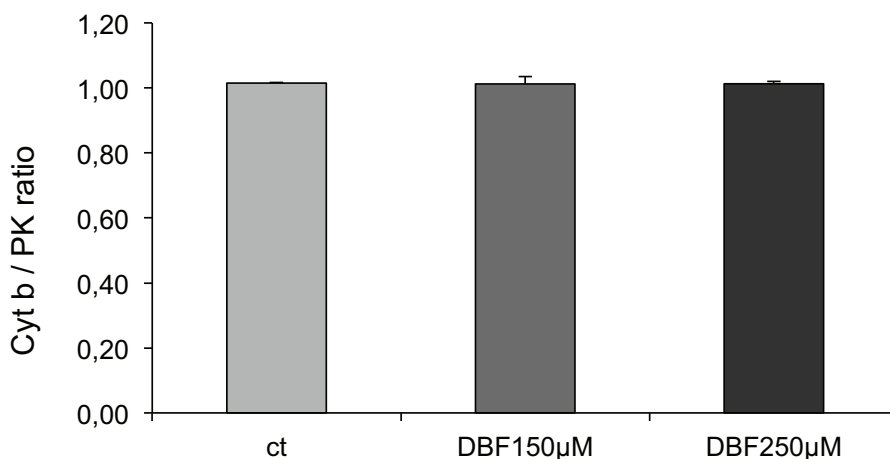


Figure 5.2.12 – mtDNA copy number per cell in A549 exposed to DBF.

A549 cells were cultured and exposed to DBF for 24h. mtDNA was quantified by means of quantitative PCR, calculating the ratio of mitochondrial gene (cytochrome b) copy number to nuclear gene (pyruvate kinase) copy number and expressing it as the mtDNA copy number per cell. Copy numbers for each gene were calculated based on standard curves. Bars represent the mean \pm S.E.M. for three different cell cultures. No statistically significant differences were found ($P < 0.05$).

5.3 – Discussion

Exposure to dioxins and other environmental pollutants, such as fuel constituents and incineration products, is associated in humans with obstructive pulmonary disease and lung cancer (Boffetta, 2006). Dibenzofuran is a widespread environmental contaminant that results from chemical and combustion processes, and exposure to it brings out several dreadful effects. Although some work has been conducted on pollutants-induced liver toxicity

using liver cells in culture and animal models (Bunger et al., 2003; Niittynen et al., 2008; Weinstein et al., 2008), the evaluation of lung cell function after exposure to this kind of toxicants is scarce. In this study we report that there is both time and concentration-dependence on DBF-induced proliferative arrest in A549 cells, related to a drop in cellular ATP content and increased lysosome accumulation and self-degradation events.

Previous studies on mitochondrial dysfunction induced by exposure to pollutants, such as TCDD or arsenic, have been carried out in liver (Mildaziene et al., 2002; Lee and Sokol, 2007), blood cells (Banerjee et al., 2008), brain (Coburn et al., 2008), or in the lung (Duarte et al., 2011). In both hepatic mitochondria isolated from TCDD-treated mice and mitochondria incubated in vitro with TCDD, a number of functional alterations have been observed, including a defect in ATP synthesis and increased ROS production (Senft et al., 2002b; Shen et al., 2005; Shertzer et al., 2006). Reported experiments with lung isolated mitochondria showed that the time that elapses from ADP-induced depolarization until total repolarization – lag phase – was significantly enlarged in mitochondria exposed to DBF (Duarte et al., 2011), suggesting that DBF may impair mitochondrial phosphorylative efficiency. Additionally, Shertzer and collaborators have also shown a decreased hepatic ATP content related to a defect in the mitochondrial ATP synthase in rats treated with TCDD for 1 week. Thus, the mitochondrial phosphorylative system is probably a target for pollutant-induced mitochondrial dysfunction.

In this study we evaluated cell death induced by exposure of A549 cells to Dibenzofuran. Previous works with A549 cells have shown that anti-cancer agents and toxicants from gasoline engine exhaust harm normal cell function (Catassi et al., 2006). These compounds have been shown to decrease cell viability and mitochondrial dehydrogenases activity, induce apoptotic cell death, increase the formation of micronucleated cells and enhance DNA damage, in a dose-response manner (Catassi et al., 2006; Zhang et al., 2007). In our study, exposure of A549 cells in culture to DBF revealed a dose- and time-dependent decrease in relative cell proliferation and MTT reduction, but no alterations in cell death/viability, assessed by staining with annexin V-PI or LDH release. DBF exposure did not induce apoptotic cell death; this result can be related to the ATP dependence of apoptosis execution, given that the

exposure to the pollutant caused a decrease in the ATP levels in lung cells. Additionally, the absence of an increase in LDH release suggested that inhibition of cell proliferation by DBF exposure was not due to increased necrotic cell death, suggesting a specific effect of DBF on cell division and/or the induction of self-digestion mechanisms (autophagy), that can be considered as a rescue mechanism from dysfunction caused by the pollutant in the lung cells.

ATP content in A549 cells exposed to DBF was found to be decreased, and this data is in agreement with the lower mitochondrial membrane potential and reduced oxygen consumption observed in A549 cells exposed to 250 μ M for 24h, suggesting an impairment of mitochondrial function. Remarkably, when we analysed ROS generation in lung cells incubated with DBF, we found a decrease in the rate of ROS formation. Some studies have reported that mitochondrial dysfunction/loss of mitochondrial membrane potential (Kim et al., 2007) and oxidative stress (Kaushik and Cuervo, 2006) induce autophagic mechanisms (Kaushik and Cuervo, 2006; Chen et al., 2007; Azad et al., 2009). In its turn, autophagy will end up removing damaged proteins and damaged/dysfunctional mitochondria, therefore reducing ROS levels (Scherz-Shouval and Elazar, 2011).

The occurrence of increased autophagosomes in dying/dead cells in certain contexts led to the idea that autophagy may be a primary death mediator. This phenomenon was termed type-II cell death, to differentiate it from apoptotic (or type-I cell death) (Schweichel and Merker, 1973). Since increased numbers of autophagosomes can result both from increased autophagosome synthesis, as well as from decreased autophagosome–lysosome fusion, cells showing type-II cell death may not always have increased autophagic flux. Although there is mounting evidence that this may be a relevant pathway in *Drosophila* metamorphosis (Denton et al., 2009), the role of autophagy as a positive mediator of cell death is unclear and not well understood in mammalian systems. On the other hand, many studies suggest that impaired autophagy sensitises cells and organisms to toxic insults (Takacs-Vellai et al., 2005; Levine and Yuan, 2005). One of the first studies that addressed this question in mammalian cells (Boya et al., 2005) reported that cells exhibit type-II cell death morphology when lysosome–

autophagosome fusion is inhibited, suggesting that autophagy may be cytoprotective. The lysosomotropic agent hydroxychloroquine (HCQ) leads to the accumulation of autophagic vacuoles (AV) that triggers a pre-lethal program, which can be suppressed by mitochondrial membrane permeability inhibitors, or caspase antagonists. AV accumulation precedes $\Delta\Psi_m$ loss, which marks imminent cell death and apoptosis (Boya et al., 2005). Consistent with these data, other group (Ravikumar et al., 2006) showed that genetic or chemical inhibition of autophagy sensitised cells to pro-apoptotic insults and that autophagy induction with rapamycin or Beclin 1 overexpression protected cells and *Drosophila* from pro-apoptotic agents. These data suggested that the ability of autophagy to reduce the mitochondrial load in cells and thereby lower the amount of pro-apoptotic molecules (like cytochrome *c*) released from mitochondria after apoptotic insults, was an important contributor to the protective effects of autophagy (Moreau et al., 2010).

An evident increase in lysosomal vacuoles in cells exposed to DBF, along with accumulation of LC3 in punctuate structures, suggest an increase in autophagosome formation in cells exposed to DBF; thus, these results put forward that exposure to DBF induces autophagy in A549 cells. However, the lack of differences in the mtDNA copy number of cells exposed to DBF does not permit to make an assertion about specific autophagy degrading mitochondria (mitophagy), at 24h of exposure to DBF. In our experimental settings, we found ROS generation to be decreased in lung cells after 24h of exposure to DBF; this is probably the consequence of a salvage mechanism that is triggered to prevent and/or recover from cellular damage caused by DBF, particularly autophagy mechanisms.

Different autophagic pathways have been described, all sharing in common the import of cytoplasmic components into the lysosome. Autophagy induction and alterations in the autophagic-lysosomal compartment have been linked to neuronal death in many neurodegenerative disorders as well as in transmissible neuronal pathologies (Larsen and Sulzer, 2002; Qin et al., 2003; Webb et al., 2003; Yu et al., 2003; Mariño and López-Otín, 2004; Alirezai et al., 2008). LC3-II is the only protein marker that is reliably associated with completed autophagosomes. In mammalian cells, the total levels of LC3 do

not necessarily change, as there may be increases in the conversion of LC3-I to LC3-II, or a decrease in LC3-II relative to LC3-I if degradation of LC3-II via lysosomal turnover is particularly rapid. Western blotting was used to monitor changes in LC3 amounts, showing an increase of LC3-I to LC3-II conversion in A549 cells exposed to DBF for 48h. For 24h exposure we could only see an increase in LC3-I content in comparison with control, although LC3-II didn't change significantly; this may probably be due to the fact that, at this time, autophagosomal number was not yet large enough to break out the normal and rapid degradation, that way not being accumulated. Given that the amount of LC3-II is correlated with the extent of autophagosome formation, data shows that DBF toxic effects include triggering of autophagy in lung cells in culture. Additionally, we wanted to evaluate another marker that can be associated with autophagy induction. Thus we estimated the degradation of p62 protein, other established indicator of the activation of autophagy (Ichimura et al., 2008). We found that exposure of A549 cells to Dibenzofuran also caused a small decrease in p62 protein content, which is in agreement with the established degradation of p62 after activation of autophagy, since that the levels of p62 protein are regulated also by autophagy through an interaction of this protein with LC3 (Ichimura et al., 2008).

In summary, our results indicate that mitochondria are probably a target in DBF-induced lung toxicity. A decrease in the mitochondrial phosphorylative efficiency elicited by Dibenzofuran, with subsequent decrease in ATP content, are damaging results from exposure to Dibenzofuran; also inhibition of lung cell proliferation and mitochondrial activity, as well as autophagy triggering seem to be critical events in DBF-induced impairment of pulmonary function.

Chapter 6

General discussion

Environmental pollutants such as polychlorinated dibenzo-*p*-dioxins (PCDDs) and polychlorinated dibenzofurans (PCDFs) constitute a category of chlorinated aromatic hydrocarbons containing 210 structurally related congeners (US EPA, 2004). These compounds are associated with a wide range of physiological and toxicological effects, many of which are mediated via a common underlying mechanism of action involving chemical binding to the aryl hydrocarbon receptor (AhR) (Goodman et al., 2010). Effects associated with dioxins and dioxin-like compounds (DLCs) range from distinctive acute effects that can be readily observed following high level exposures (e.g., chloracne) to more subtle effects (e.g., potential impacts on the levels or functioning of endogenous hormones) for which the biological and clinical significance may be less certain.

In humans, exposure to noxious agents such as PCBs, B[a]P, and dioxin-like compounds in cigarette smoke have the potential to induce inflammation or exacerbate chronic bronchitis, asthma, COPD, and lung cancer (Patel and Homnick, 2000; Baginski et al., 2006; Marshall and Kerkvliet, 2010; Chiba et al., 2012). In addition to lung and liver as primary target organs of toxicity, reproductive, hormonal and immunological defects have also been shown following exposure to different types of environmental pollutants (Fisher et al., 2005; van Grevenynghe et al., 2005; Kobayashi et al., 2009; Ferecatu et al., 2010; Helgason et al., 2010; Martin and Klaassen, 2010). Various combustion and industrial processes contribute to the widespread environmental contamination with Dibenzofuran (US EPA, 2004). These compounds also have high persistence in the environment, but humans can also be exposed via sources such as the diet, leading to long-term accumulation in fatty tissues. However, the wide range of physiological and toxicological effects of these compounds is still uncertain, especially those caused by chronic exposure comparatively to distinct acute effects observed after high level exposures.

Binding to AhR and related ROS generation has been suggested as the mechanism of action underlying the toxic and biological effects of these dioxins and dioxin-like compounds (Senft et al., 2002b; Chiba et al., 2011a). The AR/AHR nuclear translocator (ARNT) complex binds to canonical DNA recognition sequences found in the genes coding for many phase I and phase

II detoxification enzymes, such as the cytochromes P450 CYP1A1, CYP1A2, and CYP1B1, and initiates gene transcription (Whitlock, 1999). Besides its role in the regulation of drug metabolism, the AhR also has an important physiologic role in the control of cell-cycle progression, liver and vascular development, immune system function, and cell growth and differentiation (Fernandez-Salguero et al., 1995; Schmidt and Bradfield, 1996; Elizondo et al., 2000). Therefore, AhR activation has been described as necessary for the teratogenic, immunotoxic, carcinogenic, and biochemical effects of dioxins and dioxin-like compounds (Rowlands and Gustafsson, 1997), by inducing gene alteration, cell-cell adhesion interaction, cytokine expression, and mucin production, which are involved in the induction of cancer or inflammation (Watabe et al., 2010; Chiba et al., 2011b; Chiba et al., 2011a; Barouki et al., 2012).

However, the underlying mechanisms are not fully understood and toxic mechanisms activated by dioxins and dioxin-like compounds, independent of AhR activation, must be considered (Fernandez-Salguero et al., 1995; Hossain et al., 1998; Ahmed et al., 2005). 2,3,7,8-tetrachlorodibenzo-*p*-dioxin (TCDD) induces apoptosis in the human lymphoblastic T-cell line L-MAT, although these cells do not express the AhR (Hossain et al., 1998; Kobayashi et al., 2009). Also, previous work with Ahr knockout mice revealed the existence of dioxin-independent functions of Ahr, including developmental functions and ageing-related detoxification (Fernandez-Salguero et al., 1995). The relationship between these two types of biological actions (AhR-dependent and independent) remains unclear, which hampers understanding and treatment of dioxin and dioxin-like compounds toxicity. Recently, siRNA-mediated knockdown of the AhR in lung epithelial cells and fibroblasts was shown to increase sensitivity to smoke-induced apoptosis (Rico de Souza et al., 2011). This involved mitochondrial dysfunction, decreased antioxidant enzymes and oxidative stress.

Mitochondria are intracellular organelles with many cellular roles besides the first described energy production by oxidative phosphorylation, namely fatty acid β -oxidation, heat generation, ROS metabolism and cell death regulation (Martel et al., 2012). Mitochondria perform diverse yet interconnected functions, producing ATP and many biosynthetic intermediates

while also contributing to cellular stress responses such as autophagy and apoptosis. Mitochondria form a dynamic, interconnected network that is intimately integrated with other cellular compartments. In addition, mitochondrial functions extend beyond the boundaries of the cell and influence an organism's physiology by regulating communication between cells and tissues. It is therefore not surprising that mitochondrial dysfunction has emerged as a key factor in a myriad of diseases, including neurodegenerative and metabolic disorders (Nunnari and Suomalainen, 2012). Indeed, mitochondrial dysfunction has been associated with a series of human diseases such as cancer, cardiopathies, nonalcoholic fatty liver diseases, neurodegenerative diseases, aging and cell dysfunction triggered by exposure to xenobiotics (Wallace, 1999; Kroemer et al., 2007; Martel et al., 2012). Decreased mitochondrial efficiency leads to metabolic impairment characterized by decreased ATP synthesis capacity, enhanced ROS production due to electron leak from the respiratory chain, as well as morphological alterations of mitochondrial network. Mitochondria also contribute to cellular stress responses such as autophagy and apoptosis, via mitochondrial membrane permeabilization (MMP) and release of proapoptotic factors contained in the intermembrane space to the cytosol (Eisenberg-Lerner et al., 2009; Okamoto and Kondo-Okamoto, 2012). Multiple lines of evidence indicate that mitochondrial ROS also influence homeostatic signaling pathways to control cell proliferation and differentiation and to contribute to adaptive stress signaling pathways, such as hypoxia (Hamanaka and Chandel, 2010).

Mitochondrial dysfunction induced by exposure to pollutants, such as TCDD or arsenic has been shown in liver (Mildaziene et al., 2002; Lee and Sokol, 2007), blood cells (Banerjee et al., 2008) and in brain (Coburn et al., 2008). In both hepatic mitochondria isolated from TCDD-treated mice and mitochondria incubated in vitro with TCDD, a number of functional alterations have been observed, including a defect in ATP synthesis and increased ROS production (Senft et al., 2002a; Shen et al., 2005; Shertzer et al., 2006; Kopf and Walker, 2010). TCDD decreases hepatic ATP levels through changes in mitochondrial F₀F₁-ATP synthase and ubiquinone and generates mitochondrial oxidative DNA damage, which is exacerbated by increasing

mitochondrial glutathione redox state and by inner membrane hyperpolarization. These mitochondrial effects of TCDD are also associated with altered expression of nuclear encoded mitochondrial genes (Forgacs et al., 2010), as well as apoptosis induction involving calcium/calmodulin signaling (Kobayashi et al., 2009). In primary hepatocytes, TCDD has been shown to induce an oxidative stress response involving mitochondrial dysfunction (Aly and Domènech, 2009), and in mice exposure to TCDD would caused a loss in mitochondrial membrane potential mediated by AhR-dependent production of ROS (Fisher et al., 2005).

Experiments with isolated mitochondria from lungs showed that the generation of mitochondrial membrane potential was not compromised by exposure to DBF, neither was mitochondrial oxygen consumption (Chapter 3). Nevertheless, the time that elapses from ADP-induced depolarization until total repolarization – lag phase – was significantly enlarged in mitochondria exposed to DBF, suggesting that DBF may impair the mitochondrial phosphorylative system. Additionally, Shertzer and collaborators have also shown a decrease in hepatic ATP levels related to a defect in the mitochondrial ATP synthase in rats treated with TCDD for 1 week (Shertzer et al., 2006). Mitochondrial ATPase (ATPsynthase) activity, one of the components of the mitochondrial phosphorylative sub-system, was then evaluated through phosphate (P_i) production from ATP hydrolysis (Chapter 3). Interestingly, no significant differences were found between lung mitochondria incubated with DBF and control, indicating that other components of the phosphorylative system are being affected by DBF and then causing the impairment on ATP synthesis. In isolated liver mitochondria, DBF also did not affect mitochondrial capacity to generate and sustain membrane potential, created by the electron transport chain and used to drive production of ATP from ADP in the matrix (Chapter 4). However, similarly to the effects on lung mitochondria, DBF decreased mitochondrial phosphorylative efficiency (increased lag phase), thus impairing ATP synthesis. This was also reflected by the decrease in respiratory state 3 (active phosphorylation) after exposure to DBF. Hence, in liver mitochondria, DBF exposure decreased ATPase efficiency, while not excluding action at the level of other components of the phosphorylative system (Chapter 4). Titrations with CAT showed that, in

mitochondria incubated with DBF, less CAT was needed to completely inhibit repolarization after ADP addition when compared to control. Also, the lag phase in DBF-exposed mitochondria during a phosphorylative cycle was larger in the presence of CAT, comparatively to control. This suggested that DBF inhibits ANT activity (Chapter 4), at least in isolated mitochondria.

Increases in mitochondrial permeability are also manifestations of mitochondrial dysfunction and are associated with induction of apoptotic and necrotic death (Kroemer et al., 2007; Millay et al., 2008; Varela et al., 2008; Halestrap and Pasdois, 2009; Mbye et al., 2009; Nicholls, 2009; Russmann et al., 2009; Varela et al., 2010). Mitochondrial permeability transition is caused by the mitochondrial permeability transition pore (mPTP), a voltage- and Ca^{2+} -dependent, cyclosporine A (CsA)-sensitive, high conductance channel (Rasola et al., 2010). This causes cell death by uncoupling oxidative phosphorylation, inducing mitochondrial swelling and collapsing mitochondrial membrane potential, thus blocking cellular ATP formation. Such defective mitochondria have the potential to further damage the population of healthy mitochondria, by exposure to accelerated ROS generation and increased calcium concentrations. MPT induction is associated with pathological conditions and is triggered by high Ca^{2+} , oxidative stress, ATP depletion, high inorganic phosphate and mitochondrial depolarization. In both lung (Chapter 3) and liver mitochondria (Chapter 4), exposure to DBF inhibited calcium-induced mitochondrial swelling, cytochrome *c* release and calcium-induced mitochondrial calcium efflux sensitive to CsA. DBF also prevented mitochondrial swelling induced by CAT in liver mitochondria (Chapter 4). Taking also into account the suggested inhibition of the ANT activity, based on the lag phase experiments, DBF inhibitory effect on the MPT is probably dependent on the ANT. CAT induces MPT induction by facilitating changes in the conformational state of the ANT, stabilizing the “c” conformation where the nucleotide binding site faces the cytoplasmic side of the membrane (Zoratti and Szabò, 1995). The calcium-dependency of the MPT suggested that there might be a calcium trigger site exposed on the ANT associated with the “c” conformation (Halestrap and Brenner, 2003). The requirement for the ANT in MPT induction was questioned when liver mitochondria of mice genetically modified to lack the two major isoforms of ANT (ANT1 and ANT2) still

exhibited CsA-sensitive MPT (Kokoszka et al., 2004). However, ANT-deficient mitochondria require much higher calcium concentrations to open the permeability pore, suggesting if not a physical at least a regulatory role for the ANT in MPT induction, sensitizing to adenine nucleotides and ANT ligands (Kokoszka et al., 2004; Baines and Molkentin, 2009). Early on, it was demonstrated that ANT binds cyclophilin D (CypD) in a CsA-sensitive manner and that role of CypD in mPTP formation was to induce a conformational change in the ANT (Crompton et al., 1998; Woodfield et al., 1998; Rasola et al., 2010; Hansson et al., 2011). CypD was detected by immunoprecipitating the ANT after calcium-induced mitochondrial swelling (thus bound previously to ANT) (Chapter 4). When MPT induction was prevented, either with CsA or DBF exposure, the ratio CypD/ANT in the samples was decreased when compared to control or CAT, also supporting that DBF interacts with the ANT and somehow prevents CypD binding and MPT induction (Chapter 4). It has been described that the MPT can also operate in a more “limited size” or “low conductance” mode, which allows passage of only small ions across the inner mitochondrial membrane (Novgorodov and Guduz, 1996; Ichas and Mazat, 1998). Because opening of the low conductance mPTP does not allow passage of large molecules, but does allow the passage of small ions, mitochondrial ion gradients and energy production are affected. As such, it is thought that the low conductance MPT functions not to induce cell death but to aid in the fine regulation of cell metabolism (Ichas and Mazat, 1998). The low-conductance state also allows fine dissipation of mitochondrial membrane potential, preventing mitochondrial ROS generation due to mitochondrial hyperpolarization.

Studies with lung epithelial A549 cells exposed to DBF showed that DBF exposure decreases ATP content, thus inhibiting cell proliferation, without inducing necrotic or apoptotic cell death (Chapter 5). The decreased mitochondrial activity was associated with a reduced rate of oxygen consumption and decreased ROS generation, which could be explained by increased autophagy and mitochondria removal. It is currently known that autophagy might mediate cytoprotective effects; the mechanisms include the ability of autophagy to buffer against starvation-induced stress, protect against apoptotic insults and clear mitochondria, aggregate-prone proteins and

pathogens (Moreau et al., 2010). These effects are pertinent to the roles of autophagy in normal human physiology, including the early neonatal period and ageing, as well as a variety of diseases, including cancer, neurodegenerative conditions and infectious diseases (Moreau et al., 2010). Concerning DBF exposure of A549 lung cells, autophagy will end up removing damaged proteins and dysfunctional mitochondria, therefore reducing ROS levels (Chapter 5) and preventing the extension of the initial damage induced by DBF. The same rescue mechanism has already been reported by other authors (Scherz-Shouval and Elazar, 2011). The mechanisms whereby autophagy mediates its cytoprotective effects are still the subject of active investigation by a number of laboratories. It is likely that these may vary according to the stress that the relevant cells and organisms are exposed to, and the cell types involved (Moreau et al., 2010).

Controversy exists as to whether autophagy promotes or prevents cell death (Hait et al., 2006; Levine and Kroemer, 2008). Autophagy removes damaged mitochondria that would otherwise activate caspases and apoptosis, suggesting that autophagy should be protective. Also, disruption of autophagic processing and/or lysosomal function promotes caspase-dependent cell death, as well as excessive and dysregulated autophagy may promote cell death (Narendra et al., 2008; Narendra et al., 2010; Kim and Lemasters, 2011; Green et al., 2011; Michel et al., 2012; Mai et al., 2012). Compromised mitochondrial function and autophagic overload have been described for several pathologies. Compromising mitochondrial function with the antiretroviral drug efavirenz induces cell survival-promoting autophagy (Apostolova et al., 2011). Increased autophagy contributes to COPD pathogenesis by promoting epithelial cell death (Ryter and Choi, 2010) and exposure to cigarette smoke extract induces ER stress and autophagy in human umbilical vein endothelial cells (HUVECs) (Csordas et al., 2011).

In summary, this work aimed to evaluate the effects that are elicited by Dibenzofuran exposure. Since mitochondria are key players in cellular life/death regulation, besides being its primary energy supplier, isolated mitochondria were used as models. *In vitro* exposure to the toxicant caused mitochondrial impairment, mainly at the phosphorylative system level but also deregulation of mitochondrial permeability transition (which is one of the main

mechanisms involved in cell death regulation, calcium homeostasis and global mitochondrial and cellular fitness). Both mitochondria from the lung (primary exposure source for gaseous toxicants like DBF) and the liver (the organ that most accumulates and metabolizes xenobiotics) were affected by DBF, which exerted its deleterious effects at least in part by interacting with the mitochondrial ANT carrier. Also A549 lung cells were exposed to DBF and showed impaired function. DBF caused a decrease in cellular proliferation, mitochondrial potential and cellular energy levels (reduced ATP), and the harmful effects of the toxicant trigger a rescue mechanism that involves autophagy induction after DBF exposure. The main toxic effects of DBF are depicted in Figure 6.1.

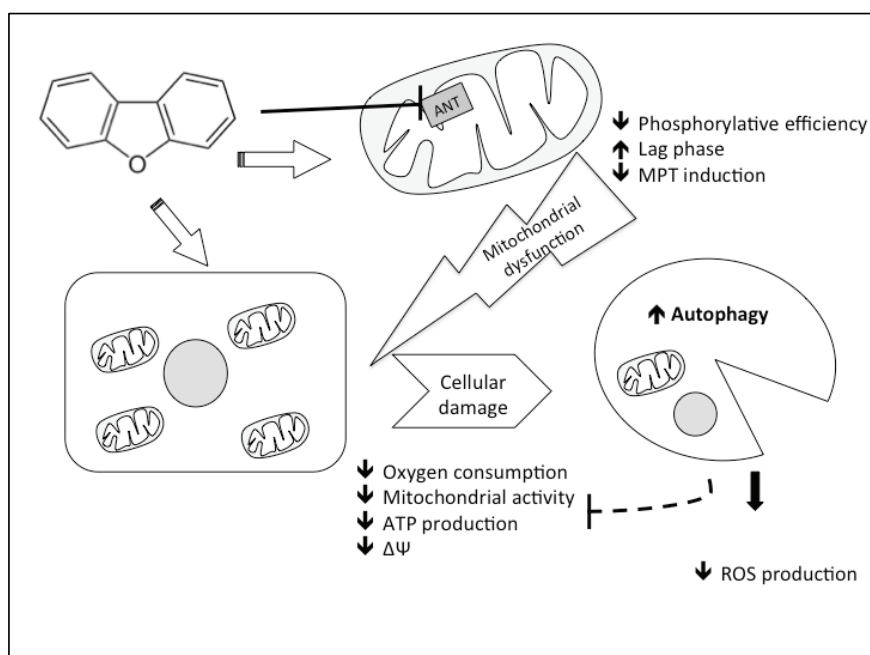


Figure 6.1 – Scheme illustrating the main effects of DBF exposure.

DBF affects mitochondrial function, impairing phosphorylative efficiency and interfering with MPT induction. These effects are related to an interaction with the ANT carrier. Mitochondrial dysfunction can help to explain cellular damage. At least in lung cells, DBF exposure triggers autophagy as a rescue mechanism to block the progression of the damage, and therefore improve cellular function, by mitigating the origin of the damage (dysfunctional mitochondria and ROS production).

Clarifying some of the molecular mechanisms that motivate environmental pollutants-induced damage, may help to develop better and more effective strategies to ameliorate health condition that is continuously threatened by today's continuously increasing environmental pollution.

Bibliography

- Abramov, A. Y., Gegg, M., Grünewald, A., Wood, N. W., Klein, C. and Schapira, A. H. V.** (2011). Bioenergetic Consequences of PINK1 Mutations in Parkinson Disease. *PLoS ONE* **6**, e25622.
- Ahmed, S., Shibazaki, M., Takeuchi, T. and Kikuchi, H.** (2005). Protein kinase C θ activity is involved in the 2,3,7,8-tetrachlorodibenzo-p-dioxin-induced signal transduction pathway leading to apoptosis in L-MAT, a human lymphoblastic T-cell line. *FEBS J* **272**, 903–915.
- Alexander, C., Votruba, M., Pesch, U. E., Thiselton, D. L., Mayer, S., Moore, A., Rodriguez, M., Kellner, U., Leo-Kottler, B., Auburger, G., et al.** (2000). OPA1, encoding a dynamin-related GTPase, is mutated in autosomal dominant optic atrophy linked to chromosome 3q28. *Nat Genet* **26**, 211–215.
- Alirezaei, M., Kiosses, W. B., Flynn, C. T., Brady, N. R. and Fox, H. S.** (2008). Disruption of neuronal autophagy by infected microglia results in neurodegeneration. *PLoS ONE* **3**, e2906.
- Aly, H. A. A. and Domènech, O.** (2009). Cytotoxicity and mitochondrial dysfunction of 2,3,7,8-tetrachlorodibenzo-p-dioxin (TCDD) in isolated rat hepatocytes. *Toxicol Lett* **191**, 79–87.
- Aoki, Y.** (2001). Polychlorinated biphenyls, polychlorinated dibenzo-p-dioxins, and polychlorinated dibenzofurans as endocrine disrupters--what we have learned from Yusho disease. *Environ Res* **86**, 2–11.
- Apostolova, N., Gomez-Sucerquia, L. J., Gortat, A., Blas-Garcia, A. and Esplugues, J. V.** (2011). Compromising mitochondrial function with the antiretroviral drug efavirenz induces cell survival-promoting autophagy. *Hepatology* **54**, 1009–1019.
- Argaud, L., Gateau-Roesch, O., Raisky, O., Loufouat, J., Robert, D. and Ovize, M.** (2005). Postconditioning inhibits mitochondrial permeability transition. *Circulation* **111**, 194–197.
- Aristizábal, B., Cobo, M., Hoyos, A., Montes de Correa, C., Abalos, M., Martínez, K., Abad, E. and Rivera, J.** (2008). Baseline levels of dioxin and furan emissions from waste thermal treatment in Colombia. *CHEMOSPHERE* **73**, S171–5.
- Ashford, T. and Porter, K.** (1962). Cytoplasmic components in hepatic cell lysosomes. *J Cell Biol* **12**, 198–202.
- Attardi, G. and Schatz, G.** (1988). Biogenesis of mitochondria. *Annu. Rev. Cell Biol.* **4**, 289–333.
- Azad, M. B., Chen, Y. and Gibson, S. B.** (2009). Regulation of autophagy by reactive oxygen species (ROS): implications for cancer progression and treatment. *Antioxid Redox Signal* **11**, 777–790.
- Azarashvili, T., Stricker, R. and Reiser, G.** (2010). The mitochondria permeability transition pore complex in the brain with interacting proteins - promising targets for protection in neurodegenerative diseases. *Biological Chemistry* **391**, 619–629.
- Azoulay-Zohar, H., Israelson, A., Abu-Hamad, S. and Shoshan-Barmatz, V.** (2004). In self-defence: hexokinase promotes voltage-dependent anion channel closure and prevents mitochondria-mediated apoptotic cell death. *Biochem J* **377**, 347–

355.

- Azzolin, L., Stockum, von, S., Basso, E., Petronilli, V., Forte, M. A. and Bernardi, P.** (2010). The mitochondrial permeability transition from yeast to mammals. *FEBS Lett* **584**, 2504–2509.
- Bae, Y. S., Oh, H., Rhee, S. G. and Yoo, Y. D.** (2011). Regulation of reactive oxygen species generation in cell signaling. *Mol. Cells* **32**, 491–509.
- Baginski, T. K., Dabbagh, K., Satjawatcharaphong, C. and Swinney, D. C.** (2006). Cigarette smoke synergistically enhances respiratory mucin induction by proinflammatory stimuli. *Am J Respir Cell Mol Biol* **35**, 165–174.
- Baines, C. P.** (2009). The molecular composition of the mitochondrial permeability transition pore. *J Mol Cell Cardiol* **46**, 850–857.
- Baines, C. P. and Molkentin, J. D.** (2009). Adenine nucleotide translocase-1 induces cardiomyocyte death through upregulation of the pro-apoptotic protein Bax. *J Mol Cell Cardiol* **46**, 969–977.
- Baines, C. P., Kaiser, R. A., Purcell, N. H., Blair, N. S., Osinska, H., Hambleton, M. A., Brunskill, E. W., Sayen, M. R., Gottlieb, R. A., Dorn, G. W., et al.** (2005). Loss of cyclophilin D reveals a critical role for mitochondrial permeability transition in cell death. *Nature* **434**, 658–662.
- Baines, C. P., Kaiser, R. A., Sheiko, T., Craigen, W. J. and Molkentin, J. D.** (2007). Voltage-dependent anion channels are dispensable for mitochondrial-dependent cell death. *Nat Cell Biol* **9**, 550–555.
- Baines, C. P., Song, C.-X., Zheng, Y.-T., Wang, G.-W., Zhang, J., Wang, O.-L., Guo, Y., Bolli, R., Cardwell, E. M. and Ping, P.** (2003). Protein kinase Cepsilon interacts with and inhibits the permeability transition pore in cardiac mitochondria. *Circ Res* **92**, 873–880.
- Bakeeva, L. E., Chentsov YuS and Skulachev, V. P.** (1978). Mitochondrial framework (reticulum mitochondriale) in rat diaphragm muscle. *Biochim Biophys Acta* **501**, 349–369.
- Bakke, B., Stewart, P. A. and Waters, M. A.** (2007). Uses of and exposure to trichloroethylene in U.S. industry: a systematic literature review. *J Occup Environ Hyg* **4**, 375–390.
- Banerjee, N., Banerjee, M., Ganguly, S., Bandyopadhyay, S., Das, J. K., Bandyopadhyay, A., Chatterjee, M. and Giri, A. K.** (2008). Arsenic-induced mitochondrial instability leading to programmed cell death in the exposed individuals. *Toxicology* **246**, 101–111.
- Barouki, R., Aggerbeck, M., Aggerbeck, L. and Coumoul, X.** (2012). The aryl hydrocarbon receptor system. *Drug Metabol Drug Interact* **27**, 3–8.
- Basso, E., Fante, L., Fowlkes, J., Petronilli, V., Forte, M. A. and Bernardi, P.** (2005). Properties of the permeability transition pore in mitochondria devoid of Cyclophilin D. *J Biol Chem* **280**, 18558–18561.
- Basso, E., Petronilli, V., Forte, M. A. and Bernardi, P.** (2008). Phosphate is essential for inhibition of the mitochondrial permeability transition pore by cyclosporin A and

by cyclophilin D ablation. *J Biol Chem* **283**, 26307–26311.

- Bauer, M. K., Schubert, A., Rocks, O. and Grimm, S.** (1999). Adenine nucleotide translocase-1, a component of the permeability transition pore, can dominantly induce apoptosis. *J Cell Biol* **147**, 1493–1502.
- Bayir, H. and Kagan, V. E.** (2008). Bench-to-bedside review: Mitochondrial injury, oxidative stress and apoptosis--there is nothing more practical than a good theory. *Crit Care* **12**, 206.
- Bereiter-Hahn, J. and Vöth, M.** (1994). Dynamics of mitochondria in living cells: shape changes, dislocations, fusion, and fission of mitochondria. *Microsc. Res. Tech.* **27**, 198–219.
- Bernales, S., McDonald, K. L. and Walter, P.** (2006). Autophagy counterbalances endoplasmic reticulum expansion during the unfolded protein response. *PLoS Biol* **4**, e423.
- Bernardi, P.** (1992). Modulation of the mitochondrial cyclosporin A-sensitive permeability transition pore by the proton electrochemical gradient. Evidence that the pore can be opened by membrane depolarization. *J Biol Chem* **267**, 8834–8839.
- Bernardi, P.** (1999). Mitochondrial transport of cations: channels, exchangers, and permeability transition. *Physiol Rev* **79**, 1127–1155.
- Bernardi, P. and Stockum, von, S.** (2012). The permeability transition pore as a Ca(2+) release channel: New answers to an old question. *Cell Calcium*.
- Bernardi, P., Broekemeier, K. M. and Pfeiffer, D. R.** (1994). Recent progress on regulation of the mitochondrial permeability transition pore; a cyclosporin-sensitive pore in the inner mitochondrial membrane. *J Bioenerg Biomembr* **26**, 509–517.
- Bernardi, P., Krauskopf, A., Basso, E., Petronilli, V., Blachly-Dyson, E., Blachly-Dyson, E., Di Lisa, F. and Forte, M. A.** (2006). The mitochondrial permeability transition from in vitro artifact to disease target. *FEBS J* **273**, 2077–2099.
- Bernardi, P., Petronilli, V., Di Lisa, F. and Forte, M.** (2001). A mitochondrial perspective on cell death. *Trends Biochem Sci* **26**, 112–117.
- Bernardi, P., Vassanelli, S., Veronese, P., Colonna, R., Szabò, I. and Zoratti, M.** (1992). Modulation of the mitochondrial permeability transition pore. Effect of protons and divalent cations. *J Biol Chem* **267**, 2934–2939.
- Billet, S., Abbas, I., Le Goff, J., Verdin, A., André, V., Lafargue, P.-E., Hachimi, A., Cazier, F., Sichel, F., Shirali, P., et al.** (2008). Genotoxic potential of Polycyclic Aromatic Hydrocarbons-coated onto airborne Particulate Matter (PM 2.5) in human lung epithelial A549 cells. *Cancer Lett* **270**, 144–155.
- Blair, A. and Freeman, L. B.** (2006). Lung cancer among nonsmokers. *Epidemiology* **17**, 601–603.
- Boffetta, P.** (2006). Human cancer from environmental pollutants: the epidemiological evidence. *Mutat Res* **608**, 157–162.
- Bolaños-Meade, J., Zhou, L., Hoke, A., Corse, A., Vogelsang, G. and Wagner, K.**

- R. (2005). Hydroxychloroquine causes severe vacuolar myopathy in a patient with chronic graft-versus-host disease. *Am. J. Hematol.* **78**, 306–309.
- Boya, P., González-Polo, R.-A., Casares, N., Perfettini, J.-L., Dessen, P., Larochette, N., Métivier, D., Meley, D., Souquere, S., Yoshimori, T., et al.** (2005). Inhibition of macroautophagy triggers apoptosis. *Mol Cell Biol* **25**, 1025–1040.
- Brautigan, D., Ferguson-Miller, S. and Margoliash, E.** (1978). Mitochondrial cytochrome c: preparation and activity of native and chemically modified cytochromes c. *Meth Enzymol* **53**, 128–164.
- Brdiczka, D., Beutner, G., Rück, A., Dolder, M. and Wallimann, T.** (1998). The molecular structure of mitochondrial contact sites. Their role in regulation of energy metabolism and permeability transition. *Biofactors* **8**, 235–242.
- Brody, J. G., Moysich, K. B., Humblet, O., Attfield, K. R., Beehler, G. P. and Rudel, R. A.** (2007). Environmental pollutants and breast cancer: epidemiologic studies. *Cancer* **109**, 2667–2711.
- Broekemeier, K. M. and Pfeiffer, D. R.** (1989). Cyclosporin A-sensitive and insensitive mechanisms produce the permeability transition in mitochondria. *Biochem Biophys Res Commun* **163**, 561–566.
- Broekemeier, K. M., Carpenter-Deyo, L., Reed, D. J. and Pfeiffer, D. R.** (1992). Cyclosporin A protects hepatocytes subjected to high Ca²⁺ and oxidative stress. *FEBS Lett* **304**, 192–194.
- Brunekreef, B. and Forsberg, B.** (2005). Epidemiological evidence of effects of coarse airborne particles on health. *Eur Respir J* **26**, 309–318.
- Bunger, M. K., Moran, S. M., Glover, E., Thomae, T. L., Lahvis, G. P., Lin, B. C. and Bradfield, C. A.** (2003). Resistance to 2,3,7,8-tetrachlorodibenzo-p-dioxin toxicity and abnormal liver development in mice carrying a mutation in the nuclear localization sequence of the aryl hydrocarbon receptor. *J Biol Chem* **278**, 17767–17774.
- Carlson, D. E., Pumplun, D. W., Ghavam, S., Fiedler, S. M., Chiu, W. C. and Scalea, T. M.** (2005). ATP accelerates respiration of mitochondria from rat lung and suppresses their release of hydrogen peroxide. *J Bioenerg Biomembr* **37**, 327–338.
- Catassi, A., Cesario, A., Arzani, D., Menichini, P., Alama, A., Bruzzo, C., Imperatori, A., Rotolo, N., Granone, P. and Russo, P.** (2006). Characterization of apoptosis induced by marine natural products in non small cell lung cancer A549 cells. *Cell Mol Life Sci* **63**, 2377–2386.
- Cave, M., Appana, S., Patel, M., Falkner, K. C., McClain, C. J. and Brock, G.** (2010). Polychlorinated biphenyls, lead, and mercury are associated with liver disease in American adults: NHANES 2003-2004. *Environ Health Perspect* **118**, 1735–1742.
- Cecconi, F. and Levine, B.** (2008). The role of autophagy in mammalian development: cell makeover rather than cell death. *Dev Cell* **15**, 344–357.
- Chance, B. and Williams, G.** (1956). The respiratory chain and oxidative phosphorylation. *Adv Enzymol Relat Subj Biochem* **17**, 65–134.

- Chang, H. J., Wang, S., Li, H. W., Lin, K. H., Chao, C. C. and Lai, Y. C.** (2010). Polychlorinated dibenzo-p-dioxins and dibenzofuran contents in fish and sediment near a pentachlorophenol contaminated site. *J Environ Sci Health A Tox Hazard Subst Environ Eng* **45**, 923–931.
- Chen, H. and Chan, D. C.** (2009). Mitochondrial dynamics--fusion, fission, movement, and mitophagy--in neurodegenerative diseases. *Human Molecular Genetics* **18**, R169–76.
- Chen, H. and Chan, D. C.** (2010). Physiological functions of mitochondrial fusion. *Ann N Y Acad Sci* **1201**, 21–25.
- Chen, H., Detmer, S. A., Ewald, A. J., Griffin, E. E., Fraser, S. E. and Chan, D. C.** (2003). Mitofusins Mfn1 and Mfn2 coordinately regulate mitochondrial fusion and are essential for embryonic development. *J Cell Biol* **160**, 189–200.
- Chen, K., Pociask, D. A., McAleer, J. P., Chan, Y. R., Alcorn, J. F., Kreindler, J. L., Keyser, M. R., Shapiro, S. D., Houghton, A. M., Kolls, J. K., et al.** (2011). IL-17RA is required for CCL2 expression, macrophage recruitment, and emphysema in response to cigarette smoke. *PLoS ONE* **6**, e20333.
- Chen, Y. and Klionsky, D. J.** (2011). The regulation of autophagy - unanswered questions. *Journal of Cell Science* **124**, 161–170.
- Chen, Y., McMillan-Ward, E., Kong, J., Israels, S. J. and Gibson, S. B.** (2007). Mitochondrial electron-transport-chain inhibitors of complexes I and II induce autophagic cell death mediated by reactive oxygen species. *Journal of Cell Science* **120**, 4155–4166.
- Cheng, Z., Tseng, Y. and White, M. F.** (2010). Insulin signaling meets mitochondria in metabolism. *Trends Endocrinol Metab* **21**, 589–598.
- Cheon, H., Woo, Y.-S., Lee, J. Y., Kim, H. S., Kim, H. J., Cho, S., Won, N. H. and Sohn, J.** (2007). Signaling pathway for 2,3,7,8-tetrachlorodibenzo-p-dioxin-induced TNF-alpha production in differentiated THP-1 human macrophages. *Exp Mol Med* **39**, 524–534.
- Chevrollier, A., Loiseau, D., Chabi, B., Renier, G., Douay, O., Malthiery, Y. and Stepien, G.** (2005). ANT2 isoform required for cancer cell glycolysis. *J Bioenerg Biomembr* **37**, 307–316.
- Chiara, F., Castellaro, D., Marin, O., Petronilli, V., Brusilow, W. S., Juhaszova, M., Sollott, S. J., Forte, M., Bernardi, P. and Rasola, A.** (2008). Hexokinase II detachment from mitochondria triggers apoptosis through the permeability transition pore independent of voltage-dependent anion channels. *PLoS ONE* **3**, e1852.
- Chiba, T., Chihara, J. and Furue, M.** (2012). Role of the Arylhydrocarbon Receptor (AhR) in the Pathology of Asthma and COPD. *J Allergy (Cairo)* **2012**, 372384.
- Chiba, T., Uchi, H., Tsuji, G., Gondo, H., Moroi, Y. and Furue, M.** (2011a). Arylhydrocarbon receptor (AhR) activation in airway epithelial cells induces MUC5AC via reactive oxygen species (ROS) production. *Pulm Pharmacol Ther* **24**, 133–140.
- Chiba, T., Uchi, H., Yasukawa, F. and Furue, M.** (2011b). Role of the

- arylhydrocarbon receptor in lung disease. *Int. Arch. Allergy Immunol.* **155 Suppl 1**, 129–134.
- Chinopoulos, C. and Adam-Vizi, V.** (2012). Modulation of the mitochondrial permeability transition by cyclophilin D: moving closer to F(0)-F(1) ATP synthase? *Mitochondrion* **12**, 41–45.
- Chomyn, A. and Attardi, G.** (2003). MtDNA mutations in aging and apoptosis. *Biochem Biophys Res Commun* **304**, 519–529.
- Clark, G. C., Taylor, M. J., Tritscher, A. M. and Lucier, G. W.** (1991). Tumor necrosis factor involvement in 2,3,7,8-tetrachlorodibenzo-p-dioxin-mediated endotoxin hypersensitivity in C57BL/6J mice congenic at the Ah locus. *Toxicol Appl Pharmacol* **111**, 422–431.
- Coburn, C. G., Currás-Collazo, M. C. and Kodavanti, P. R. S.** (2008). In vitro effects of environmentally relevant polybrominated diphenyl ether (PBDE) congeners on calcium buffering mechanisms in rat brain. *Neurochem Res* **33**, 355–364.
- Cohen, A. J., Ross Anderson, H., Ostro, B., Pandey, K. D., Krzyzanowski, M., Künzli, N., Gutschmidt, K., Pope, A., Romieu, I., Samet, J. M., et al.** (2005). The global burden of disease due to outdoor air pollution. *Journal of Toxicology and Environmental Health Part A* **68**, 1301–1307.
- Contreras, L., Drago, I., Zampese, E. and Pozzan, T.** (2010). Mitochondria: the calcium connection. *Biochim Biophys Acta* **1797**, 607–618.
- Couraud, S., Zalczman, G., Milleron, B., Morin, F. and Souquet, P.-J.** (2012). Lung cancer in never smokers--a review. *Eur J Cancer* **48**, 1299–1311.
- Crichton, D., Wilkinson, S., O'Prey, J., Syed, N., Smith, P., Harrison, P. R., Gasco, M., Garrone, O., Crook, T. and Ryan, K. M.** (2006). DRAM, a p53-induced modulator of autophagy, is critical for apoptosis. *Cell* **126**, 121–134.
- Crompton, M., Barksby, E., Johnson, N. and Capano, M.** (2002). Mitochondrial intermembrane junctional complexes and their involvement in cell death. *Biochimie* **84**, 143–152.
- Crompton, M., Virji, S. and Ward, J. M.** (1998). Cyclophilin-D binds strongly to complexes of the voltage-dependent anion channel and the adenine nucleotide translocase to form the permeability transition pore. *Eur J Biochem* **258**, 729–735.
- Csordas, A., Kreutmayer, S., Ploner, C., Braun, P. R., Karlas, A., Backovic, A., Wick, G. and Bernhard, D.** (2011). Cigarette smoke extract induces prolonged endoplasmic reticulum stress and autophagic cell death in human umbilical vein endothelial cells. *Cardiovasc Res* **92**, 141–148.
- Davis, J. W., Burdick, A. D., Lauer, F. T. and Burchiel, S. W.** (2003). The aryl hydrocarbon receptor antagonist, 3-methoxy-4-nitroflavone, attenuates 2,3,7,8-tetrachlorodibenzo-p-dioxin-dependent regulation of growth factor signaling and apoptosis in the MCF-10A cell line. *Toxicol Appl Pharmacol* **188**, 42–49.
- de Duve, C.** (1963). The lysosome. *Sci. Am.* **208**, 64–72.
- de Duve, C. and Wattiaux, R.** (1966). Functions of lysosome. *Annu. Rev. Physiol.* **28**, 435–492.

- Delettre, C., Lenaers, G., Griffoin, J. M., Gigarel, N., Lorenzo, C., Belenguer, P., Pelloquin, L., Grosgeorge, J., Turc-Carel, C., Perret, E., et al.** (2000). Nuclear gene OPA1, encoding a mitochondrial dynamin-related protein, is mutated in dominant optic atrophy. *Nat Genet* **26**, 207–210.
- Denton, D., Shrivage, B., Simin, R., Mills, K., Berry, D. L., Baehrecke, E. H. and Kumar, S.** (2009). Autophagy, not apoptosis, is essential for midgut cell death in *Drosophila*. *Curr Biol* **19**, 1741–1746.
- Detmer, S. A. and Chan, D. C.** (2007). Functions and dysfunctions of mitochondrial dynamics. *Nat Rev Mol Cell Biol* **8**, 870–879.
- Di Lisa, F. and Bernardi, P.** (2006). Mitochondria and ischemia-reperfusion injury of the heart: fixing a hole. *Cardiovasc Res* **70**, 191–199.
- Di Lisa, F. and Bernardi, P.** (2009). A CaPful of mechanisms regulating the mitochondrial permeability transition. *J Mol Cell Cardiol* **46**, 775–780.
- Di Lisa, F. and Ziegler, M.** (2001). Pathophysiological relevance of mitochondria in NAD(+) metabolism. *FEBS Lett* **492**, 4–8.
- Di Lisa, F., Canton, M., Menabò, R., Kaludercic, N. and Bernardi, P.** (2007). Mitochondria and cardioprotection. *Heart Fail Rev* **12**, 249–260.
- Di Lisa, F., Menabò, R., Canton, M., Barile, M. and Bernardi, P.** (2001). Opening of the mitochondrial permeability transition pore causes depletion of mitochondrial and cytosolic NAD⁺ and is a causative event in the death of myocytes in postischemic reperfusion of the heart. *J Biol Chem* **276**, 2571–2575.
- Doczi, J., Turiák, L., Vajda, S., Mándi, M., Töröcsik, B., Gerencser, A. A., Kiss, G., Konrád, C., Adam-Vizi, V. and Chinopoulos, C.** (2011). Complex contribution of cyclophilin D to Ca²⁺-induced permeability transition in brain mitochondria, with relation to the bioenergetic state. *J Biol Chem* **286**, 6345–6353.
- Doll, R. and Hill, A.** (1950). Smoking and carcinoma of the lung; preliminary report. *Br Med J* **2**, 739–748.
- Du, C., Fang, M., Li, Y., Li, L. and Wang, X.** (2000). Smac, a mitochondrial protein that promotes cytochrome c-dependent caspase activation by eliminating IAP inhibition. *Cell* **102**, 33–42.
- Duarte, F. V., Simões, A. M., Teodoro, J. S., Rolo, A. P. and Palmeira, C. M.** (2011). Exposure to dibenzofuran affects lung mitochondrial function in vitro. *Toxicology mechanisms and methods* **21**, 571–576.
- Duarte, F. V., Teodoro, J. S., Rolo, A. P. and Palmeira, C. M.** (2012). Exposure to dibenzofuran triggers autophagy in lung cells. *Toxicol Lett* **209**, 35–42.
- Duchen, M. R.** (2004a). Roles of mitochondria in health and disease. *Diabetes* **53** Suppl 1, S96–102.
- Duchen, M. R.** (2004b). Mitochondria in health and disease: perspectives on a new mitochondrial biology. *Mol Aspects Med* **25**, 365–451.
- Ehrenberg, B., Montana, V., Wei, M. D., Wuskell, J. P. and Loew, L. M.** (1988). Membrane potential can be determined in individual cells from the nernstian

distribution of cationic dyes. *Biophys J* **53**, 785–794.

Eisenberg-Lerner, A., Bialik, S., Simon, H.-U. and Kimchi, A. (2009). Life and death partners: apoptosis, autophagy and the cross-talk between them. *Cell Death Differ* **16**, 966–975.

Elizondo, G., Fernandez-Salguero, P., Sheikh, M. S., Kim, G. Y., Fornace, A. J., Lee, K. S. and Gonzalez, F. J. (2000). Altered cell cycle control at the G(2)/M phases in aryl hydrocarbon receptor-null embryo fibroblast. *Mol Pharmacol* **57**, 1056–1063.

Elmore, S. P., Qian, T., Grissom, S. F. and Lemasters, J. J. (2001). The mitochondrial permeability transition initiates autophagy in rat hepatocytes. *The FASEB Journal* **15**, 2286–2287.

Elrod, J. W., Wong, R., Mishra, S., Vagnozzi, R. J., Sakthivel, B., Goonasekera, S. A., Karch, J., Gabel, S., Farber, J., Force, T., et al. (2010). Cyclophilin D controls mitochondrial pore-dependent Ca(2+) exchange, metabolic flexibility, and propensity for heart failure in mice. *J Clin Invest* **120**, 3680–3687.

Estabrook, R. (1967). Mitochondrial respiratory control and the polarographic measurement of ADP/O ratios. *Methods Enzymol* **10**, 41–47.

Fader, C. M. and Colombo, M. I. (2009). Autophagy and multivesicular bodies: two closely related partners. *Cell Death Differ* **16**, 70–78.

Feng, Z., Zhang, H., Levine, A. J. and Jin, S. (2005). The coordinate regulation of the p53 and mTOR pathways in cells. *Proc Natl Acad Sci USA* **102**, 8204–8209.

Ferecatu, I., Borot, M.-C., Bossard, C., Leroux, M., Boggetto, N., Marano, F., Baeza-Squiban, A. and Andreau, K. (2010). Polycyclic aromatic hydrocarbon components contribute to the mitochondria-antiapoptotic effect of fine particulate matter on human bronchial epithelial cells via the aryl hydrocarbon receptor. *Particle and Fibre Toxicology* **7**, 18.

Ferlay, J., Shin, H.-R., Bray, F., Forman, D., Mathers, C. and Parkin, D. M. (2010). Estimates of worldwide burden of cancer in 2008: GLOBOCAN 2008. *Int J Cancer* **127**, 2893–2917.

Fernandez-Salguero, P., Pineau, T., Hilbert, D. M., McPhail, T., Lee, S. S., Kimura, S., Nebert, D. W., Rudikoff, S., Ward, J. M. and Gonzalez, F. J. (1995). Immune system impairment and hepatic fibrosis in mice lacking the dioxin-binding Ah receptor. *Science* **268**, 722–726.

Fimia, G. M., Stoykova, A., Romagnoli, A., Giunta, L., Di Bartolomeo, S., Nardacci, R., Corazzari, M., Fuoco, C., Ucar, A., Schwartz, P., et al. (2007). Ambra1 regulates autophagy and development of the nervous system. *Nature* **447**, 1121–1125.

Fisher, M. T., Nagarkatti, M. and Nagarkatti, P. S. (2005). Aryl hydrocarbon receptor-dependent induction of loss of mitochondrial membrane potential in epididymal spermatozoa by 2,3,7,8-tetrachlorodibenzo-p-dioxin (TCDD). *Toxicol Lett* **157**, 99–107.

Forgacs, A. L., Burgoon, L. D., Lynn, S. G., LaPres, J. J. and Zacharewski, T. (2010). Effects of TCDD on the expression of nuclear encoded mitochondrial

- genes. *Toxicol Appl Pharmacol* **246**, 58–65.
- Gendy, El, M. A. M., Soshilov, A. A., Denison, M. S. and El-Kadi, A. O. S.** (2012). Transcriptional and posttranslational inhibition of dioxin-mediated induction of CYP1A1 by harmine and harmol. *Toxicol Lett* **208**, 51–61.
- Gentner, N. J. and Weber, L. P.** (2010). Intranasal benzo[a]pyrene alters circadian blood pressure patterns and causes lung inflammation in rats. *Arch Toxicol*.
- Giorgi, C., Agnoletto, C., Bononi, A., Bonora, M., De Marchi, E., Marchi, S., Missiroli, S., Patergnani, S., Poletti, F., Rimessi, A., et al.** (2012). Mitochondrial calcium homeostasis as potential target for mitochondrial medicine. *Mitochondrion* **12**, 77–85.
- Giorgio, V., Soriano, M. E., Basso, E., Bisetto, E., Lippe, G., Forte, M. A. and Bernardi, P.** (2010). Cyclophilin D in mitochondrial pathophysiology. *Biochim Biophys Acta* **1797**, 1113–1118.
- Gomes, A. P., Duarte, F. V., Nunes, P., Hubbard, B. P., Teodoro, J. S., Varela, A. T., Jones, J. G., Sinclair, D. A., Palmeira, C. M. and Rolo, A. P.** (2012). Berberine protects against high fat diet-induced dysfunction in muscle mitochondria by inducing SIRT1-dependent mitochondrial biogenesis. *Biochim Biophys Acta* **1822**, 185–195.
- Gomez, L., Li, B., Mewton, N., Sanchez, I., Piot, C., Elbaz, M. and Ovize, M.** (2009). Inhibition of mitochondrial permeability transition pore opening: translation to patients. *Cardiovasc Res* **83**, 226–233.
- Goodman, J. E., Kerper, L. E., Boyce, C. P., Prueitt, R. L. and Rhomberg, L. R.** (2010). Weight-of-evidence analysis of human exposures to dioxins and dioxin-like compounds and associations with thyroid hormone levels during early development. *Regul Toxicol Pharmacol* **58**, 79–99.
- Gornall, A., Bardawill, C. and David, M.** (1949). Determination of serum proteins by means of the biuret reaction. *J Biol Chem* **177**, 751–766.
- Gozuacik, D. and Kimchi, A.** (2006). DAPK protein family and cancer. *Autophagy* **2**, 74–79.
- Gozuacik, D. and Kimchi, A.** (2007). Autophagy and cell death. pp. 217–245. *Current Topics in Developmental Biology*.
- Green, D. R. and Kroemer, G.** (2004). The pathophysiology of mitochondrial cell death. *Science* **305**, 626–629.
- Green, D. R., Galluzzi, L. and Kroemer, G.** (2011). Mitochondria and the autophagy-inflammation-cell death axis in organismal aging. *Science* **333**, 1109–1112.
- Griffiths, E. J. and Halestrap, A. P.** (1995). Mitochondrial non-specific pores remain closed during cardiac ischaemia, but open upon reperfusion. *Biochem J* **307 (Pt 1)**, 93–98.
- Gunter, T. E. and Pfeiffer, D. R.** (1990). Mechanisms by which mitochondria transport calcium. *Am J Physiol* **258**, C755–86.
- Hailey, D. W., Rambold, A. S., Satpute-Krishnan, P., Mitra, K., Sougrat, R., Kim, P.**

- K. and Lippincott-Schwartz, J.** (2010). Mitochondria supply membranes for autophagosome biogenesis during starvation. *Cell* **141**, 656–667.
- Hait, W. N., Jin, S. and Yang, J.-M.** (2006). A matter of life or death (or both): understanding autophagy in cancer. *Clin Cancer Res* **12**, 1961–1965.
- Halappanavar, S., Wu, D., Williams, A., Kuo, B., Godschalk, R. W., Van Schooten, F. J. and Yauk, C. L.** (2011). Pulmonary gene and microRNA expression changes in mice exposed to benzo(a)pyrene by oral gavage. *Toxicology* **285**, 133–141.
- Halestrap, A. P.** (2009). What is the mitochondrial permeability transition pore? *J Mol Cell Cardiol* **46**, 821–831.
- Halestrap, A. P. and Brenner, C.** (2003). The adenine nucleotide translocase: a central component of the mitochondrial permeability transition pore and key player in cell death. *Curr Med Chem* **10**, 1507–1525.
- Halestrap, A. P. and Davidson, A. M.** (1990). Inhibition of Ca²⁺(+)-induced large-amplitude swelling of liver and heart mitochondria by cyclosporin is probably caused by the inhibitor binding to mitochondrial-matrix peptidyl-prolyl cis-trans isomerase and preventing it interacting with the adenine nucleotide translocase. *Biochem J* **268**, 153–160.
- Halestrap, A. P. and Pasdois, P.** (2009). The role of the mitochondrial permeability transition pore in heart disease. *Biochim Biophys Acta* **1787**, 1402–1415.
- Halestrap, A. P., Clarke, S. J. and Javadov, S. A.** (2004). Mitochondrial permeability transition pore opening during myocardial reperfusion--a target for cardioprotection. *Cardiovasc Res* **61**, 372–385.
- Halestrap, A. P., Clarke, S. J. and Khaliulin, I.** (2007). The role of mitochondria in protection of the heart by preconditioning. *Biochim Biophys Acta* **1767**, 1007–1031.
- Hamanaka, R. B. and Chandel, N. S.** (2010). Mitochondrial reactive oxygen species regulate cellular signaling and dictate biological outcomes. *Trends Biochem Sci* **35**, 505–513.
- Hansson, M. J., Morota, S., Chen, L., Matsuyama, N., Suzuki, Y., Nakajima, S., Tanoue, T., Omi, A., Shibasaki, F., Shimazu, M., et al.** (2011). Cyclophilin D-sensitive mitochondrial permeability transition in adult human brain and liver mitochondria. *J. Neurotrauma* **28**, 143–153.
- Hausenloy, D. J. and Yellon, D. M.** (2003). The mitochondrial permeability transition pore: its fundamental role in mediating cell death during ischaemia and reperfusion. *J Mol Cell Cardiol* **35**, 339–341.
- Hausenloy, D. J., Yellon, D. M., Mani-Babu, S. and Duchon, M. R.** (2004). Preconditioning protects by inhibiting the mitochondrial permeability transition. *Am J Physiol Heart Circ Physiol* **287**, H841–9.
- Haynes, C. M. and Ron, D.** (2010). The mitochondrial UPR - protecting organelle protein homeostasis. *Journal of Cell Science* **123**, 3849–3855.
- Helgason, L. B., Verreault, J., Braune, B. M., Borgå, K., Primicerio, R., Jenssen, B. M. and Gabrielsen, G. W.** (2010). Relationship between persistent halogenated organic contaminants and TCDD-toxic equivalents on EROD activity and retinoid

- and thyroid hormone status in northern fulmars. *Sci Total Environ* **408**, 6117–6123.
- Hengartner, M. O.** (2000). The biochemistry of apoptosis. *Nature* **407**, 770–776.
- Hombach-Klonisch, S., Pocar, P., Kauffold, J. and Klonisch, T.** (2006). Dioxin exerts anti-estrogenic actions in a novel dioxin-responsive telomerase-immortalized epithelial cell line of the porcine oviduct (TERT-OPEC). *Toxicol Sci* **90**, 519–528.
- Hossain, A., Tsuchiya, S., Minegishi, M., Osada, M., Ikawa, S., Tezuka, F. A., Kaji, M., Konno, T., Watanabe, M. and Kikuchi, H.** (1998). The Ah receptor is not involved in 2,3,7,8-tetrachlorodibenzo-*p*-dioxin-mediated apoptosis in human leukemic T cell lines. *J Biol Chem* **273**, 19853–19858.
- Hu, C., Jiang, L., Geng, C., Zhang, X., Cao, J. and Zhong, L.** (2008). Possible involvement of oxidative stress in trichloroethylene-induced genotoxicity in human HepG2 cells. *Mutat Res* **652**, 88–94.
- Hu, M.-T., Chen, S.-J., Huang, K.-L., Lin, Y.-C., Chang-Chien, G.-P. and Tsai, J.-H.** (2009). Characterization of polychlorinated dibenzo-*p*-dioxin/dibenzofuran emissions from joss paper burned in a furnace with air pollution control devices. *Science of the Total Environment, The* **407**, 3290–3294.
- Ichas, F. and Mazat, J. P.** (1998). From calcium signaling to cell death: two conformations for the mitochondrial permeability transition pore. Switching from low- to high-conductance state. *Biochim Biophys Acta* **1366**, 33–50.
- Ichimura, Y., Kumanomidou, T., Sou, Y.-S., Mizushima, T., Ezaki, J., Ueno, T., Kominami, E., Yamane, T., Tanaka, K. and Komatsu, M.** (2008). Structural basis for sorting mechanism of p62 in selective autophagy. *J Biol Chem* **283**, 22847–22857.
- Iida, A., Emi, M., Matsuoka, R., Hiratsuka, E., Okui, K., Ohashi, H., Inazawa, J., Fukushima, Y., Imai, T. and Nakamura, Y.** (2000). Identification of a gene disrupted by inv(11)(q13.5;q25) in a patient with left-right axis malformation. *Hum. Genet.* **106**, 277–287.
- Iida, T., Todaka, T., Hirakawa, H., Hori, T., Tobiishi, K., Matsueda, T., Watanabe, S. and Yamada, T.** (2007). Concentration and distribution of dioxins and related compounds in human tissues. *CHEMOSPHERE* **67**, S263–71.
- Ishida, T., Hirono, Y., Yoshikawa, K., Hutei, Y., Miyagawa, M., Sakaguchi, I., Pinkerton, K. E. and Takeuchi, M.** (2009). Inhibition of immunological function mediated DNA damage of alveolar macrophages caused by cigarette smoke in mice. *Inhal Toxicol* **21**, 1229–1235.
- James, D. I., Parone, P. A., Mattenberger, Y. and Martinou, J.-C.** (2003). hFis1, a novel component of the mammalian mitochondrial fission machinery. *J Biol Chem* **278**, 36373–36379.
- Javadov, S., Hunter, J. C., Barreto-Torres, G. and Parodi-Rullan, R.** (2011). Targeting the mitochondrial permeability transition: cardiac ischemia-reperfusion versus carcinogenesis. *Cell. Physiol. Biochem.* **27**, 179–190.
- Javadov, S., Rajapurohitam, V., Kilić, A., Zeidan, A., Choi, A. and Karmazyn, M.** (2009). Anti-hypertrophic effect of NHE-1 inhibition involves GSK-3beta-dependent

- attenuation of mitochondrial dysfunction. *J Mol Cell Cardiol* **46**, 998–1007.
- Jemal, A., Bray, F., Center, M. M., Ferlay, J., Ward, E. and Forman, D.** (2011). Global cancer statistics. *CA Cancer J Clin* **61**, 69–90.
- Jobe, S. M., Wilson, K. M., Leo, L., Raimondi, A., Molkenin, J. D., Lentz, S. R. and Di Paola, J.** (2008). Critical role for the mitochondrial permeability transition pore and cyclophilin D in platelet activation and thrombosis. *Blood* **111**, 1257–1265.
- Jules, G. E., Pratap, S., Ramesh, A. and Hood, D. B.** (2012). In utero exposure to benzo(a)pyrene predisposes offspring to cardiovascular dysfunction in later-life. *Toxicology*.
- Jung, W.-W., Kim, E.-M., Lee, E.-H., Yun, H.-J., Ju, H.-R., Jeong, M.-J., Hwang, K. W., Sul, D. and Kang, H.-S.** (2007). Formaldehyde exposure induces airway inflammation by increasing eosinophil infiltrations through the regulation of reactive oxygen species production. *Environ. Toxicol. Pharmacol.* **24**, 174–182.
- Kabeya, Y., Mizushima, N., Yamamoto, A., Oshitani-Okamoto, S., Ohsumi, Y. and Yoshimori, T.** (2004). LC3, GABARAP and GATE16 localize to autophagosomal membrane depending on form-II formation. *Journal of Cell Science* **117**, 2805–2812.
- Kamimoto, T., Shoji, S., Hidvegi, T., Mizushima, N., Umebayashi, K., Perlmutter, D. H. and Yoshimori, T.** (2006). Intracellular inclusions containing mutant alpha-1-antitrypsin Z are propagated in the absence of autophagic activity. *J Biol Chem* **281**, 4467–4476.
- Kamo, N., Muratsugu, M., Hongoh, R. and Kobatake, Y.** (1979). Membrane potential of mitochondria measured with an electrode sensitive to tetraphenyl phosphonium and relationship between proton electrochemical potential and phosphorylation potential in steady state. *J. Membr. Biol.* **49**, 105–121.
- Katanoda, K., Sobue, T., Satoh, H., Tajima, K., Suzuki, T., Nakatsuka, H., Takezaki, T., Nakayama, T., Nitta, H., Tanabe, K., et al.** (2011). An association between long-term exposure to ambient air pollution and mortality from lung cancer and respiratory diseases in Japan. *J Epidemiol* **21**, 132–143.
- Kaushik, S. and Cuervo, A. M.** (2006). Autophagy as a cell-repair mechanism: activation of chaperone-mediated autophagy during oxidative stress. *Mol Aspects Med* **27**, 444–454.
- Khuder, S. A.** (2001). Effect of cigarette smoking on major histological types of lung cancer: a meta-analysis. *Lung Cancer* **31**, 139–148.
- Kim, I. and Lemasters, J. J.** (2011). Mitochondrial degradation by autophagy (mitophagy) in GFP-LC3 transgenic hepatocytes during nutrient deprivation. *AJP: Cell Physiology* **300**, C308–17.
- Kim, I., Rodriguez-Enriquez, S. and Lemasters, J. J.** (2007). Selective degradation of mitochondria by mitophagy. pp. 245–253.
- Kinnally, K. W., Peixoto, P. M., Ryu, S.-Y. and Dejean, L. M.** (2011). Is mPTP the gatekeeper for necrosis, apoptosis, or both? *Biochim Biophys Acta* **1813**, 616–622.
- Klingenberg, M.** (2008). The ADP and ATP transport in mitochondria and its carrier.

Biochim Biophys Acta **1778**, 1978–2021.

Klionsky, D. J., Abeliovich, H., Agostinis, P., Agrawal, D. K., Aliev, G., Askew, D. S., Baba, M., Baehrecke, E. H., Bahr, B. A., Ballabio, A., et al. (2008).

Guidelines for the use and interpretation of assays for monitoring autophagy in higher eukaryotes. *Autophagy* **4**, 151–175.

Kobayashi, D., Ahmed, S., Ishida, M., Kasai, S. and Kikuchi, H. (2009).

Calcium/calmodulin signaling elicits release of cytochrome c during 2,3,7,8-tetrachlorodibenzo-p-dioxin-induced apoptosis in the human lymphoblastic T-cell line, L-MAT. *Toxicology* **258**, 25–32.

Kokoszka, J. E., Waymire, K. G., Levy, S. E., Sligh, J. E., Cai, J., Jones, D. P., MacGregor, G. R. and Wallace, D. C. (2004).

The ADP/ATP translocator is not essential for the mitochondrial permeability transition pore. *Nature* **427**, 461–465.

Komatsu, M. and Ichimura, Y. (2010). Selective autophagy regulates various cellular functions. *Genes Cells* **15**, 923–933.

Konrád, C., Kiss, G., Töröcsik, B., Lábár, J. L., Gerencser, A. A., Mándi, M., Adam-Vizi, V. and Chinopoulos, C. (2011).

A distinct sequence in the adenine nucleotide translocase from *Artemia franciscana* embryos is associated with insensitivity to bongkrekate and atypical effects of adenine nucleotides on Ca²⁺ uptake and sequestration. *FEBS J* **278**, 822–836.

Kopf, P. G. and Walker, M. K. (2010). 2,3,7,8-tetrachlorodibenzo-p-dioxin increases reactive oxygen species production in human endothelial cells via induction of cytochrome P4501A1. *Toxicol Appl Pharmacol* **245**, 91–99.

Koshiba, T., Detmer, S. A., Kaiser, J. T., Chen, H., McCaffery, J. M. and Chan, D. C. (2004).

Structural basis of mitochondrial tethering by mitofusin complexes. *Science* **305**, 858–862.

Krauskopf, A., Eriksson, O., Craigen, W. J., Forte, M. A. and Bernardi, P. (2006).

Properties of the permeability transition in VDAC1(-/-) mitochondria. *Biochim Biophys Acta* **1757**, 590–595.

Krestinina, O. V., Grachev, D. E., Odinkova, I. V., Reiser, G., Evtodienko, Y. V. and Azarashvili, T. S. (2009).

Effect of peripheral benzodiazepine receptor (PBR/TSPO) ligands on opening of Ca²⁺-induced pore and phosphorylation of 3.5-kDa polypeptide in rat brain mitochondria. *Biochemistry Mosc.* **74**, 421–429.

Krishnan, K. J., Greaves, L. C., Reeve, A. K. and Turnbull, D. (2007). The ageing mitochondrial genome. *Nucleic Acids Research* **35**, 7399–7405.

Kroemer, G., Galluzzi, L. and Brenner, C. (2007). Mitochondrial membrane permeabilization in cell death. *Physiol Rev* **87**, 99–163.

Kroemer, G., Zamzami, N. and Susin, S. A. (1997). Mitochondrial control of apoptosis. *Immunol. Today* **18**, 44–51.

Kushnareva, Y. and Newmeyer, D. D. (2010). Bioenergetics and cell death. *Ann N Y Acad Sci* **1201**, 50–57.

Landes, T., Leroy, I., Bertholet, A., Diot, A., Khosrobakhsh, F., Daloyau, M., Davezac, N., Miquel, M.-C., Courilleau, D., Guillou, E., et al. (2010). OPA1

- (dys)functions. *Semin Cell Dev Biol* **21**, 593–598.
- Larsen, K. E. and Sulzer, D.** (2002). Autophagy in neurons: a review. *Histol. Histopathol.* **17**, 897–908.
- Larsson, N.-G.** (2010). Somatic mitochondrial DNA mutations in mammalian aging. *Annu. Rev. Biochem.* **79**, 683–706.
- Lecureur, V., Arzel, M., Ameziane, S., Houlbert, N., Le Vee, M., Jouneau, S. and Fardel, O.** (2012). MAPK- and PKC/CREB-dependent induction of interleukin-11 by the environmental contaminant formaldehyde in human bronchial epithelial cells. *Toxicology* **292**, 13–22.
- Lee, A. C., Xu, X. and Colombini, M.** (1996). The role of pyridine dinucleotides in regulating the permeability of the mitochondrial outer membrane. *J Biol Chem* **271**, 26724–26731.
- Lee, J., Giordano, S. and Zhang, J.** (2012). Autophagy, mitochondria and oxidative stress: cross-talk and redox signalling. *Biochem J* **441**, 523–540.
- Lee, W. S. and Sokol, R. J.** (2007). Liver disease in mitochondrial disorders. *Semin. Liver Dis.* **27**, 259–273.
- Lehmann, I., Rehwagen, M., Diez, U., Seiffart, A., Rolle-Kampczyk, U., Richter, M., Wetzig, H., Borte, M., Herbarth, O. Leipzig Allergy Risk Children Study** (2001). Enhanced in vivo IgE production and T cell polarization toward the type 2 phenotype in association with indoor exposure to VOC: results of the LARS study. *Int J Hyg Environ Health* **204**, 211–221.
- Lehmann, I., Röder-Stolinski, C., Nieber, K. and Fischäder, G.** (2008). In vitro models for the assessment of inflammatory and immuno-modulatory effects of the volatile organic compound chlorobenzene. *Exp. Toxicol. Pathol.* **60**, 185–193.
- Lehmann, I., Thoenke, A., Weiss, M., Schlink, U., Schulz, R., Diez, U., Sierig, G., Emmrich, F., Jacob, B., Belcredi, P., et al.** (2002). T cell reactivity in neonates from an East and a West German city--results of the LISA study. *Allergy* **57**, 129–136.
- Lemasters, J. J.** (2005). Selective mitochondrial autophagy, or mitophagy, as a targeted defense against oxidative stress, mitochondrial dysfunction, and aging. *Rejuvenation Res* **8**, 3–5.
- Lemasters, J. J., Qian, T., He, L., Kim, J.-S., Elmore, S. P., Cascio, W. E. and Brenner, D. A.** (2002). Role of mitochondrial inner membrane permeabilization in necrotic cell death, apoptosis, and autophagy. *Antioxid Redox Signal* **4**, 769–781.
- Lemasters, J. J., Theruvath, T. P., Zhong, Z. and Nieminen, A.-L.** (2009). Mitochondrial calcium and the permeability transition in cell death. *Biochim Biophys Acta* **1787**, 1395–1401.
- Lenaz, G.** (2012). Mitochondria and reactive oxygen species. Which role in physiology and pathology? *Adv. Exp. Med. Biol.* **942**, 93–136.
- Leung, A. W. C. and Halestrap, A. P.** (2008). Recent progress in elucidating the molecular mechanism of the mitochondrial permeability transition pore. *Biochim Biophys Acta* **1777**, 946–952.

- Leung, A. W. C., Varanyuwatana, P. and Halestrap, A. P.** (2008). The mitochondrial phosphate carrier interacts with cyclophilin D and may play a key role in the permeability transition. *J Biol Chem* **283**, 26312–26323.
- Levine, B. and Kroemer, G.** (2008). Autophagy in the pathogenesis of disease. *Cell* **132**, 27–42.
- Levine, B. and Yuan, J.** (2005). Autophagy in cell death: an innocent convict? *Journal of Clinical Investigation* **115**, 2679–2688.
- Li, L. Y., Luo, X. and Wang, X.** (2001). Endonuclease G is an apoptotic DNase when released from mitochondria. *Nature* **412**, 95–99.
- Li, X.-D., Yan, M., Chen, T., Lu, S.-Y., Yan, J.-H. and Cen, K.-F.** (2010). Levels of PCDD/Fs in soil in the vicinity of a medical waste incinerator in China: the temporal variation during 2007-2009. *Journal of Hazardous Materials* **179**, 783–789.
- Lin, D.-T. and Lechleiter, J. D.** (2002). Mitochondrial targeted cyclophilin D protects cells from cell death by peptidyl prolyl isomerization. *J Biol Chem* **277**, 31134–31141.
- Liu, X., Kim, C. N., Yang, J., Jemmerson, R. and Wang, X.** (1996). Induction of apoptotic program in cell-free extracts: requirement for dATP and cytochrome c. *Cell* **86**, 147–157.
- Liu, X., Weaver, D., Shirihai, O. and Hajnóczky, G.** (2009). Mitochondrial “kiss-and-run”: interplay between mitochondrial motility and fusion-fission dynamics. *EMBO J* **28**, 3074–3089.
- Luce, K., Weil, A. C. and Osiewacz, H. D.** (2010). Mitochondrial protein quality control systems in aging and disease. *Adv. Exp. Med. Biol.* **694**, 108–125.
- Luvisetto, S., Basso, E., Petronilli, V., Bernardi, P. and Forte, M.** (2008). Enhancement of anxiety, facilitation of avoidance behavior, and occurrence of adult-onset obesity in mice lacking mitochondrial cyclophilin D. *Neuroscience* **155**, 585–596.
- Madeira, V. M.** (1975). A rapid and ultrasensitive method to measure Ca⁺⁺ movements across biological membranes. *Biochem Biophys Res Commun* **64**, 870–876.
- Madeira, V. M., Antunes-Madeira, M. C. and Carvalho, A. P.** (1974). Activation energies of the ATPase activity of sarcoplasmic reticulum. *Biochem Biophys Res Commun* **58**, 897–904.
- Mai, S., Muster, B., Bereiter-Hahn, J. and Jendrach, M.** (2012). Autophagy proteins LC3B, ATG5 and ATG12 participate in quality control after mitochondrial damage and influence lifespan. *Autophagy* **8**, 47–62.
- Maiuri, M. C., Zalckvar, E., Kimchi, A. and Kroemer, G.** (2007). Self-eating and self-killing: crosstalk between autophagy and apoptosis. *Nat Rev Mol Cell Biol* **8**, 741–752.
- Mandal, P. K.** (2005). Dioxin: a review of its environmental effects and its aryl hydrocarbon receptor biology. *J. Comp. Physiol. B, Biochem. Syst. Environ. Physiol.* **175**, 221–230.

- Mariño, G. and López-Otín, C.** (2004). Autophagy: molecular mechanisms, physiological functions and relevance in human pathology. *Cell Mol Life Sci* **61**, 1439–1454.
- Marshall, N. B. and Kerkvliet, N. I.** (2010). Dioxin and immune regulation: emerging role of aryl hydrocarbon receptor in the generation of regulatory T cells. *Ann N Y Acad Sci* **1183**, 25–37.
- Martel, C., Huynh, L. H., Garnier, A., Ventura-Clapier, R. and Brenner, C.** (2012). Inhibition of the Mitochondrial Permeability Transition for Cytoprotection: Direct versus Indirect Mechanisms. *Biochem Res Int* **2012**, 213403.
- Martin, L. and Klaassen, C. D.** (2010). Differential effects of polychlorinated biphenyl congeners on serum thyroid hormone levels in rats. *Toxicological Sciences* **117**, 36–44.
- Martinelli, N., Girelli, D., Cigolini, D., Sandri, M., Ricci, G., Rocca, G. and Olivieri, O.** (2012). Access rate to the emergency department for venous thromboembolism in relationship with coarse and fine particulate matter air pollution. *PLoS ONE* **7**, e34831.
- Martinez-Vicente, M. and Cuervo, A. M.** (2007). Autophagy and neurodegeneration: when the cleaning crew goes on strike. *Lancet Neurol* **6**, 352–361.
- Masini, A., Ceccarelli-Stanzani, D. and Muscatello, U.** (1984). An investigation on the effect of oligomycin on state-4 respiration in isolated rat-liver mitochondria. *Biochim Biophys Acta* **767**, 130–137.
- Mathew, R., Karantza-Wadsworth, V. and White, E.** (2007). Role of autophagy in cancer. *Nat Rev Cancer* **7**, 961–967.
- Matsumoto, Y., Ide, F., Kishi, R., Akutagawa, T., Sakai, S., Nakamura, M., Ishikawa, T., Fujii-Kuriyama, Y. and Nakatsuru, Y.** (2007). Aryl hydrocarbon receptor plays a significant role in mediating airborne particulate-induced carcinogenesis in mice. *Environ Sci Technol* **41**, 3775–3780.
- Mbye, L. H. A. N., Singh, I. N., Carrico, K. M., Saatman, K. E. and Hall, E. D.** (2009). Comparative neuroprotective effects of cyclosporin A and NIM811, a nonimmunosuppressive cyclosporin A analog, following traumatic brain injury. *J. Cereb. Blood Flow Metab.* **29**, 87–97.
- McCommis, K. S. and Baines, C. P.** (2012). The role of VDAC in cell death: Friend or foe? *Biochim Biophys Acta* **1818**, 1444–1450.
- McGregor, D. B., Partensky, C., Wilbourn, J. and Rice, J. M.** (1998). An IARC evaluation of polychlorinated dibenzo-p-dioxins and polychlorinated dibenzofurans as risk factors in human carcinogenesis. *Environ Health Perspect* **106 Suppl 2**, 755–760.
- McGwin, G., Lienert, J. and Kennedy, J. I.** (2010). Formaldehyde exposure and asthma in children: a systematic review. *Environ Health Perspect* **118**, 313–317.
- Meeusen, S., McCaffery, J. M. and Nunnari, J.** (2004). Mitochondrial fusion intermediates revealed in vitro. *Science* **305**, 1747–1752.
- Meier, J.-M., Urban, P. and Goy, J.-J.** (2005). Postconditioning inhibits mitochondrial

- permeability transition. *Future Cardiol* **1**, 457–460.
- Mennear, J. H. and Lee, C. C.** (1994). Polybrominated dibenzo-p-dioxins and dibenzofurans: literature review and health assessment. *Environ Health Perspect* **102 Suppl 1**, 265–274.
- Michel, S., Wanet, A., De Pauw, A., Rommelaere, G., Arnould, T. and Renard, P.** (2012). Crosstalk between mitochondrial (dys)function and mitochondrial abundance. *J. Cell. Physiol.* **227**, 2297–2310.
- Mildaziene, V., Nauciene, Z., Baniene, R., Demin, O. and Krab, K.** (2002). Analysis of effects of 2,2',5,5'-tetrachlorobiphenyl on the flux control in oxidative phosphorylation system in rat liver mitochondria. *Mol Biol Rep* **29**, 35–40.
- Millay, D. P., Sargent, M. A., Osinska, H., Baines, C. P., Barton, E. R., Vuagniaux, G., Sweeney, H. L., Robbins, J. and Molkentin, J. D.** (2008). Genetic and pharmacologic inhibition of mitochondrial-dependent necrosis attenuates muscular dystrophy. *Nat Med* **14**, 442–447.
- Mimura, J. and Fujii-Kuriyama, Y.** (2003). Functional role of AhR in the expression of toxic effects by TCDD. *Biochim Biophys Acta* **1619**, 263–268.
- Min, L., Fulton, D. B. and Andreotti, A. H.** (2005). A case study of proline isomerization in cell signaling. *Front Biosci* **10**, 385–397.
- Minelli, C., Wei, I., Sagoo, G., Jarvis, D., Shaheen, S. and Burney, P.** (2011). Interactive effects of antioxidant genes and air pollution on respiratory function and airway disease: a HuGE review. *American Journal of Epidemiology* **173**, 603–620.
- Mizushima, N., Levine, B., Cuervo, A. M. and Klionsky, D. J.** (2008). Autophagy fights disease through cellular self-digestion. *Nature* **451**, 1069–1075.
- Moreau, K., Luo, S. and Rubinsztein, D. C.** (2010). Cytoprotective roles for autophagy. *Curr Opin Cell Biol* **22**, 206–211.
- Mögel, I., Baumann, S., Böhme, A., Kohajda, T., Bergen, von, M., Simon, J.-C. and Lehmann, I.** (2011). The aromatic volatile organic compounds toluene, benzene and styrene induce COX-2 and prostaglandins in human lung epithelial cells via oxidative stress and p38 MAPK activation. *Toxicology* **289**, 28–37.
- Murphy, E. and Steenbergen, C.** (2008). Mechanisms underlying acute protection from cardiac ischemia-reperfusion injury. *Physiol Rev* **88**, 581–609.
- Murphy, M. P.** (2009). How mitochondria produce reactive oxygen species. *Biochem J* **417**, 1–13.
- Nadal, M., Domingo, J. L., García, F. and Schuhmacher, M.** (2009). Levels of PCDD/F in adipose tissue on non-occupationally exposed subjects living near a hazardous waste incinerator in Catalonia, Spain. *CHEMOSPHERE* **74**, 1471–1476.
- Nakagawa, T., Shimizu, S., Watanabe, T., Yamaguchi, O., Otsu, K., Yamagata, H., Inohara, H., Kubo, T. and Tsujimoto, Y.** (2005). Cyclophilin D-dependent mitochondrial permeability transition regulates some necrotic but not apoptotic cell death. *Nature* **434**, 652–658.
- Narendra, D. P., Jin, S. M., Tanaka, A., Suen, D.-F., Gautier, C. A., Shen, J.,**

- Cookson, M. R. and Youle, R. J.** (2010). PINK1 is selectively stabilized on impaired mitochondria to activate Parkin. *PLoS Biol* **8**, e1000298.
- Narendra, D., Tanaka, A., Suen, D.-F. and Youle, R. J.** (2008). Parkin is recruited selectively to impaired mitochondria and promotes their autophagy. *J Cell Biol* **183**, 795–803.
- Nemmar, A., Zia, S., Subramaniyan, D., Fahim, M. A. and Ali, B. H.** (2011). Exacerbation of thrombotic events by diesel exhaust particle in mouse model of hypertension. *Toxicology* **285**, 39–45.
- Nicholls, D. G.** (2009). Mitochondrial calcium function and dysfunction in the central nervous system. *Biochim Biophys Acta* **1787**, 1416–1424.
- Niittynen, M., Tuomisto, J. T. and Pohjanvirta, R.** (2008). Effect of 2,3,7,8-tetrachlorodibenzo-p-dioxin (TCDD) on heme oxygenase-1, biliverdin IXalpha reductase and delta-aminolevulinic acid synthetase 1 in rats with wild-type or variant AH receptor. *Toxicology* **250**, 132–142.
- Nishino, I.** (2006). Autophagic vacuolar myopathy. *Semin Pediatr Neurol* **13**, 90–95.
- Novgorodov, S. A. and Gudz, T. I.** (1996). Permeability transition pore of the inner mitochondrial membrane can operate in two open states with different selectivities. *J Bioenerg Biomembr* **28**, 139–146.
- Nunnari, J. and Suomalainen, A.** (2012). Mitochondria: in sickness and in health. *Cell* **148**, 1145–1159.
- Oda, K., Matsuoka, Y., Funahashi, A. and Kitano, H.** (2005). A comprehensive pathway map of epidermal growth factor receptor signaling. *Mol Syst Biol* **1**, 2005.0010.
- Oettinghaus, B., Licci, M., Scorrano, L. and Frank, S.** (2011). Less than perfect divorces: dysregulated mitochondrial fission and neurodegeneration. *Acta Neuropathol.*
- Okamoto, K. and Kondo-Okamoto, N.** (2012). Mitochondria and autophagy: Critical interplay between the two homeostats. *Biochim Biophys Acta* **1820**, 595–600.
- Okamoto, K., Kondo-Okamoto, N. and Ohsumi, Y.** (2009). A landmark protein essential for mitophagy: Atg32 recruits the autophagic machinery to mitochondria. *Autophagy* **5**, 1203–1205.
- Olichon, A., Baricault, L., Gas, N., Guillou, E., Valette, A., Belenguer, P. and Lenaers, G.** (2003). Loss of OPA1 perturbs the mitochondrial inner membrane structure and integrity, leading to cytochrome c release and apoptosis. *J Biol Chem* **278**, 7743–7746.
- Orrenius, S., Gogvadze, V. and Zhivotovsky, B.** (2007). Mitochondrial oxidative stress: implications for cell death. *Annu Rev Pharmacol Toxicol* **47**, 143–183.
- Palmeira, C. M. and Madeira, V. M.** (1997). Mercuric chloride toxicity in rat liver mitochondria and isolated hepatocytes. *Environ. Toxicol. Pharmacol.* **3**, 229–235.
- Palmeira, C. M. and Wallace, K. B.** (1997). Benzoquinone inhibits the voltage-dependent induction of the mitochondrial permeability transition caused by redox-

- cycling naphthoquinones. *Toxicol Appl Pharmacol* **143**, 338–347.
- Palmeira, C. M., Moreno, A. J. and Madeira, V. M.** (1994). Interactions of herbicides 2,4-D and dinoseb with liver mitochondrial bioenergetics. *Toxicol Appl Pharmacol* **127**, 50–57.
- Palmeira, C. M., Rolo, A. P., Berthiaume, J., Bjork, J. A. and Wallace, K. B.** (2007). Hyperglycemia decreases mitochondrial function: the regulatory role of mitochondrial biogenesis. *Toxicol Appl Pharmacol* **225**, 214–220.
- Pantucharoensri, S., Boontee, P., Likhitsan, P., Padungtod, C. and Prasartsansoui, S.** (2004). Generalized eruption accompanied by hepatitis in two Thai metal cleaners exposed to trichloroethylene. *Ind Health* **42**, 385–388.
- Parkin, D. M., Bray, F., Ferlay, J. and Pisani, P.** (2005). Global cancer statistics, 2002. *CA Cancer J Clin* **55**, 74–108.
- Pasdois, P., Parker, J. E., Griffiths, E. J. and Halestrap, A. P.** (2011). The role of oxidized cytochrome c in regulating mitochondrial reactive oxygen species production and its perturbation in ischaemia. *Biochem J* **436**, 493–505.
- Pastorino, J. G. and Hoek, J. B.** (2003). Hexokinase II: the integration of energy metabolism and control of apoptosis. *Curr Med Chem* **10**, 1535–1551.
- Pastorino, J. G. and Hoek, J. B.** (2008). Regulation of hexokinase binding to VDAC. *J Bioenerg Biomembr* **40**, 171–182.
- Patel, D. R. and Homnick, D. N.** (2000). Pulmonary effects of smoking. *Adolesc Med* **11**, 567–576.
- Pedersen, P. L., Mathupala, S., Rempel, A., Geschwind, J. F. and Ko, Y. H.** (2002). Mitochondrial bound type II hexokinase: a key player in the growth and survival of many cancers and an ideal prospect for therapeutic intervention. *Biochim Biophys Acta* **1555**, 14–20.
- Pedraza-Chaverri, J., Barrera, D., Medina-Campos, O. N., Carvajal, R. C., Hernández-Pando, R., Macías-Ruvalcaba, N. A., Maldonado, P. D., Salcedo, M. I., Tapia, E., Saldívar, L., et al.** (2005). Time course study of oxidative and nitrosative stress and antioxidant enzymes in K2Cr2O7-induced nephrotoxicity. *BMC Nephrol* **6**, 4.
- Pelucchi, C., Negri, E., Gallus, S., Boffetta, P., Tramacere, I. and La Vecchia, C.** (2009). Long-term particulate matter exposure and mortality: a review of European epidemiological studies. *BMC Public Health* **9**, 453.
- Peralta, S., Wang, X. and Moraes, C. T.** (2011). Mitochondrial transcription: Lessons from mouse models. *Biochim Biophys Acta*.
- Perez, L., Rapp, R. and Künzli, N.** (2010). The Year of the Lung: outdoor air pollution and lung health. *Swiss Med Wkly* **140**, w13129.
- Perier, C. and Vila, M.** (2012). Mitochondrial biology and Parkinson's disease. *Cold Spring Harb Perspect Med* **2**, a009332.
- Perlmuter, D. H.** (2006). The role of autophagy in alpha-1-antitrypsin deficiency: a specific cellular response in genetic diseases associated with aggregation-prone

proteins. *Autophagy* **2**, 258–263.

- Petronilli, V., Miotto, G., Canton, M., Brini, M., Colonna, R., Bernardi, P. and Di Lisa, F.** (1999). Transient and long-lasting openings of the mitochondrial permeability transition pore can be monitored directly in intact cells by changes in mitochondrial calcein fluorescence. *Biophys J* **76**, 725–734.
- Pfeiffer, D. R. and Tchen, T. T.** (1975). The activation of adrenal cortex mitochondrial malic enzyme by Ca²⁺ and Mg²⁺. *Biochemistry* **14**, 89–96.
- Piot, C., Croisille, P., Staat, P., Thibault, H., Rioufol, G., Mewton, N., Elbelghiti, R., Cung, T. T., Bonnefoy, E., Angoulvant, D., et al.** (2008). Effect of cyclosporine on reperfusion injury in acute myocardial infarction. *N. Engl. J. Med.* **359**, 473–481.
- Polster, B. M. and Fiskum, G.** (2004). Mitochondrial mechanisms of neural cell apoptosis. *J Neurochem* **90**, 1281–1289.
- Prüss-Ustün, A., Vickers, C., Haefliger, P. and Bertollini, R.** (2011). Knowns and unknowns on burden of disease due to chemicals: a systematic review. *Environmental Health* **10**, 9.
- Puppala, D., Lee, H., Kim, K. B. and Swanson, H. I.** (2008). Development of an aryl hydrocarbon receptor antagonist using the proteolysis-targeting chimeric molecules approach: a potential tool for chemoprevention. *Mol Pharmacol* **73**, 1064–1071.
- Purdue, M. P., Bakke, B., Stewart, P., De Roos, A. J., Schenk, M., Lynch, C. F., Bernstein, L., Morton, L. M., Cerhan, J. R., Severson, R. K., et al.** (2011). A case-control study of occupational exposure to trichloroethylene and non-Hodgkin lymphoma. *Environ Health Perspect* **119**, 232–238.
- Qin, Z.-H., Wang, Y., Kegel, K. B., Kazantsev, A., Apostol, B. L., Thompson, L. M., Yoder, J., Aronin, N. and DiFiglia, M.** (2003). Autophagy regulates the processing of amino terminal huntingtin fragments. *Human Molecular Genetics* **12**, 3231–3244.
- Raaschou-Nielsen, O., Andersen, Z., Hvidberg, M., Jensen, S. S., Ketzel, M., Sørensen, M., Loft, S., Overvad, K. and Tjønneland, A.** (2011). Lung Cancer Incidence and Long-Term Exposure to Air Pollution from Traffic. *Environ Health Perspect*.
- Rasola, A., Sciacovelli, M., Chiara, F., Pantic, B., Brusilow, W. S. and Bernardi, P.** (2010a). Activation of mitochondrial ERK protects cancer cells from death through inhibition of the permeability transition. *Proc Natl Acad Sci USA* **107**, 726–731.
- Rasola, A., Sciacovelli, M., Pantic, B. and Bernardi, P.** (2010b). Signal transduction to the permeability transition pore. *FEBS Lett* **584**, 1989–1996.
- Ravikumar, B., Acevedo-Arozena, A., Imarisio, S., Berger, Z., Vacher, C., O’Kane, C. J., Brown, S. D. M. and Rubinsztein, D. C.** (2005). Dynein mutations impair autophagic clearance of aggregate-prone proteins. *Nat Genet* **37**, 771–776.
- Ravikumar, B., Berger, Z., Vacher, C., O’Kane, C. J. and Rubinsztein, D. C.** (2006). Rapamycin pre-treatment protects against apoptosis. *Human Molecular Genetics* **15**, 1209–1216.
- Ravikumar, B., Duden, R. and Rubinsztein, D. C.** (2002). Aggregate-prone proteins

with polyglutamine and polyalanine expansions are degraded by autophagy. *Human Molecular Genetics* **11**, 1107–1117.

- Reddy, P. H., Reddy, T. P., Manczak, M., Calkins, M. J., Shirendeb, U. and Mao, P.** (2011). Dynamin-related protein 1 and mitochondrial fragmentation in neurodegenerative diseases. *Brain Res Rev* **67**, 103–118.
- Ricchelli, F., Sileikytė, J. and Bernardi, P.** (2011). Shedding light on the mitochondrial permeability transition. *Biochim Biophys Acta* **1807**, 482–490.
- Rico de Souza, A., Zago, M., Pollock, S. J., Sime, P. J., Phipps, R. P. and Baglole, C. J.** (2011). Genetic ablation of the aryl hydrocarbon receptor causes cigarette smoke-induced mitochondrial dysfunction and apoptosis. *J Biol Chem* **286**, 43214–43228.
- Rizzuto, R., Bernardi, P. and Pozzan, T.** (2000). Mitochondria as all-round players of the calcium game. *J Physiol (Lond)* **529 Pt 1**, 37–47.
- Rolo, A. P. and Palmeira, C. M.** (2006). Diabetes and mitochondrial function: role of hyperglycemia and oxidative stress. *Toxicol Appl Pharmacol* **212**, 167–178.
- Rolo, A. P., Gomes, A. P. and Palmeira, C. M.** (2011). Regulation of mitochondrial biogenesis in metabolic syndrome. *Curr Drug Targets* **12**, 872–878.
- Rolo, A. P., Palmeira, C. M. and Wallace, K. B.** (2003). Mitochondrially mediated synergistic cell killing by bile acids. *Biochim Biophys Acta* **1637**, 127–132.
- Rolo, A. P., Teodoro, J. S., Peralta, C., Roselló-Catafau, J. and Palmeira, C. M.** (2009). Prevention of I/R injury in fatty livers by ischemic preconditioning is associated with increased mitochondrial tolerance: the key role of ATP synthase and mitochondrial permeability transition. *Transpl. Int.* **22**, 1081–1090.
- Rostovtseva, T. K., Komarov, A., Bezrukov, S. M. and Colombini, M.** (2002). Dynamics of nucleotides in VDAC channels: structure-specific noise generation. *Biophys J* **82**, 193–205.
- Rostovtseva, T. K., Tan, W. and Colombini, M.** (2005). On the role of VDAC in apoptosis: fact and fiction. *J Bioenerg Biomembr* **37**, 129–142.
- Roupé, K. M., Nybo, M., Sjöbring, U., Alberius, P., Schmidtchen, A. and Sørensen, O. E.** (2010). Injury is a major inducer of epidermal innate immune responses during wound healing. *J. Invest. Dermatol.* **130**, 1167–1177.
- Rowlands, J. C. and Gustafsson, J. A.** (1997). Aryl hydrocarbon receptor-mediated signal transduction. *Critical Reviews in Toxicology* **27**, 109–134.
- Rubinsztein, D. C., Gestwicki, J. E., Murphy, L. O. and Klionsky, D. J.** (2007). Potential therapeutic applications of autophagy. *Nat Rev Drug Discov* **6**, 304–312.
- Russmann, S., Kullak-Ublick, G. A. and Grattagliano, I.** (2009). Current concepts of mechanisms in drug-induced hepatotoxicity. *Curr Med Chem* **16**, 3041–3053.
- Ryter, S. W. and Choi, A. M. K.** (2010). Autophagy in the lung. *Proc Am Thorac Soc* **7**, 13–21.
- Safe, S.** (1990). Polychlorinated biphenyls (PCBs), dibenzo-p-dioxins (PCDDs),

dibenzofurans (PCDFs), and related compounds: environmental and mechanistic considerations which support the development of toxic equivalency factors (TEFs). *Critical Reviews in Toxicology* **21**, 51–88.

- Sakai, Y., Oku, M., van der Klei, I. J. and Kiel, J. A. K. W.** (2006). Pexophagy: autophagic degradation of peroxisomes. *Biochim Biophys Acta* **1763**, 1767–1775.
- Salnikow, K. and Zhitkovich, A.** (2008). Genetic and epigenetic mechanisms in metal carcinogenesis and cocarcinogenesis: nickel, arsenic, and chromium. *Chem Res Toxicol* **21**, 28–44.
- Scagliotti, G. V., Longo, M. and Novello, S.** (2009). Nonsmall cell lung cancer in never smokers. *Curr Opin Oncol* **21**, 99–104.
- Scarpulla, R. C.** (2008). Transcriptional paradigms in mammalian mitochondrial biogenesis and function. *Physiol Rev* **88**, 611–638.
- Schapira, A. H. V.** (2006). Mitochondrial disease. *Lancet* **368**, 70–82.
- Schapira, A. H. V. and Gegg, M.** (2011). Mitochondrial contribution to Parkinson's disease pathogenesis. *Parkinsons Dis* **2011**, 159160.
- Scherz-Shouval, R. and Elazar, Z.** (2011). Regulation of autophagy by ROS: physiology and pathology. *Trends Biochem Sci* **36**, 30–38.
- Schinzel, A. C., Takeuchi, O., Huang, Z., Fisher, J. K., Zhou, Z., Rubens, J., Hetz, C., Danial, N. N., Moskowitz, M. A. and Korsmeyer, S. J.** (2005). Cyclophilin D is a component of mitochondrial permeability transition and mediates neuronal cell death after focal cerebral ischemia. *Proc Natl Acad Sci USA* **102**, 12005–12010.
- Schmidt, J. V. and Bradfield, C. A.** (1996). Ah receptor signaling pathways. *Annu Rev Cell Dev Biol* **12**, 55–89.
- Schweichel, J. U. and Merker, H. J.** (1973). The morphology of various types of cell death in prenatal tissues. *Teratology* **7**, 253–266.
- Scorrano, L.** (2009). Opening the doors to cytochrome c: changes in mitochondrial shape and apoptosis. *Int J Biochem Cell Biol* **41**, 1875–1883.
- Senft, A. P., Dalton, T. P., Nebert, D. W., Genter, M. B., Hutchinson, R. J. and Shertzer, H. G.** (2002a). Dioxin increases reactive oxygen production in mouse liver mitochondria. *Toxicol Appl Pharmacol* **178**, 15–21.
- Senft, A. P., Dalton, T. P., Nebert, D. W., Genter, M. B., Puga, A., Hutchinson, R. J., Kerzee, J. K., Uno, S. and Shertzer, H. G.** (2002b). Mitochondrial reactive oxygen production is dependent on the aromatic hydrocarbon receptor. *Free Radic Biol Med* **33**, 1268–1278.
- Sewall, C. H., Clark, G. C. and Lucier, G. W.** (1995). TCDD reduces rat hepatic epidermal growth factor receptor: comparison of binding, immunodetection, and autophosphorylation. *Toxicol Appl Pharmacol* **132**, 263–272.
- Shacka, J. J., Roth, K. A. and Zhang, J.** (2008). The autophagy-lysosomal degradation pathway: role in neurodegenerative disease and therapy. *Front Biosci* **13**, 718–736.

- Shah, P. P., Saurabh, K., Pant, M. C., Mathur, N. and Parmar, D.** (2009). Evidence for increased cytochrome P450 1A1 expression in blood lymphocytes of lung cancer patients. *Mutat Res* **670**, 74–78.
- Shen, D., Dalton, T. P., Nebert, D. W. and Shertzer, H. G.** (2005). Glutathione redox state regulates mitochondrial reactive oxygen production. *J Biol Chem* **280**, 25305–25312.
- Shertzer, H. G., Genter, M. B., Shen, D., Nebert, D. W., Chen, Y. and Dalton, T. P.** (2006). TCDD decreases ATP levels and increases reactive oxygen production through changes in mitochondrial F(0)F(1)-ATP synthase and ubiquinone. *Toxicol Appl Pharmacol* **217**, 363–374.
- Shibata, M., Lu, T., Furuya, T., Degterev, A., Mizushima, N., Yoshimori, T., MacDonald, M., Yankner, B. and Yuan, J.** (2006). Regulation of intracellular accumulation of mutant Huntingtin by Beclin 1. *J Biol Chem* **281**, 14474–14485.
- Shimada, T. and Fujii-Kuriyama, Y.** (2004). Metabolic activation of polycyclic aromatic hydrocarbons to carcinogens by cytochromes P450 1A1 and 1B1. *Cancer Science* **95**, 1–6.
- Shimizu, S., Matsuoka, Y., Shinohara, Y., Yoneda, Y. and Tsujimoto, Y.** (2001). Essential role of voltage-dependent anion channel in various forms of apoptosis in mammalian cells. *J Cell Biol* **152**, 237–250.
- Shoubridge, E. A.** (2001). Nuclear genetic defects of oxidative phosphorylation. *Human Molecular Genetics* **10**, 2277–2284.
- Sileikytė, J., Petronilli, V., Zulian, A., Dabbeni-Sala, F., Tognon, G., Nikolov, P., Bernardi, P. and Ricchelli, F.** (2011). Regulation of the inner membrane mitochondrial permeability transition by the outer membrane translocator protein (peripheral benzodiazepine receptor). *J Biol Chem* **286**, 1046–1053.
- Simões, A. M., Duarte, F. V., Teodoro, J. S., Rolo, A. P. and Palmeira, C. M.** (2010). Exposure to 2, 3, 7, 8-tetrachlorodibenzo-p-dioxin and tetraethyl lead affects lung mitochondria bioenergetics. *Toxicology mechanisms and methods* **20**, 1–6.
- Singh, P., Suman, S., Chandna, S. and Das, T. K.** (2009). Possible role of amyloid-beta, adenine nucleotide translocase and cyclophilin-D interaction in mitochondrial dysfunction of Alzheimer's disease. *Bioinformation* **3**, 440–445.
- Skehan, P., Storeng, R., Scudiero, D., Monks, A., McMahon, J., Vistica, D., Warren, J. T., Bokesch, H., Kenney, S. and Boyd, M. R.** (1990). New colorimetric cytotoxicity assay for anticancer-drug screening. *J Natl Cancer Inst* **82**, 1107–1112.
- Slattery, M. L., Samowitz, W., Ma, K., Murtaugh, M., Sweeney, C., Levin, T. R. and Neuhausen, S.** (2004). CYP1A1, cigarette smoking, and colon and rectal cancer. *American Journal of Epidemiology* **160**, 842–852.
- Smeitink, J. A., Zeviani, M., Turnbull, D. M. and Jacobs, H. T.** (2006). Mitochondrial medicine: a metabolic perspective on the pathology of oxidative phosphorylation disorders. *Cell Metab* **3**, 9–13.
- Smirnova, E., Shurland, D. L., Ryazantsev, S. N. and van der Bliek, A. M.** (1998). A human dynamin-related protein controls the distribution of mitochondria. *J Cell Biol*

143, 351–358.

- Soudani, N., Ben Amara, I., Sefi, M., Boudawara, T. and Zeghal, N.** (2011). Effects of selenium on chromium (VI)-induced hepatotoxicity in adult rats. *Exp. Toxicol. Pathol.* **63**, 541–548.
- Stocchi, V., Cucchiarini, L., Magnani, M., Chiarantini, L., Palma, P. and Crescentini, G.** (1985). Simultaneous extraction and reverse-phase high-performance liquid chromatographic determination of adenine and pyridine nucleotides in human red blood cells. *Anal Biochem* **146**, 118–124.
- Su, K. G., Banker, G., Bourdette, D. and Forte, M.** (2009). Axonal degeneration in multiple sclerosis: The mitochondrial hypothesis. *Curr Neurol Neurosci* **9**, 411–417.
- Su, T.-C., Chen, S.-Y. and Chan, C.-C.** (2011). Progress of ambient air pollution and cardiovascular disease research in Asia. *Prog Cardiovasc Dis* **53**, 369–378.
- Sun, Q., Hong, X. and Wold, L. E.** (2010). Cardiovascular effects of ambient particulate air pollution exposure. *Circulation* **121**, 2755–2765.
- Sun, S., Schiller, J. H. and Gazdar, A. F.** (2007). Lung cancer in never smokers--a different disease. *Nat Rev Cancer* **7**, 778–790.
- Susin, S. A., Lorenzo, H. K., Zamzami, N., Marzo, I., Snow, B. E., Brothers, G. M., Mangion, J., Jacotot, E., Costantini, P., Loeffler, M., et al.** (1999). Molecular characterization of mitochondrial apoptosis-inducing factor. *Nature* **397**, 441–446.
- Sutter, C. H., Yin, H., Li, Y., Mammen, J. S., Bodreddigari, S., Stevens, G., Cole, J. A. and Sutter, T. R.** (2009). EGF receptor signaling blocks aryl hydrocarbon receptor-mediated transcription and cell differentiation in human epidermal keratinocytes. *Proc Natl Acad Sci USA* **106**, 4266–4271.
- Tabrez, S. and Ahmad, M.** (2009). Toxicity, biomarkers, genotoxicity, and carcinogenicity of trichloroethylene and its metabolites: a review. *J Environ Sci Health C Environ Carcinog Ecotoxicol Rev* **27**, 178–196.
- Takacs-Vellai, K., Vellai, T., Puoti, A., Passannante, M., Wicky, C., Streit, A., Kovács, A. L. and Müller, F.** (2005). Inactivation of the autophagy gene bec-1 triggers apoptotic cell death in *C. elegans*. *Curr Biol* **15**, 1513–1517.
- Tanida, I., Ueno, T. and Kominami, E.** (2004). LC3 conjugation system in mammalian autophagy. *Int J Biochem Cell Biol* **36**, 2503–2518.
- Tanida, I., Ueno, T. and Kominami, E.** (2008). LC3 and Autophagy. *Methods Mol Biol* **445**, 77–88.
- Tatsuta, T. and Langer, T.** (2008). Quality control of mitochondria: protection against neurodegeneration and ageing. *EMBO J* **27**, 306–314.
- Teodoro, J. S., Simões, A. M., Duarte, F. V., Rolo, A. P., Murdoch, R. C., Hussain, S. M. and Palmeira, C. M.** (2011). Assessment of the toxicity of silver nanoparticles in vitro: a mitochondrial perspective. *Toxicol In Vitro* **25**, 664–670.
- Terman, A. and Brunk, U. T.** (2005). Autophagy in cardiac myocyte homeostasis, aging, and pathology. *Cardiovasc Res* **68**, 355–365.

- Thiele, D. L., Eigenbrodt, E. H. and Ware, A. J.** (1982). Cirrhosis after repeated trichloroethylene and 1,1,1-trichloroethane exposure. *Gastroenterology* **83**, 926–929.
- Thornberry, N. A. and Lazebnik, Y.** (1998). Caspases: enemies within. *Science* **281**, 1312–1316.
- Thun, M. J., Henley, S. J., Burns, D., Jemal, A., Shanks, T. G. and Calle, E. E.** (2006). Lung cancer death rates in lifelong nonsmokers. *JNCI Journal of the National Cancer Institute* **98**, 691–699.
- Toyooka, T. and Ibuki, Y.** (2009). Cigarette sidestream smoke induces phosphorylated histone H2AX. *Mutat Res* **676**, 34–40.
- Tritscher, A. M., Mahler, J., Portier, C. J., Lucier, G. W. and Walker, N. J.** (2000). Induction of lung lesions in female rats following chronic exposure to 2,3,7,8-tetrachlorodibenzo-p-dioxin. *Toxicol Pathol* **28**, 761–769.
- Turner, N. and Heilbronn, L. K.** (2008). Is mitochondrial dysfunction a cause of insulin resistance? *Trends Endocrinol Metab* **19**, 324–330.
- Twig, G., Elorza, A., Molina, A. J. A., Mohamed, H., Wikstrom, J. D., Walzer, G., Stiles, L., Haigh, S. E., Katz, S., Las, G., et al.** (2008). Fission and selective fusion govern mitochondrial segregation and elimination by autophagy. *EMBO J* **27**, 433–446.
- Valavanidis, A., Vlahogianni, T., Dassenakis, M. and Scoullou, M.** (2006). Molecular biomarkers of oxidative stress in aquatic organisms in relation to toxic environmental pollutants. *Ecotoxicol. Environ. Saf.* **64**, 178–189.
- van Grevenynghe, J., Bernard, M., Langouet, S., Le Berre, C., Fest, T. and Fardel, O.** (2005). Human CD34-positive hematopoietic stem cells constitute targets for carcinogenic polycyclic aromatic hydrocarbons. *J Pharmacol Exp Ther* **314**, 693–702.
- van Loo, G., Schotte, P., van Gorp, M., Demol, H., Hoorelbeke, B., Gevaert, K., Rodriguez, I., Ruiz-Carrillo, A., Vandekerckhove, J., Declercq, W., et al.** (2001). Endonuclease G: a mitochondrial protein released in apoptosis and involved in caspase-independent DNA degradation. *Cell Death Differ* **8**, 1136–1142.
- Varela, A. T., Gomes, A. P., Simões, A. M., Teodoro, J. S., Duarte, F. V., Rolo, A. P. and Palmeira, C. M.** (2008). Indirubin-3'-oxime impairs mitochondrial oxidative phosphorylation and prevents mitochondrial permeability transition induction. *Toxicol Appl Pharmacol* **233**, 179–185.
- Varela, A. T., Simões, A. M., Teodoro, J. S., Duarte, F. V., Gomes, A. P., Palmeira, C. M. and Rolo, A. P.** (2010). Indirubin-3'-oxime prevents hepatic I/R damage by inhibiting GSK-3beta and mitochondrial permeability transition. *Mitochondrion* **10**, 456–463.
- Vassalli, P.** (1992). The pathophysiology of tumor necrosis factors. *Annu. Rev. Immunol.* **10**, 411–452.
- Verhagen, A. M., Ekert, P. G., Pakusch, M., Silke, J., Connolly, L. M., Reid, G. E., Moritz, R. L., Simpson, R. J. and Vaux, D. L.** (2000). Identification of DIABLO, a mammalian protein that promotes apoptosis by binding to and antagonizing IAP

- proteins. *Cell* **102**, 43–53.
- Wallace, D. C.** (1999). Mitochondrial diseases in man and mouse. *Science* **283**, 1482–1488.
- Wallace, D. C.** (2005). The mitochondrial genome in human adaptive radiation and disease: on the road to therapeutics and performance enhancement. *Gene* **354**, 169–180.
- Wang, C.-Y. and Zhao, Z.-B.** (2012). Somatic mtDNA mutations in lung tissues of pesticide-exposed fruit growers. *Toxicology* **291**, 51–55.
- Wang, P. and Heitman, J.** (2005). The cyclophilins. *Genome Biol.* **6**, 226.
- Watabe, Y., Nazuka, N., Tezuka, M. and Shimba, S.** (2010). Aryl hydrocarbon receptor functions as a potent coactivator of E2F1-dependent transcription activity. *Biol Pharm Bull* **33**, 389–397.
- Waterham, H. R., Koster, J., van Roermund, C. W. T., Mooyer, P. A. W., Wanders, R. J. A. and Leonard, J. V.** (2007). A lethal defect of mitochondrial and peroxisomal fission. *N. Engl. J. Med.* **356**, 1736–1741.
- Webb, J. L., Ravikumar, B., Atkins, J., Skepper, J. N. and Rubinsztein, D. C.** (2003). Alpha-Synuclein is degraded by both autophagy and the proteasome. *J Biol Chem* **278**, 25009–25013.
- Weinstein, D. A., Gogal, R. M., Mustafa, A., Prater, M. R. and Holladay, S. D.** (2008). Mid-gestation exposure of C57BL/6 mice to 2,3,7,8-tetrachlorodibenzo-p-dioxin causes postnatal morphologic changes in the spleen and liver. *Toxicol Pathol* **36**, 705–713.
- West, A. P., Shadel, G. S. and Ghosh, S.** (2011). Mitochondria in innate immune responses. *Nat Rev Immunol* **11**, 389–402.
- Westermann, B.** (2010). Mitochondrial fusion and fission in cell life and death. *Nat Rev Mol Cell Biol* **11**, 872–884.
- Whitlock, J. P.** (1999). Induction of cytochrome P4501A1. *Annu Rev Pharmacol Toxicol* **39**, 103–125.
- Wojtczak, L., Zaluska, H., Wroniszewska, A. and Wojtczak, A. B.** (1972). Assay for the intactness of the outer membrane in isolated mitochondria. *Acta Biochim Pol* **19**, 227–234.
- Woodfield, K., Rück, A., Brdiczka, D. and Halestrap, A. P.** (1998). Direct demonstration of a specific interaction between cyclophilin-D and the adenine nucleotide translocase confirms their role in the mitochondrial permeability transition. *Biochem J* **336 (Pt 2)**, 287–290.
- Wu, Y.-T., Wu, S.-B., Lee, W.-Y. and Wei, Y.-H.** (2010). Mitochondrial respiratory dysfunction-elicited oxidative stress and posttranslational protein modification in mitochondrial diseases. *Ann N Y Acad Sci* **1201**, 147–156.
- Yang, C.-Y., Huang, T.-S., Lin, K.-C., Kuo, P., Tsai, P.-C. and Guo, Y. L.** (2011). Menstrual effects among women exposed to polychlorinated biphenyls and dibenzofurans. *Environ Res* **111**, 288–294.

- Yang, C.-Y., Wang, Y.-J., Chen, P.-C., Tsai, S.-J. and Guo, Y. L.** (2008). Exposure to a mixture of polychlorinated biphenyls and polychlorinated dibenzofurans resulted in a prolonged time to pregnancy in women. *Environ Health Perspect* **116**, 599–604.
- Yang, X., Jiang, Y., Li, J., Hong, W.-X., Wu, D., Huang, X., Huang, H., Zhou, L., Yang, L., Yuan, J., et al.** (2012). Lentivirus-mediated silencing of I2PP2A through RNA interference attenuates trichloroethylene-induced cytotoxicity in human hepatic L-02 cells. *Toxicol Lett* **209**, 232–238.
- Yarden, Y. and Schlessinger, J.** (1987). Epidermal growth factor induces rapid, reversible aggregation of the purified epidermal growth factor receptor. *Biochemistry* **26**, 1443–1451.
- Yorimitsu, T. and Klionsky, D. J.** (2007). Eating the endoplasmic reticulum: quality control by autophagy. *Trends Cell Biol* **17**, 279–285.
- Yoshioka, W., Peterson, R. E. and Tohyama, C.** (2011). Molecular targets that link dioxin exposure to toxicity phenotypes. *J. Steroid Biochem. Mol. Biol.* **127**, 96–101.
- Yu, L.-Y., Jokitalo, E., Sun, Y.-F., Mehlen, P., Lindholm, D., Saarna, M. and Arumae, U.** (2003). GDNF-deprived sympathetic neurons die via a novel nonmitochondrial pathway. *J Cell Biol* **163**, 987–997.
- Yue, Z., Horton, A., Bravin, M., DeJager, P. L., Selimi, F. and Heintz, N.** (2002). A novel protein complex linking the delta 2 glutamate receptor and autophagy: implications for neurodegeneration in lurcher mice. *Neuron* **35**, 921–933.
- Yue, Z., Jin, S., Yang, C., Levine, A. J. and Heintz, N.** (2003). Beclin 1, an autophagy gene essential for early embryonic development, is a haploinsufficient tumor suppressor. *Proc Natl Acad Sci USA* **100**, 15077–15082.
- Zangar, R. C., Davydov, D. R. and Verma, S.** (2004). Mechanisms that regulate production of reactive oxygen species by cytochrome P450. *Toxicol Appl Pharmacol* **199**, 316–331.
- Zhang, Y. and Chan, D. C.** (2007). Structural basis for recruitment of mitochondrial fission complexes by Fis1. *Proc Natl Acad Sci USA* **104**, 18526–18530.
- Zhang, Y., Qi, H., Taylor, R., Xu, W., Liu, L. F. and Jin, S.** (2007a). The role of autophagy in mitochondria maintenance: characterization of mitochondrial functions in autophagy-deficient *S. cerevisiae* strains. *Autophagy* **3**, 337–346.
- Zhang, Z., Che, W., Liang, Y., Wu, M., Li, N., Shu, Y., Liu, F. and Wu, D.** (2007b). Comparison of cytotoxicity and genotoxicity induced by the extracts of methanol and gasoline engine exhausts. *Toxicol In Vitro* **21**, 1058–1065.
- Zheng, Y. T., Shahnazari, S., Brech, A., Lamark, T., Johansen, T. and Brumell, J. H.** (2009). The adaptor protein p62/SQSTM1 targets invading bacteria to the autophagy pathway. *J Immunol* **183**, 5909–5916.
- Zheng, Y., Shi, Y., Tian, C., Jiang, C., Jin, H., Chen, J., Almasan, A., Tang, H. and Chen, Q.** (2004). Essential role of the voltage-dependent anion channel (VDAC) in mitochondrial permeability transition pore opening and cytochrome c release induced by arsenic trioxide. *Oncogene* **23**, 1239–1247.

- Zoratti, M. and Szabò, I.** (1995). The mitochondrial permeability transition. *Biochim Biophys Acta* **1241**, 139–176.
- Zorov, D. B., Juhaszova, M., Yaniv, Y., Nuss, H. B., Wang, S. and Sollott, S. J.** (2009). Regulation and pharmacology of the mitochondrial permeability transition pore. *Cardiovasc Res* **83**, 213–225.
- Zou, H., Henzel, W. J., Liu, X., Lutschg, A. and Wang, X.** (1997). Apaf-1, a human protein homologous to *C. elegans* CED-4, participates in cytochrome c-dependent activation of caspase-3. *Cell* **90**, 405–413.
- Züchner, S., Mersyanova, I. V., Muglia, M., Bissar-Tadmouri, N., Rochelle, J., Dadali, E. L., Zappia, M., Nelis, E., Patitucci, A., Senderek, J., et al.** (2004). Mutations in the mitochondrial GTPase mitofusin 2 cause Charcot-Marie-Tooth neuropathy type 2A. *Nat Genet* **36**, 449–451.
- US EPA, 2004. Exposure and Human Health Reassessment of 2,3,7,8-Tetrachlorodibenzo-p-dioxin (TCDD) and Related Compounds, National Academy of Sciences (NAS) Review Draft. EPA/600/P-00/001Cb. Available from: <http://www.epa.gov/ncea/pdfs/dioxin/nas-review>.